THE ROLE OF THE HERPES SIMPLEX VIRUS TYPE 1 UL28 PROTEIN IN TERMINASE COMPLEX ASSEMBLY AND FUNCTION

by

Jason Don Heming

Bachelor of Science, Clarion University of Pennsylvania, 2004

Submitted to the Graduate Faculty of

the School of Medicine in partial fulfillment

of the requirements for the degree of

Doctor of Philosophy

University of Pittsburgh

2013

UNIVERSITY OF PITTSBURGH

SCHOOL OF MEDICINE

This dissertation was presented

by

Jason Don Heming

It was defended on

April 18, 2013

and approved by

Michael Cascio, Associate Professor, Bayer School of Natural and Environmental Sciences

James Conway, Associate Professor, Department of Structural Biology

Neal DeLuca, Professor, Department of Microbiology and Molecular Genetics

Saleem Khan, Professor, Department of Microbiology and Molecular Genetics

Dissertation Advisor: Fred Homa, Associate Professor, Department of Microbiology and Molecular Genetics

THE ROLE OF THE HERPES SIMPLEX VIRUS TYPE 1 UL28 PROTEIN IN TERMINASE COMPLEX ASSEMBLY AND FUNCTION

Jason Don Heming, PhD

University of Pittsburgh, 2013

Herpes simplex virus type I (HSV-1) is the causative agent of several pathologies ranging in severity from the common cold sore to life-threatening encephalitic infection. During productive lytic infection, over 80 viral proteins are expressed in a highly regulated manner, resulting in the replication of viral genomes and assembly of progeny virions. Cleavage and packaging of replicated, concatemeric viral DNA into newly assembled capsids is critical to virus proliferation and requires seven viral genes: UL6, UL15, UL17, UL25, UL28, UL32, and UL33. Analogy with the well-characterized cleavage and packaging systems of double-stranded DNA bacteriophage suggests that HSV-1 encodes for a viral terminase complex to perform these essential functions, and several studies have indicated that this complex consists of the viral UL15, UL28, and UL33 proteins. However, the inability to purify the terminase proteins has hampered biochemical analysis of these proteins. The goal of the following studies was to isolate a functional terminase complex from HSV-1-infected cells by affinity chromatography using a virus expressing a UL28-TAP fusion protein. The tandem affinity purification (TAP) procedure resulted in the isolation of soluble UL28 complexes containing the UL15 and UL33 proteins. Biochemical studies were performed to determine the protein composition and stoichiometry of the purified complex, and the associated nuclease activity was examined. Mass spectrometry was utilized to identify viral and cellular proteins that associate with the complex during infection. Finally, mutations or deletions within the nuclease domain of UL15 or the

metal-binding domain of UL28 were introduced into the genome of the NTAP-UL28 fusion virus. Characterization of these viruses followed by the isolation of terminase complexes revealed that the domain mutations did not preclude complex formation but each virus was deficient in viral DNA cleavage, further demonstrating the importance of these domains during DNA encapsidation. The ability to purify the endogenous terminase complex is novel to the field and we view these studies as a critical step in understanding how the terminase complex functions in the context of productive HSV-1 infection.

TABLE OF CONTENTS

LIST OF TABLES

LIST OF FIGURES

PREFACE

The data presented in this dissertation are the culmination of many individual contributions. I would like to thank Shelley Cockrell and Jamie Huffman who provided technical assistance in the laboratory. Jamie Huffman performed the capsid preparation and Southern blot assays. Lisa Jones performed the mass spectrometry at the NIH/NCRR Mass Spectrometry Resource at Washington University in St. Louis (NCRR 5P41RR000954-35, NIGMS 8 P41 GM103422-35). Other reagents and technical assistance were kindly provided by Neal DeLuca (University of Pittsburgh), Carolyn Coyne (University of Pittsburgh), Paul "Kip" Kinchington (University of Pittsburgh), Joel Baines (Cornell University), Sandra Weller (University of Connecticut), Greg Smith (Northwestern University), Roselyn Eisenberg (University of Pennsylvania), and Gary Cohen (University of Pennsylvania).

Commonly used abbreviations in this dissertation include: bp, base pairs; min, minutes; h or hr, hour(s); ORF, open reading frame; MOI, multiplicity of infection; PFU, plaque forming units; nm, nanometers; ATP, adenosine triphosphate; PCR, polymerase chain reaction; kDa, kilodalton; mM, millimolar.

1.0 INTRODUCTION

1.1 HSV-1 LINEAGE AND PATHOGENESIS

1.1.1 The Human herpesviruses

Herpesviruses are highly prevalent among mammals, to the point that a unique infecting herpesvirus has been identified in the majority of studied animal species (168). Currently, nine herpesviruses are known to infect humans and these have been classified, based largely upon four architectural features shared between the mature virus particles, into the family *Herpesviridae* (Table 1) (2, 53, 168). Herpesvirions are typically comprised of i) an inner core of linear double-stranded DNA (dsDNA) contained within ii) an icosahedral capsid composed of 161 capsomers and 125 nm in diameter, which is surrounded by iii) a proteinaceous, asymmetric layer called the tegument, and iv) an outer lipid envelope that is studded with glycoproteins. Herpesviruses also share the following four biological criterion: i) expression of numerous enzymes required for viral processes such as nucleotide metabolism, DNA synthesis, and protein processing; ii) nuclear synthesis of viral DNA and capsids, with the final virion maturation steps occurring in the cytoplasm; iii) virus proliferation resulting in cell death; and iv) persistence in host cells in a latent form that can later reactivate to cause productive infection. The family *Herpesviridae* is further divided into three specific subfamilies, *Alpha-*, *Beta-*, and

Gammaherpesvirinae that differ based upon viral characteristics such as host range and reproductive cycle length. Herpes simplex virus type I (HSV-1) is the prototypical alphaherpesvirus and like other members of this subfamily, possesses a relatively short reproductive cycle (18-20 hr), spreads rapidly in cultured cells, and efficiently destroys infected cells (168).

Table 1. The human *Herpesviridae*

Common Name (Abbr)	Species (Abbr)	Genome size (kb)[a]
Subfamily *Alphaherpesvirinae*		
Herpes simplex virus type 1 (HSV-1)	*Human herpesvirus 1* (HHV-1)	152
Herpes simplex virus type 2 (HSV-2)	*Human herpesvirus 2* (HHV-2)	155
Varicella-zoster virus (VZV)	*Human herpesvirus 3* (HHV-3)	125
Subfamily *Betaherpesvirinae*		
Human cytomegalovirus (HCMV)	*Human herpesvirus 5* (HHV-5)	236
	Human herpesvirus 6A (HHV-6A)	159
	Human herpesvirus 6B (HHV-6B)	162
	Human herpesvirus 7 (HHV-7)	145
Subfamily *Gammaherpesvirinae*		
Epstein-Barr virus (EBV)	*Human herpesvirus 4* (HHV-4)	172
Kaposi's sarcoma-associated herpesvirus (KSHV)	*Human herpesvirus 8* (HHV-8)	138

[a]Kilobase pairs; Sizes are approximate and not representative of every sequenced strain (53)

1.1.2 Pathogenesis and treatment

A typical HSV-1 infection begins when the virus comes into contact with mucosal surfaces or abraded skin, entering host epithelial cells at these sites (Figure 1). In the cell, the virus

proliferates resulting in a lytic or productive primary infection that spreads to adjacent sensory nerve cells. Within neurons, the virus will traffic along the axon until it reaches the neuronal cell body, typically located within the trigeminal ganglia. Here, the lytic gene expression cascade is repressed resulting in HSV-1 latency, a hallmark of the herpesviruses that allows viral infection to persist for the lifetime of the host. Periodically during latency, numerous internal or external factors such as stress, fatigue, or immunosuppression, can trigger the virus to reenter the lytic phase resulting in the production of virions. These viral progeny will traffic back along the neuronal axon to the periphery, at or near the site of initial infection, and this process is the basis of HSV-1 recurrent infection (71, 259).

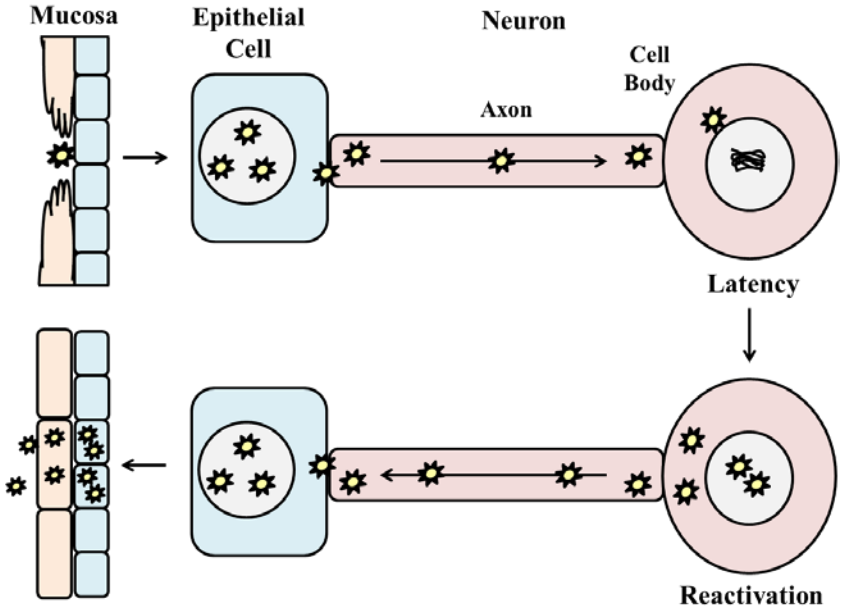

Figure 1. Model of recurrent HSV-1 infection.

The majority of primary HSV-1 infections are asymptomatic; however symptomatic recurrences can occur and this depends largely on the immune status of the host (71, 259). There are several clinical manifestations of HSV-1 disease, with the most common form being

orolabial lesions or cold sores (57). Ocular herpes, or herpes keratitis, is a leading cause of blindness in developed countries, while other less common presentations of HSV-1 disease include herpes gladiatorum, herpetic whitlow, and eczema herpeticum (57, 71). Life-threatening infections are rare but include: neonatal herpes, virus transmission from an infected mother to the baby during delivery; herpes encephalitis, infection of the brain; and severe infections of immunocompromised patients (57). Infection incidence is lower through adolescence in developed countries, but by adulthood the majority (60-80%) of humans worldwide are seropositive for HSV-1 (57, 143). It is also very likely that the incidence rate is much higher due to a lack of self-reporting by infected individuals (57).

Nucleoside analogues represent the standard for treatment of HSV-1 infection and include aciclovir, valaciclovir, penciclovir, and famciclovir. These antiviral agents are guanosine analogues that cause inhibition of viral DNA polymerase activity and chain termination when added to a replicating viral DNA strand (71). They exhibit low toxicity towards uninfected host cells and are very effective in immunocompetent individuals; however, resistant strains have been isolated from bone marrow transplantation recipients at rates as high as 14% (57). In patients with resistant HSV-1, other drugs such as foscarnet and cidofovir may be used, but both exhibit significant toxicity toward host cells (71). With the immunocompromised population world-wide expanding due to factors such as aging, cancer, and AIDS, there is an increasing demand for novel HSV-1 antivirals that target essential viral processes or structures other than viral DNA replication.

1.2 THE HSV-1 VIRION

1.2.1 Virion morphology

The mature HSV-1 virion is pleiomorphic but largely spherical, with an average diameter of 186 nm at the base of the envelope that extends to approximately 225 nm when the glycoprotein spikes are included (85). As previously discussed (Section 1.1.1), like all members of the *Herpesviridae* the HSV-1 virion is composed of four main architectural features: envelope, tegument, capsid, and core (Figure 2) (168).

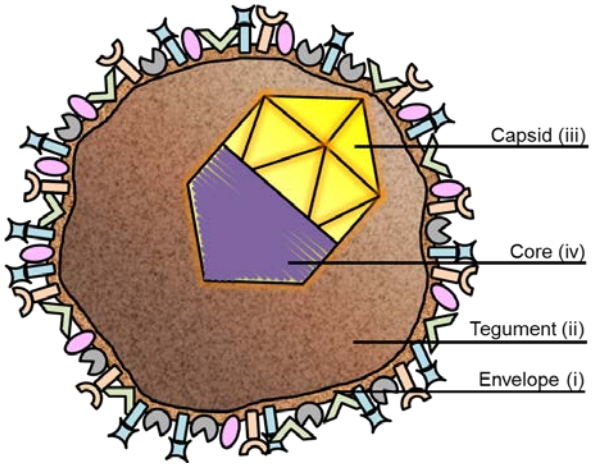

Figure 2. Structure of the HSV-1 virion. The diagram depicts the four major structural components of the HSV-1 virion: (i) the outer envelope studded with various glycoproteins, (ii) the proteinaceous tegument layer, and (iii) the icosahedral capsid that houses (iv) the dsDNA core.

The outer envelope is arranged as a lipid bilayer containing multiple copies of approximately eleven viral glycoproteins that protrude externally and a small number of intrinsic membrane proteins (68). Experimental evidence supports that the envelope is obtained from the

host cell and possesses lipid content similar to that found in the cellular cytoplasmic membrane (214, 239).

The viral tegument layer is located in the space between the envelope and capsid, and occupies approximately two-thirds of the volume within the virion. Cryo-electron tomography of the HSV-1 virion revealed that the tegument is asymmetrical in structure; where at one side of the virion there is approximately 35 nm of tegument between the envelope and the capsid, and at the opposite side the capsid resides in close proximity to the envelope. These studies also showed that the tegument substructure was particulate in appearance and contained short actin-like filaments (85). The tegument is largely proteinaceous, containing multiple copies of twenty-three viral proteins, but has also been shown to contain viral and cellular gene transcripts (126, 202). Mass spectrometry analysis of purified virions has also identified several cellular proteins that may be tegument components; however these results are yet to be verified (126).

The structure of the HSV-1 capsid has been described in great detail owing to numerous studies utilizing cryo-electron microscopy (cryo-EM) and three-dimensional image reconstruction of isolated capsids (26). The viral capsid is 125 nm in diameter, with its component proteins positioned on a T=16 icosahedral lattice (Figure 3) (31, 201, 261). Each capsid is composed of 161 major structural protein subunits termed capsomers, which can be divided more specifically into the 150 hexons that constitute the edges and faces of the icosahedron, and eleven pentons that reside at all but one vertex of the capsid (155, 261). Respectively, the pentamers and hexamers are composed of five and six copies of the major capsid protein, VP5 (157). The unique capsid vertex not occupied by a VP5 pentamer is the site of the portal complex through which DNA enters or exits the capsid. The portal is cylindrical in geometry and composed of twelve copies of the UL6 protein (155). Positioned at the tip of each

VP5 protein of every capsid hexamer is one copy of the VP26 protein, which totals 900 copies per capsid (24, 157). Located just above the capsid floor at positions of threefold capsomer symmetry is the triplex complex, which functions in linking capsomers during capsid formation (157, 234, 279). There are 320 triplexes per capsid and each is composed of one subunit of VP19C and two subunits of VP23 (157). Recent cryo-EM studies have determined the presence of an additional capsid component residing around each vertex, termed the capsid vertex specific component (CVSC). Each CVSC is a heterodimer of the UL25 and UL17 proteins, and is thought to stabilize the capsid during and after completion of DNA packaging (41, 45, 229, 232, 236). One final capsid component is the VP24 protease, which cleaves the scaffolding proteins during capsid maturation; however the precise location and function of this protein within virions is not yet known (126, 215).

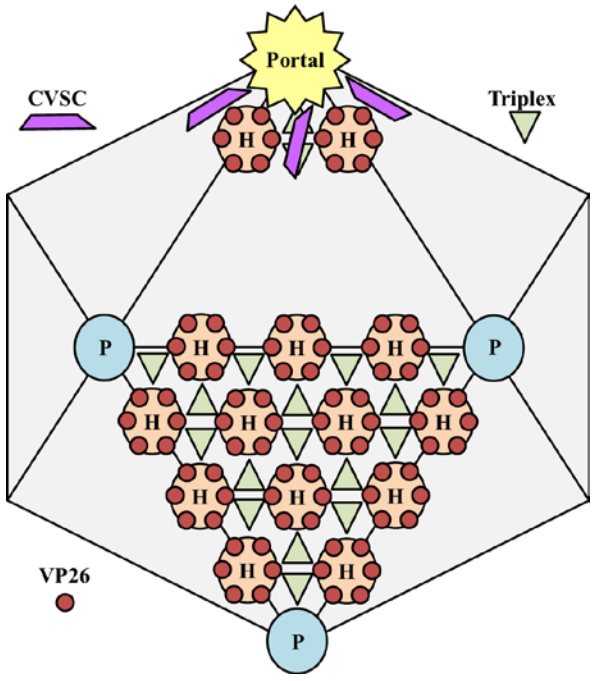

Figure 3. The capsid structural proteins. The schematic diagram depicts the location of the major and minor capsid components. (Top) The UL6 portal situated at a unique penton vertex and the location of the CVSC. Of note, CVSC molecules are situated between hexons at each capsid vertex but for simplicity are only depicted at a single vertex. (Bottom) Position of the pentons (P, blue), hexons (H, orange), VP26 (red circles) and triplexes (green triangles) on one face of the T=16 icosahedral lattice.

The HSV-1 virion core is located within the viral capsid and contains the linear, dsDNA genome (69, 261). Cryo-EM analysis of purified virions suggests that the packaged DNA resides in a liquid-crystalline state as a toroid or spool structure, with strands spaced approximately 2.6 nm apart (23, 77, 278).

1.2.2 Genome structure and sequence arrangement

The linear, dsDNA genome of HSV-1 has been sequenced and totals 152,261 base pairs (bp), with a G+C content of 68.3% (66, 110, 131). This large molecule consists of covalently linked long and short regions of unique viral sequence (U_L and U_S respectively) that are both flanked by repeated sequences (Figure 4). The U_L component is bracketed by inverted copies of the *b* sequence, which differ in size and sequence arrangement from inverted copies of the *c* sequence that flank the U_S component (247). Repeated *a* sequences are located at the termini of both the U_L and U_S components and at the junction between both components, and vary in orientation and copy number depending on their position in the genome (125, 188, 189, 247, 248). The *a* sequences are highly conserved and mediate processes (i.e. cleavage and packaging of viral DNA) critical to the research described in the remainder of this document (237). A detailed discussion of *a* sequence structure and function can be found in section 1.4.5.

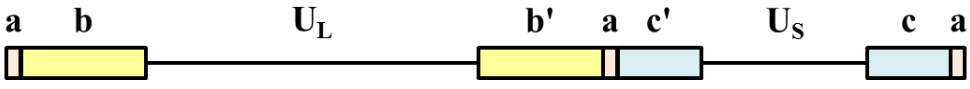

Figure 4. Structure and sequence arrangement of the HSV-1 genome.

An interesting characteristic of the HSV-1 genome is the ability of the long and short regions to invert relative to one another. Genomic DNA isolated from cells infected with wild-type HSV-1 is observed as four linear, isomeric forms in an equimolar concentration and designated as P (prototype), I_L (inversion of the long component), I_S (inversion of the short component), and I_{SL} (inversion of the both components) (61, 87). Sites within the viral *a* sequences have been shown to be responsible for the recombination events leading to genome isomerization, however the physiological significance of these isomers is not known (38, 137, 209, 210).

1.3 MOLECULAR BIOLOGY OF HSV-1 LYTIC INFECTION

1.3.1 Virus entry and capsid transport

The HSV-1 replication cycle begins with virus entry into the host cell. This process, although not fully understood, has been shown to occur through a series of highly regulated interactions between several viral glycoproteins and host cell receptors. Five viral glycoproteins participate in binding and entry and include: gC, gB, gD, gH, and gL (68). The virion initially attaches to heparan sulfate proteoglycans on the host cell surface via gC and/or gB, followed by the interaction of gD with one of three cellular receptors; nectin-1, herpesvirus entry mediator, or 3-*O*-sulfated heparan sulfate (213). The gD/receptor interaction initiates a series of protein conformational changes and interactions that lead to fusion of the viral and cellular membranes. First, gD bound to a cellular receptor interacts with a heterodimer of the gH and gL proteins. The gH/gL proteins then bind gB, activating it to a fusogenic form that brings the viral and

cellular membranes into close proximity and ultimately results in membrane fusion (68). It is important to note that fusion has been observed to occur at the cell surface or within an endocytic vesicle. However, what determines the specific route of entry is not fully known, but appears to be based largely upon the cell type that the virus infects (88).

Membrane fusion releases the viral capsid and tegument proteins into the host cell cytoplasm, where they travel to varying locations within the cell. Many of the tegument proteins remain in the cytoplasm at the cellular membrane while others localize to the nucleus. Some tegument proteins remain associated with the viral capsid which exploits the cellular microtubular network for transport to the nucleus (120). Specifically, the cellular dynein-dynactin motor complex is recruited to the capsid, where it is thought to interact with the remaining components of the inner tegument. The UL36 and UL37 tegument proteins appear most likely to mediate this interaction, while there is also evidence suggesting that the VP26 capsid protein plays a role in stabilizing this interaction. The capsid is transported along microtubules, in a bidirectional manner, to the cytoplasmic side of the infected cell nucleus, where it localizes to a nuclear pore complex. The capsid binds the nuclear pore, releasing viral DNA into the nucleus, and recent evidence suggests that both processes are mediated by the UL36 and/or UL25 proteins (65, 120, 161, 177).

1.3.2 The viral gene expression cascade and genome replication

Upon entering the nucleus, the host cell recognizes the incoming viral DNA and will begin to modify it into condensed chromatin structures. It is during these early time points that the viral "decision" to actively proliferate or establish a latent infection is thought to occur (111). The viral tegument proteins VP16 and VP22 are thought to promote lytic infection by reducing

histone association with viral DNA, therefore maintaining active forms of chromatin (89, 240). It is important to note that, although interesting, the details surrounding the latent infection process are beyond the scope of this manuscript and will not be covered.

During lytic infection, over 80 HSV-1 genes are coordinately expressed in an ordered cascade that is highly regulated by several viral proteins, and involves three expression groups of immediate early (IE), early, or late genes (40, 97, 98). Transcription occurs within the nucleus and translation occurs in the cytoplasm, with both processes utilizing viral and cellular components. The viral gene expression cascade coincides with a series of nuclear remodeling events that together allow for efficient gene expression, DNA replication, and assembly and egress of newly synthesized virus capsids (191), and the details of these processes are described below.

Soon after entering the nucleus and before viral protein synthesis, the input viral DNA is thought to circularize (79, 172, 220, 221) and localize to specific nuclear domains termed ND-10 sites (129). During this process, the IE or α genes are transcribed by the host RNA polymerase II and this expression is stimulated by the viral tegument protein VP16 (8, 27, 50, 174). The α genes are unique compared to the other HSV-1 gene groups in that they require no prior viral protein synthesis for expression. There are five α genes; ICP0, ICP4, ICP22, ICP27, and ICP47, and they are expressed approximately 2-4 hpi (97). The α proteins perform numerous functions including the promotion of viral gene expression by inhibiting host transcription, RNA splicing and transport, and protein synthesis. The α proteins also play a large role in the regulation of viral gene expression, and with the exception of ICP47, stimulate transcription of the viral early genes (98, 130).

Expression of the viral early or β gene class is dependent on the presence of functional α proteins, especially ICP4, and does not require viral replication (98, 107, 253). The β genes are expressed 4-8 hpi but are further classified as β_1 or β_2 depending largely on the timing of expression within this 4-8 hr period (97, 276). Expression of β_1 genes occurs early in infection and very shortly after expression of the α genes, while β_2 gene synthesis is delayed after α protein expression. The β gene class encodes proteins that function largely in nucleotide metabolism and viral DNA replication, and the synthesis of β_2 genes signals the beginning of viral DNA synthesis within the host cell nucleus (191).

Replication of the HSV-1 genome requires seven β proteins; UL30, UL42, UL9, UL29, UL5, UL8, and UL52, and their functions during replication are shown in Table 2 (34, 265). These proteins localize to viral genomes at ND-10 structures where they assemble onto the circular viral DNA molecule to form replication complexes [reviewed in (251)]. The prevailing model for HSV-1 DNA synthesis begins with the production of new genomes via a theta mechanism. However the replication machinery quickly converts to a rolling circle mechanism, producing the head-to-tail, branched, concatemeric molecules that are typically observed in the nuclei of infected cells [reviewed in (20)]. During this process, the replication compartments expand to fill the nucleus, coinciding with the condensation and marginalization of host chromatin to provide optimal space for viral DNA synthesis (191).

Table 2. Essential viral replication proteins

Protein	Function
UL30	DNA polymerase catalytic subunit
UL42	DNA polymerase processivity factor
UL9	origin binding protein
UL29	ssDNA-binding protein
UL5	helicase primase complex
UL8	helicase primase complex
UL52	helicase primase complex

Throughout the replication process, numerous host factors and proteins are recruited to the replication compartments to perform varying functions (257). Several host replication proteins such as DNA polymerase α and DNA ligase have been observed, and may be required for HSV-1 DNA synthesis (58, 260). During viral genome replication, host DNA repair pathways are activated to high levels and several host DNA repair, damage response, and recombination proteins have also been shown to localize to replication compartments (121, 262). Of note, it is during viral DNA synthesis when recombination occurs between genomes to produce the four isomeric genome types (254). However, the exact mechanism or proteins required for this process has not been fully elucidated.

The final set of HSV-1 genes expressed during lytic infection are the late or γ genes. The γ genes are classified by expression that starts after, and is enhanced by, viral genome replication (97). More specifically, γ gene transcription is stimulated by viral DNA replication, resulting in the net effect of greater protein expression (82, 99). Several α proteins and the β protein ICP8 also enhance γ gene transcription (78, 162). As with the β genes, the γ genes are further classified as γ_1 or γ_2 depending on time of, and requirements for, expression. The γ_1 genes, also known as early/late or leaky late genes, are expressed relatively early with slight stimulation by

DNA synthesis, while the γ_2, or true late genes, are expressed late and have a more strict requirement on DNA replication for expression (44, 48, 94, 107, 175). At this point in the discussion, it is important to note that the β and γ gene groupings are not hard and fast, and viewing β_2 through γ_2 gene expression as more of a continuum, is probably a more realistic representation of the events during lytic infection (191).

The majority of γ genes encode for structural proteins required for the assembly of infectious virions, and many of these proteins are needed in large amounts (74). The extensive remodeling events that take place in the host cell nucleus throughout the lytic infection process are critical for high efficiency expression of the γ genes. By the onset of γ gene expression, the viral replication compartments have expanded to fill the nucleus, and it is here that high efficiency transcription of the γ genes occurs (133).

1.3.3 Capsid assembly and DNA packaging

HSV-1 capsid formation and the subsequent packaging of capsids with replicated viral DNA are processes that are central to this manuscript and will be covered in greater detail below (Section 1.4). Briefly, the proteins required for capsid assembly and DNA encapsidation are synthesized with γ gene class kinetics within the cytoplasm, and localize to the infected cell nucleus. Both processes occur within replication compartments at sites near viral DNA replication, and to date, have not been shown to require cellular proteins (46). Capsid formation consists of capsid structural proteins assembling around an internal scaffold to produce empty, spherical, precursor capsids that are competent for DNA packaging. Replicated viral DNA concatemers are then cleaved into monomeric genomes that are packaged into capsids. DNA packaging is thought to

trigger cleavage of the internal scaffold protein, resulting in the structural transformation of the capsid into a mature, polyhedral form. During encapsidation, additional proteins are added to the outer capsid shell that function in stabilization and may also aid in the egress of DNA-filled capsids from the nucleus (28, 46).

1.3.4 Egress and envelopment

After the completion of DNA packaging, viral nucleocapsids exit the host cell nucleus and traverse the cytoplasm to ultimately exit the host cell. Along the way, the nucleocapsids will acquire necessary tegument and envelope components resulting in the assembly of a mature infectious HSV-1 virion. The details surrounding this process have not been fully elucidated and the model for HSV-1 egress and envelopment has been contested within the field. However, a model consisting of sequential envelopment, de-envelopment, and re-envelopment steps has become more widely accepted and will be described below (reviewed in (106, 134)).

Initially, completed viral nucleocapsids utilize nuclear actin filaments for transport to the inner nuclear membrane (224), where they are thought to interact with a heterodimeric complex of the viral UL34 and UL31 proteins (75, 181, 182), termed the nuclear envelopment complex (NEC). The nucleocapsids bud through the inner nuclear membrane, releasing primary-enveloped virions into the perinuclear space, and during this initial envelopment, the virion acquires a small subset of tegument components. Virions within the perinuclear space possess viral glycoproteins on the outer surface of the primary envelope (106). Glycoproteins gB and gH are essential for membrane fusion during virion entry into the host cell (discussed in Section 1.3.1) and these proteins may also mediate fusion of the primary envelope of perinuclear virions with the outer nuclear membrane (70). Fusion results in the release of de-enveloped

nucleocapsids into the cytosol, where they acquire the bulk of the virion tegument proteins. Secondary envelopment occurs when the tegument-coated nucleocapsids bud through membranes of the *trans*-Golgi network, producing mature virions that possess a full complement of tegument and envelope proteins. The assembled virions exit the *trans*-Golgi network within vesicles that are transported to, and released from, the plasma membrane via an exocytic mechanism; resulting in extracellular HSV-1 virions that can go on to infect additional host cells (106, 134).

Critical to the above model is the NEC, with both the UL34 and UL31 proteins being required for primary envelopment at the inner nuclear membrane (37, 181, 192). The NEC also recruits viral and cellular kinases, such as US3, UL13, and protein kinase C that phosphorylate components of the nuclear lamina. Phosphorylation results in disruption of the lamina and expansion of the nucleus; effects that aid in the egress of nucleocapsids (19, 118, 127, 140, 141, 164, 180, 207).

Also of interest is the suggestion that the NEC may preferentially associate with DNA-containing C-capsids versus other immature capsid forms, thus enhancing infection efficiency (106, 190). One explanation for this phenomenon is the potential interaction of the NEC with the CVSC component (UL25/UL17 heterodimer) of viral capsids (106, 236), and it has been shown that UL25 is found on all capsid forms but in increasing amounts from procapsids to B-, A-, C-capsids and virions (149, 204). Components of the HSV-1 terminase complex have also been implicated, as enveloped capsids lacking DNA have been observed in cells infected with viruses encoding nonfunctional UL33, UL15, or UL28 proteins (9, 225, 269), and it has been proposed that terminase subunits inhibit the NEC/capsid interaction based upon the observation that the UL15 and UL28 proteins appear to only transiently associate with immature capsid forms, as

they are not observed on C-capsids (11, 15, 16, 194, 204, 274). On the other hand, the UL33 terminase subunit, which associates equally well with each capsid type (15, 179, 263), has been shown to interact with both UL31 and UL34, and this interaction is conserved in varicella zoster virus (VZV), Kaposi sarcoma-associated herpesvirus, Epstein-Barr virus, and murine cytomegalovirus (73). Clearly further experiments need to be performed in order to elucidate the importance of the NEC interaction with the capsid surface.

1.4 HSV-1 CAPSID ASSEMBLY AND DNA ENCAPSIDATION

1.4.1 Similarities with dsDNA bacteriophage

HSV-1 capsid formation and DNA encapsidation are vital for virus proliferation, and numerous biochemical and electron microscopic studies have provided researchers with a wealth of data concerning capsid structure, essential capsid proteins, and the capsid assembly pathway (26, 28, 46). Common to many of these studies are the observed similarities between HSV-1 capsid structure and formation compared to that seen with tailed dsDNA bacteriophages such as HK97, P22, and T4, and it has been proposed that capsids from both families may have descended from a common ancestor (13, 28, 115, 216). Several lines of evidence also suggest that the DNA cleavage and packaging reaction is similar between HSV-1 and dsDNA phage (12). Key features shared between these virus families include: i) utilization of a scaffolding protein for capsid formation that is not observed in capsids of the mature virion or phage; ii) a spherical procapsid intermediate form that precedes the mature polyhedral form; iii) the incorporation of a dodecameric portal protein at a unique capsid vertex through which DNA is packaged in an

ATP-dependent manner; iv) endonucleolytic cleavage of DNA concatemers to generate individual, unit-length genomes; and v) conformational changes within the capsid that coincide with DNA packaging, termed expansion (12, 28, 46). These similarities have aided greatly in elucidating the roles of the individual HSV-1 subunits during capsid formation and DNA encapsidation.

1.4.2 The four viral capsid forms

During HSV-1 lytic infection, four types of capsids are formed within the infected cell nucleus. Procapsids are a fragile, precursor form of the more stable A-, B-, and C-capsids (80, 151, 186). Each capsid type possesses a distinct morphology when viewed by EM, and the A-, B- and C-capsids can be separated relative to each other by sucrose density gradient ultracentrifugation (Figure 5) (80, 151, 158). The four capsid types share a similar shell structure [detailed in Section 1.2.1], but differ in the minor proteins of the capsid exterior and in the contents of the capsid cavity (Table 3).

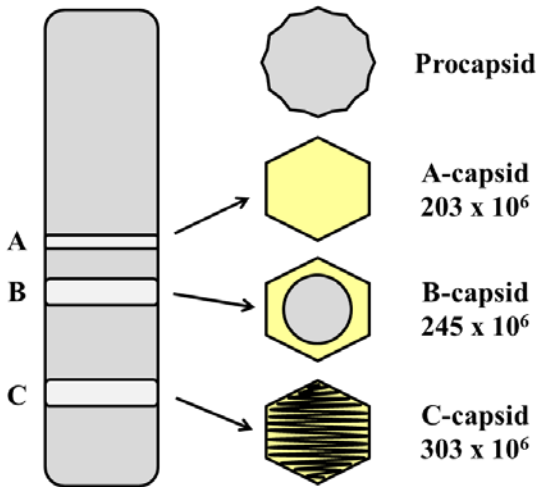

Figure 5. Isolation and morphology of the four capsid types. Schematic representation of capsids isolated by sucrose density gradient centrifugation and the salient morphological features differentiating the four capsid types. Procapsids are unstable and cannot be isolated by gradient centrifugation. The relative molecular mass (M_r) of each capsid is shown (157).

Table 3. Protein components of the four capsid types. An "X" indicates the protein is not present.

	Capsid Component									Cleavage and Packaging					
	Major				Minor										
Capsid Type	VP5	VP19C	VP23	VP26	pre-VP22a	VP22a	UL26	VP24	VP21	UL6	UL25	UL17	UL15	UL28	UL33
Pro				X		X		X	X						
A-					X	X	X		X						
B-					X		X								
C-					X	X	X		X				X	X	

Procapsids represent the first completely enclosed structures formed during the capsid assembly process, and possess an outer shell that is porous and largely spherical in shape (151-153, 158, 222). Procapsids are a precursor form of the other capsid types and have the potential to mature into a more angularized form, package DNA, and assemble into infectious virions

(Table 4) (39, 90, 176, 234). A-capsids are essentially hollow, containing very little DNA or protein content within the capsids cavity, and are thought to form as a result of unsuccessful DNA packaging (23, 80, 201, 205). The cavity of B-capsids possesses a core largely composed of VP22a, the cleaved form of the scaffolding protein, and considerably lower amounts of the UL26 gene products, VP21 and VP24 (122, 123, 147). B-capsids are angularized and thought to mature without ever encountering the DNA encapsidation machinery (80, 151). C-capsids represent the products of successful DNA packaging events and contain a single, complete HSV-1 genome (23, 201). C-capsids can exit the nucleus for further assembly into infectious virions, and are similar, if not identical, to the capsids found within mature virions (23, 80, 170). Each of the four capsid types are assembled in varying quantities during wild-type HSV-1 infection, but a specific capsid form will accumulate to higher levels within the infected cell nucleus if a particular viral protein(s) is missing or nonfunctional (Table 4) (95, 158). This observation has provided researchers with the ability to isolate relatively large quantities of the individual capsid types, which has proven invaluable toward the determination of capsid structure and elucidation of the overarching capsid assembly process.

Table 4. Role of the four capsid types during infection.

Capsid Type	Function	Cause of accumulation
Pro	Precursor/can package DNA	Missing functional maturational protease (VP24)
A-	Abortive packaging	Missing functional UL25 protein
B-	Never encounters packaging machinery	Missing functional UL6, UL15, UL28, UL33, UL32, or UL17 protein
C-	Successful packaging; contain DNA	Normal productive infection

1.4.3 The internal scaffold and maturational protease

Viral capsids co-assemble with an internal protein scaffold that is subsequently cleaved and expelled from the capsid during, or before, DNA packaging [reviewed in (12)]. The scaffolding proteins and protease responsible for scaffold cleavage are gene products of the overlapping UL26 and UL26.5 ORFs of HSV-1 (Figure 6). UL26 encodes the maturational protease, while UL26.5 encodes pre-VP22a, the primary scaffolding protein utilized during capsid assembly (56, 123, 124, 171, 185). Pre-VP22a is identical in sequence to the C-terminal 329 residues of UL26 (123). Therefore, the C-terminus of UL26 can also serve as a scaffold, and both proteins interact with the major capsid protein, VP5, during capsid assembly (63, 100, 122, 227, 252).

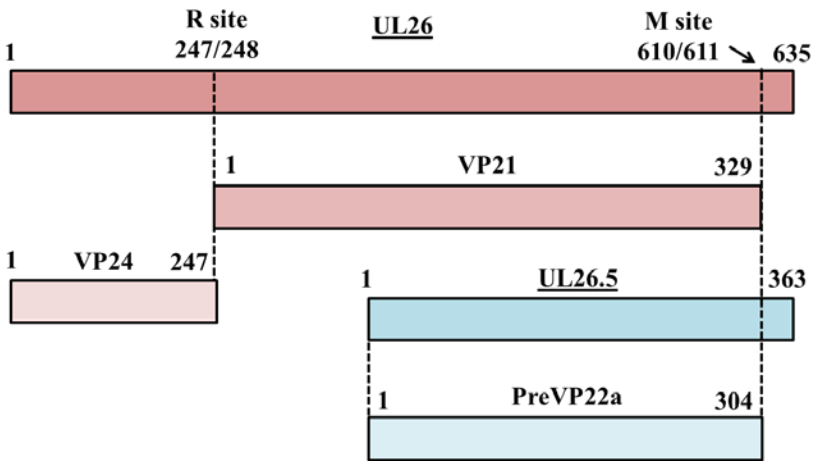

Figure 6. Proteolytic processing of the scaffolding proteins by the maturational protease. Gene names are underlined, protein names are not. Dashed lines through genes indicate cleavage sites. Numbers indicate amino acid residues.

Upon successful assembly of a spherical procapsid, the maturational protease autocleaves itself at two specific sites termed R and M (Figure 6). Cleavage releases the N-terminal VP24 protease and C-terminal VP21 scaffold domains, leaving the final 25 amino acids at the interface

with VP5. Pre-VP22a also contains the C-terminal M-site and is cleaved by the liberated VP24 protease, releasing the VP22a scaffold domain and leaving the final 25 residues bound to VP5 (64, 122, 171, 185, 255).

1.4.4 Assembly of viral capsids

In vitro assembly assays utilizing HSV-1 capsid proteins expressed by recombinant baculoviruses have been critical towards unraveling the mechanism of capsid formation [reviewed in (95)]. Using an *in vitro* assembly system, it was determined that VP5, VP19C, VP23, and either pre-VP22a or the maturational protease (UL26 gene product), were the minimum proteins required for the formation of morphologically normal capsids (151, 153, 222, 228). The *in vitro* system also identified the formation of intermediate or partial procapsid structures during assembly and identified that HSV-1 utilizes a procapsid structure that is similar to the empty proheads seen during dsDNA bacteriophage assembly [(151-153, 234), reviewed in (32)].

Soon after protein synthesis, molecules of VP5, VP23, and VP26, which cannot translocate to the nucleus independently, interact with either pre-VP22a or VP19C for nuclear localization (62, 159, 184). Once in the nucleus, capsid formation is thought to initiate around the UL6 portal protein (Figure 7A) (150). Interacting VP5/pre-VP22a subunits will begin to assemble around the portal via an interaction between pre-VP22a and UL6 (100, 101, 152, 156, 227). Assembly continues as interacting VP5/pre-VP22a subunits interact with other VP5/pre-VP22a complexes, due to the ability of the pre-VP22a molecules to self-associate (152, 169, 264). Triplex proteins are added to the partial procapsid structure, which continues to grow into a spherical procapsid (151-153, 222, 228, 234). Of note, the UL17/UL25 CVSC complex and

proposed terminase complex of UL15, UL28, and UL33 have been detected on procapsids, suggesting they assemble onto the capsid before the start of DNA encapsidation (204, 230). At a time point before, or coinciding with, DNA packaging the scaffold is cleaved from the procapsid interior, resulting in the angularization of the spherical procapsid shell to a mature, icosahedral form (Figure 7B) (39, 90, 151, 170). Procapsids that proceed through this structural transformation without encountering the DNA packaging machinery form the B-capsids (151). DNA packaging results in the expulsion of the cleaved scaffolding proteins from the capsid cavity (80, 185). However, the cleaved VP24 protease remains within the capsid (56, 80), although its function after scaffold cleavage and DNA encapsidation is not known. Capsids that have initiated DNA packaging but are unstable, or abort the packaging process early, release the viral DNA resulting in the hollow A-capsid form (205). Stable capsids containing a complete viral genome represent the C-capsids that can egress from the nucleus and assemble into mature virions (170).

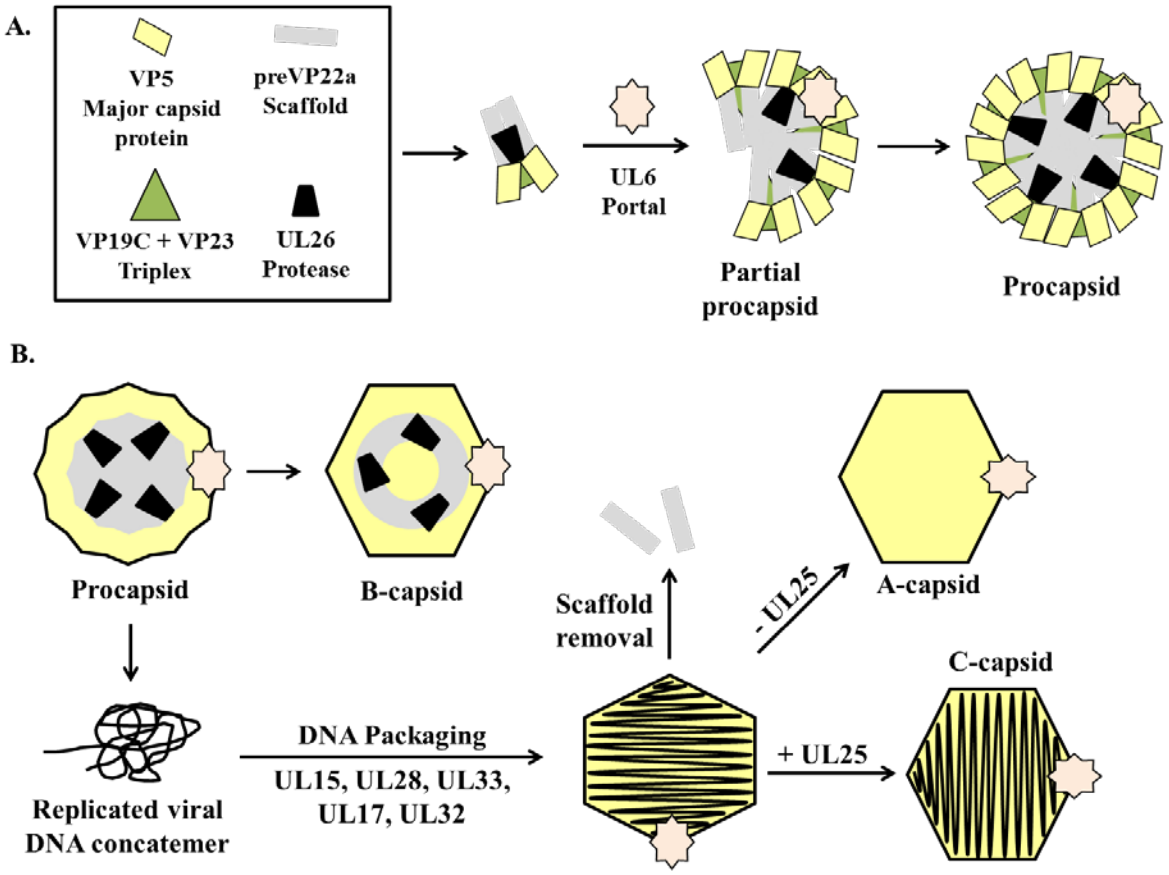

Figure 7. Capsid assembly and DNA packaging. (A) The procapsid assembly pathway. (B) Cleavage and packaging of viral DNA results in the formation of A-, B-, and C-capsids

1.4.5 Specific cleavage and packaging sequences within the HSV-1 genome

HSV-1 DNA replication produces branched, head-to-tail concatemers of viral genomes that must be cleaved and packaged into capsids as individual, unit-length monomers. The specific signals for DNA cleavage are located within the repeated *a* sequences, which contain all of the necessary *cis*-acting sequences for genome maturation (59, 60, 139, 211, 212, 218, 219, 241, 246). The viral *a* sequences are located within the inverted repeats that flank the U_L and U_S segments of the viral genome. As discussed above (Section 1.2.2), the U_L component is flanked by the repeats

ab and *b'a'*, while the U_S component is flanked by *a'c'* and *ca* (Figure 8A). The number of *a* sequence repeats located at the U_L terminus and at the junction between the U_L and U_S segments vary, while there is only one *a* sequence at the termini of the U_S segment (247, 248). The *a* sequences are highly conserved in structure, but contain many variably repeated elements (Figure 8B) (237). Each *a* sequence consists of directly repeated elements (DR1) at each end that flank unique sequence stretches (U_B and U_C). Located between the unique sequences are two additional directly repeated elements (DR2 and DR4) that vary widely in their number of copies per *a* sequence. Due to the variation in copy number of the DR2 and DR4 elements, the size of each *a* sequence can vary from approximately 465-550 bp (55, 138). In regions of the genome containing multiple *a* sequences (ie. the L-S junction), adjacent *a* sequences share the intervening DR1 element (138).

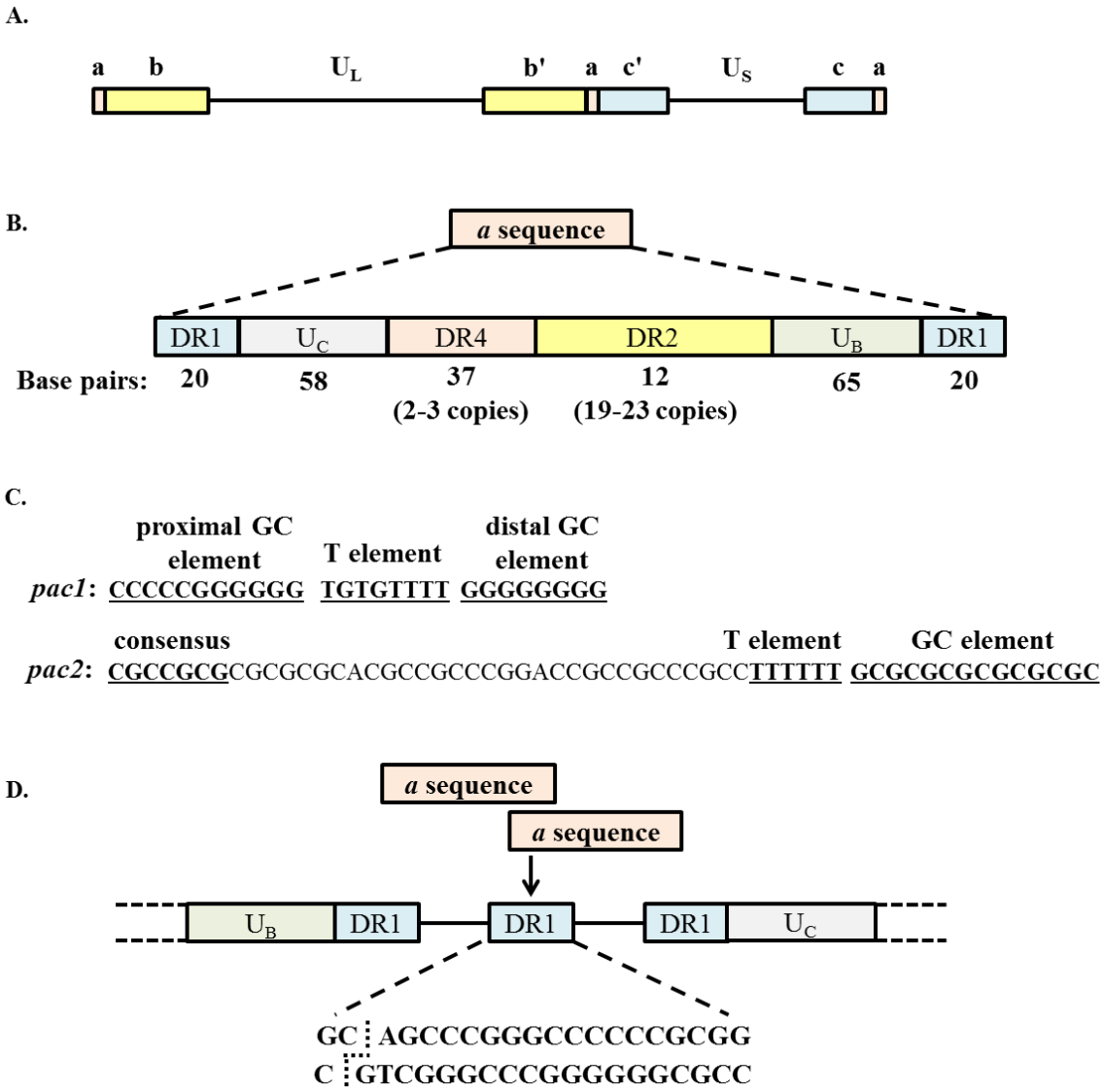

Figure 8. Structure and essential *cis*-acting elements within the viral *a* sequences. (A) **Structure and sequence arrangement of the HSV-1 genome. (B) *a* sequence elements. (C) Sequence of the *pac* motifs. (D) Cleavage within the shared DR1 element of adjacent *a* sequences.**

The *cis*-acting signals for DNA cleavage have been mapped to specific domains termed *pac1* and *pac2*, located within the U_B and U_C sequences respectively (Figure 8C) (59, 60, 136, 144, 241). The *pac1* domain is characterized by two stretches of 5-8 G nucleotides that are separated by a 3-7 nucleotide T-rich region, while *pac2* contains a conserved CGCCGCG motif near a run of 5-10 T nucleotides (59). Cleavage of the dsDNA occurs at a defined distance from

both the *pac1* and *pac2* elements (241), making a site-specific cut within DR1 (59). However, it is important to note that although DR1 contains the site of cleavage, the specific sequence is not required; only the defined distance from either *pac* element (241).

Replication of the viral genome produces concatemers where only the L component terminus is exposed. The S component terminus is covalently bound to the L component of the following genome within the concatemer (128, 203, 275). This observation has led to the suggestion that DNA packaging initiates at the L component terminus and completes at the S component terminus, and *in vitro* uncoating assays have demonstrated that the S component terminus exits the capsid first (148). Following this model, it is thought that the initial cleavage of the concatemer is directed by *pac2*, resulting in the terminal *a* sequence of the L component possessing a truncated, beginning DR1 element of 18 base pairs with a 3' G nucleotide extension (Figure 8D). Cleavage by *pac1* results in the terminal *a* sequence of the S component possessing a final truncated DR1 element of one base pair with a 3' C nucleotide overhang (12, 139). The second *pac1*-mediated cleavage frees the linear, monomeric genome from the concatemer for packaging to complete. During subsequent rounds of infection, the DR1 overhangs allow for circularization of the viral genome for replication (139).

1.4.6 Essential DNA encapsidation proteins

Studies utilizing HSV-1 mutants encoding temperature-sensitive or null mutations have revealed that successful encapsidation of HSV-1 DNA requires the protein products of seven viral genes; UL6, UL15, UL17, UL25, UL28, UL32, and UL33 (3, 4, 6, 10, 33, 116, 117, 132, 165, 166, 173, 195, 198, 205, 206, 225, 256, 272). Six of these proteins are required for viral DNA cleavage (UL6, UL15, UL17, UL28, UL32, UL33), and when even one is missing or nonfunctional,

concatemeric DNA and B-capsids accumulate within the infected cell nucleus. In the absence of a functional UL25 protein, cleaved viral genomes and A-capsids accumulate within the infected cell nucleus, indicating a defect in packaging. With the exception of UL32, each of the essential cleavage and packaging proteins have been identified as minor components of the HSV-1 capsid, and interact in varying amounts with each capsid type (15, 16, 84, 132, 165, 194, 204, 230, 263, 274). Proposed functions for each protein have been ascribed based upon analogy with essential DNA encapsidation proteins utilized by dsDNA bacteriophage (32). More recently the roles of several of the essential HSV-1 cleavage and packaging proteins have been better defined using genetic and biochemical methods, along with electron microscopy.

Twelve copies of the UL6 protein form the ring-like portal structure through which viral DNA enters and exits the capsid (30, 35, 155, 235). This observation was initially determined from immunoelectron microscopy analysis of portal structures from isolated capsids, and EM examination of portal structures formed *in vitro*, using soluble UL6 monomers purified from recombinant baculovirus infected cells (155). The formation of stable portal ring structures has been shown to require a putative leucine zipper domain within UL6, and disulfide bond formation between UL6 monomers (7, 145). EM analysis has determined that the HSV-1 portal structure is similar to the portals of dsDNA bacteriophage, and that it resides at a single, unique capsid vertex (14, 30, 35, 235). *In vitro* capsid assembly assays revealed that UL6 interacts directly with the pre-VP22a scaffold protein (150, 156), and further studies using deletion mutants determined that amino acids 143-151 of the scaffold are required for this interaction (102, 208, 266). The *in vitro* capsid assembly assays also demonstrated that not only is the scaffold/portal interaction required for portal incorporation, but the portal proteins must be present when capsid assembly initiates in order to be incorporated into the capsid (150, 156).

These results suggest that capsid assembly initiates around the portal and that a regulatory mechanism must be in place to ensure that each capsid contains only one portal (30, 35, 150, 156).

The UL25 protein is unique relative to the six other essential DNA encapsidation proteins, in that when UL25 is not functional viral DNA concatemers are cleaved and A-capsids accumulate within the nucleus (3, 41, 42, 132, 163, 217). Analysis of replicated viral DNA from UL25 mutants revealed that the L terminus was cleaved correctly, while cleavage at the S end of the genome was aberrant or did not occur (217). Taken together, these data suggest that UL25 plays a role in capsid stabilization during DNA packaging not unlike the "head-completion" proteins utilized by dsDNA bacteriophage (32). The UL25 protein is also observed in increasing amounts from procapsids, to B-, A-, then C-capsids, and finally virions, further supporting a role in capsid stabilization, with increasing amounts of UL25 protein added as encapsidation progresses (132, 149, 204). Visual confirmation of this role has come from cryo-EM analysis of capsids, revealing that UL25 interacts with the capsid surface in a 1:1 heterodimer with a second essential encapsidation protein, UL17 (41, 232, 236). This complex has been observed on A-, B-, and C-capsids, surrounding the vertices and has been aptly named the capsid vertex specific component (CVSC) (41). The CVSC contacts triplexes and hexons surrounding the pentons, and specifically UL25 has been shown to interact with the triplex protein VP19c and the VP5 major capsid protein (41, 42, 45, 163, 232, 236). UL25 also appears to interact directly with the C-terminus of UL17 (232), supporting previous data demonstrating that UL25 capsid binding is greatly enhanced by the presence of UL17 (230). It is thought that as encapsidation progress, conformational changes occur within proteins of the capsid shell, revealing binding sites for UL25 (29). Outside of capsid stabilization, the UL25 protein may play additional roles relating

to the capsid tegument. An HSV-1 strain encoding a temperature-sensitive lesion within UL25 demonstrated a viral uncoating defect at the nonpermissive temperature early in infection (177). Another study revealed an interaction between UL25 and the large tegument protein, UL36, at the capsid surface, implicating UL25 in tegumentation of the viral capsid during assembly (43).

Although the UL32 protein is essential for cleavage and packaging, its role during this process is largely unknown. In the absence of UL32, capsids do not accumulate within replication compartments, but in perinuclear regions near the nuclear membrane, possibly suggesting a role in the transport of assembled capsids to sites for DNA encapsidation (36, 116).

The remaining three essential DNA encapsidation proteins, UL15, UL28, and UL33, are thought to form the viral terminase complex (46). Analogy with terminase complexes of dsDNA bacteriophage suggests that the DNA-binding, cleavage, and translocation activities, required for successful cleavage and packaging of viral DNA, are performed by the UL15, UL28, and UL33 proteins (32). The following section of this introduction will detail the current state of knowledge regarding the HSV-1 terminase complex and propose a model for the cleavage and packaging of HSV-1 DNA into capsids.

1.5 THE HSV-1 TERMINASE COMPLEX

1.5.1 Evidence for an HSV-1 terminase complex composed of interacting UL15, UL28, and UL33 subunits

Initial evidence suggesting an interaction between the HSV-1 UL28 and UL15 proteins came from studies using the closely related herpesviruses, pseudorabies virus (PRV) and human

cytomegalovirus (HCMV). Koslowski et al. (113) utilized cell lines stably expressing the PRV UL28 protein to demonstrate that UL28 was predominantly cytoplasmic in the absence of other PRV proteins, but entered the nucleus upon PRV infection. Furthermore, they showed that PRV UL28 localized to the nucleus of cells infected with HSV-1 and that the UL15 protein of HSV-1 enabled this nuclear localization (113). In studies using HCMV, mutant viruses were isolated that were resistant to benzimidazole ribonucleoside antivirals, which inhibit HCMV infection by specifically preventing the cleavage of viral DNA concatemers. The mutations that conferred resistance were mapped to the HCMV UL89 and UL56 proteins, which are homologs of the HSV-1 UL15 and UL28 proteins respectively, suggesting that these proteins not only interact, but play an essential role during DNA encapsidation (114).

Koslowski et al. (112) were the first to provide direct evidence that the UL15 and UL28 proteins interact within HSV-1-infected cells. Ion-exchange and DNA affinity chromatography of infected cell lysates was followed by sucrose gradient centrifugation of the purified proteins. Immunoblotting of gradient fractions for UL15 and UL28 revealed that both proteins comigrated through the gradient to a position suggestive of a 1:1 heterodimeric complex (112). It was later revealed by coimmunoprecipitation of proteins from HSV-1-infected cells that the UL33 protein also interacts with the complex of UL15 and UL28 (17). Numerous additional experiments have corroborated the interaction between the HSV-1 UL15, UL28, and UL33 proteins using a variety of methods including immunofluorescence assay to determine protein localization (1, 91, 112, 179, 258), and coimmunoprecipitation experiments using either proteins expressed by recombinant baculoviruses within infected insect cells (1, 17, 258) or proteins from HSV-1-infected cells (17, 104, 267, 268, 271). Further confirmation has come from the observed interaction between homologues of the HSV-1 UL15, UL28, and UL33 proteins in VZV (243-

245), HCMV (25, 226, 250), and PRV (76) demonstrating the level of conservation of these genes and implied importance during infection (54, 73).

Proper formation of the UL15/UL28/UL33 protein complex is essential for virus replication. Several studies have demonstrated that in cells infected with HSV-1 recombinant viruses encoding mutations that preclude the interaction of these proteins, replicated viral DNA is not cleaved or packaged into capsids, suggesting that the UL15/UL28/UL33 complex functions as the viral terminase (18, 104, 225, 267, 269). The most compelling evidence that the UL15/UL28 interaction is required for terminase activity came from a study examining a panel of recombinant viruses encoding linker-insertion or nonsense mutations within UL28 (104). One particular mutant contained a four amino acid insertion after residue 334 of UL28 that allowed terminase complex formation but precluded cleavage and packaging of viral DNA. Spontaneous revertant viruses were isolated that possessed a second-site mutation within UL15 that restored the ability of the virus to cleave and package DNA; providing direct genetic evidence of the interaction between UL15 and UL28, and demonstrating the importance of this interaction during virus replication. The interaction with UL28 has also been shown to stabilize UL33 from degradation (104, 267), while in reverse, UL33 appears to enhance the interaction between UL15 and UL28, increasing the number of properly formed complexes (104, 267, 269).

It is important to note that little is known concerning the subunit stoichiometry within the HSV-1 terminase complex. Complexes purified from HSV-1-infected cells were shown to migrate through a sucrose gradient to a position corresponding to a 1:1 heterodimeric complex of UL15 and UL28 (112). However, immunoprecipitation experiments have demonstrated that the UL15 protein can self-interact (1). It has also been shown that the amount of UL15 and UL28 bound to the surface of B-capsids was approximately one and two copies respectively, while A-

capsids contained less than one copy of UL28 and twelve copies of UL15 (16). Terminases of dsDNA bacteriophage are typically comprised of subunits with higher order stoichiometry (72) and the HCMV terminase appears to be composed of oligomeric subunits (197, 199, 226); therefore it seems likely that the HSV-1 terminase consists of multiple copies of each subunit, but this remains to be elucidated.

The results of coimmunoprecipitation and colocalization studies suggest that the complex of UL15, UL28 and UL33 proteins forms within the cytoplasm of the infected cell (268). Although it was initially thought that all three subunits could directly interact (17), the use of UL28 mutants has revealed that the UL15 and UL33 proteins interact indirectly via their direct interaction with the C-terminus of UL28 (104, 267). Specifically the C-terminal 44 amino acids of UL28 appear essential for the interaction with both UL15 and UL33 (104). Recent mutational analysis of UL33 has also suggested that residues 51-74 of UL33 mediate the interaction with UL28 (18), while residues within the second exon of UL15 may be required for the interaction with UL28 and possibly other UL15 subunits (1, 269).

Once formed, the viral terminase complex is thought to translocate to the infected cell nucleus (268). Initial studies using transiently expressed proteins indicated that a cytoplasmic interaction with the UL6 portal protein was required for nuclear import of terminase components (258). However, it was later shown within HSV-1-infected cells that UL15 encodes a canonical nuclear localization signal (NLS) (residues 183-189) that is essential for complex nuclear localization, and that mutation or deletion of the NLS resulted in the cytoplasmic localization of both UL15 and UL28 (268). Of note, the UL33 protein (~19 kDa) is smaller than the passive diffusion size limit (~60 kDa) of the nuclear pore complex and can therefore diffuse freely between the nucleus and cytoplasm, making the requirements for UL33 nuclear localization

difficult to elucidate. However, the coimmunoprecipitation of UL33 from cytoplasmic extracts of HSV-1-infected cells supports the interaction of UL33 before nuclear localization of the terminase (268).

Within the nucleus, the terminase is proposed to cleave and package replicated viral DNA into capsids and this has been indirectly supported by several studies examining the interaction between terminase subunits and the components of viral capsids (15, 16, 179, 194, 196, 204, 223, 263, 270, 274). A recent study identified key residues within the UL6 portal protein that mediate the interaction of the portal with UL15 and UL28, and demonstrated that these residues are essential for cleavage and packaging of viral DNA (270). This study also determined that deletion of these critical UL6 residues resulted in a reduced interaction between the UL15, UL28, and UL33 proteins and viral B-capsids (270). However, UL15, UL28, and UL33 are observed on capsids isolated from cells infected with a UL6 deletion mutant, suggesting that the terminase can associate with viral capsids independently of the portal (15, 16). Several studies have also indicated that the UL15 and UL28 proteins interact with procapsids and B-capsids, but these interactions are diminished with DNA-filled C-capsids (16, 204, 223, 274), and that these proteins are not observed to associate with the capsids of virions (126, 223). This is similar to the terminase proteins of dsDNA bacteriophage which display a transient association with unpackaged “proheads” (analogous to HSV-1 procapsids), further supporting the role of UL15 and UL28 during cleavage and packaging of replicated HSV-1 DNA. The UL33 protein has been shown to associate with each of the capsid forms and the deletion of key UL6 residues only slightly reduced the association of UL33 with B-capsids compared to the reduction seen in UL15 and UL28 protein levels (15, 179, 263, 270), suggesting that the role of UL33 during DNA encapsidation may differ from that of the UL15 and UL28 terminase subunits.

The lack of an HSV-1 *in vitro* packaging assay has limited the direct biochemical analysis of the terminase. However, genetic experiments utilizing temperature-sensitive mutants, or viruses bearing deletions or insertions, have identified several critical protein domains within the individual terminase subunits that are essential for complex formation and function (4, 6, 9, 10, 18, 33, 104, 114, 142, 173, 178, 225, 238, 268, 269, 271-273). These studies have also been aided greatly by the high degree of observed sequence conservation between the terminase proteins of the herpesviruses and phage (54, 67). UL15 is the most highly conserved gene within the family *Herpesviridae* and contains several protein domains that are proposed, or have been demonstrated, to be critical for the cleavage and packaging of viral DNA (52, 67, 104, 142, 178, 238, 268, 269, 271, 273). The UL15 protein is relatively unique within HSV-1 in that it is encoded by two exons and expressed from a spliced transcript (49). Exon I and the N-terminal region of exon II contain conserved amino acid motifs, such as Walker A and B boxes, that are typically found in proteins that metabolize ATP, therefore implicating UL15 as the "motor" for the translocation of DNA into capsids during packaging (52, 67, 249, 273). A recombinant HSV-1 encoding a point mutation of the conserved glycine residue (G263A) within the Walker A box was shown to be deficient in cleavage and packaging, and three additional viruses with point mutations within exon I displayed the same phenotype (178, 273). The UL15 protein in each of these mutants still retained the ability to localize to the nucleus and associate with capsids suggesting this region functions in cleavage and packaging (178). Further evidence implicating the importance of this region during cleavage and packaging includes: i) HCMV isolates resistant to an inhibitor of viral DNA cleavage possessed a single amino acid mutation within this region of the UL89 protein (UL15 homolog), and this amino acid is conserved in HSV-1 UL15 (238); and ii) a second-site mutation in UL15 that conferred the ability of a UL28

mutant virus to cleave and package DNA occurred in this region (104). Based mainly on studies examining the UL15 homolog in HCMV, UL89, exon II of UL15 is implicated to possess nuclease activity (142, 199). The UL89 protein has been shown to possess endonuclease activity that is enhanced by the interaction with UL56 (homolog of UL28) (199). Most recently, Nadal et al purified a soluble fragment of exon II of the HCMV UL89 protein and demonstrated that this fragment possessed nuclease activity in the presence of manganese (Mn^{2+}) ions (142). The crystal structure of the fragment was solved and identified three Mn^{2+} coordinating amino acids that are conserved within the HSV-1 UL15 protein. Recently, an interesting UL15 mutant virus was generated that encodes a deletion of amino acids 400-420, which are located in a position between the proposed ATPase and nuclease domains (271). Analysis of this virus revealed a slight defect in DNA cleavage, but DNA packaging efficiency was drastically reduced. Taken together, this suggests that the DNA translocation function of UL15 is separable from cleavage; two processes that have long been considered closely linked. This also may suggest that the terminase can cleave viral DNA in the absence of the portal protein.

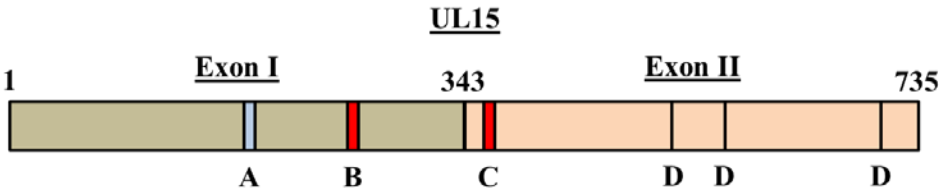

A) Nuclear localization signal: 183-PKKRAKV-189

B) Walker A box: 258-VPRRHGKT-265

C) Walker B box: 352-LLFVDE-357

D) Mn^{2+}-coordination: D509, E581, D707

Figure 9. Conserved amino acid domains within the UL15 protein.

The UL28 protein has long been implicated as the DNA-binding subunit of the terminase complex based on studies performed in HCMV (22). Strains of HCMV that were resistant to DNA cleavage inhibitors were found to encode a single amino acid mutation within a motif bearing similarity to a canonical metal-binding domain (114). Further analysis determined that this stretch of amino acids was conserved throughout the family *Herpesviridae*. The lone biochemical data regarding terminase activity was generated in a set of experiments examining the DNA-binding capability of transiently expressed UL28 protein purified from bacteria (5). The results demonstrated the interaction of UL28 with specific *pac1* sequences of the viral *a* sequence region. Specifically, UL28 only interacted with one strand of the *pac1* motif suggesting that during packaging viral DNA may adopt novel structures and extrude single-stranded regions that are recognized by UL28. Studies performed with the homolog of UL28 in HCMV, UL56, have also demonstrated an interaction with HCMV *pac1* sequences (21).

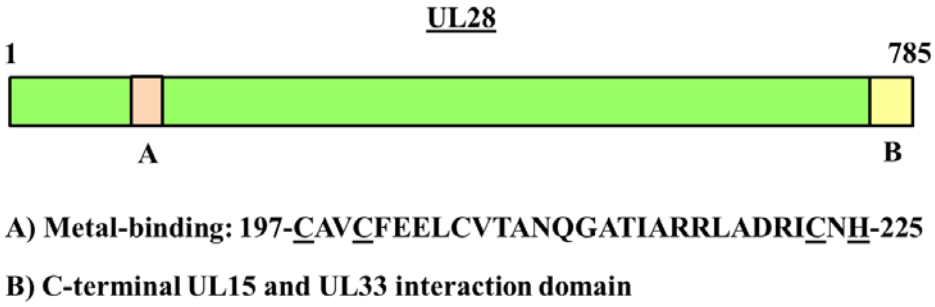

Figure 10. Conserved amino acid domains within the UL28 protein.

The role of UL33 in terminase complex formation and function is not well-elucidated and it is intriguing why HSV-1 would utilize a three subunit complex when most of the well-studied

dsDNA bacteriophages utilize two subunit complexes (32). However, numerous studies clearly indicate that the interaction between UL33 and UL28 is critical for proper terminase function (18, 104, 267, 269). Genetic experiments have identified two regions of UL33 that are essential for terminase function (18, 269). Viruses encoding temperature-sensitive or insertion mutations clustered near the center of the protein precluded the interaction with UL28, while mutations at the C-terminus allowed complex formation. However, all of the mutants were deficient in the cleavage and packaging of viral DNA suggesting that the C-terminus is critical for a specific function early in the encapsidation process. This is in contrast to a recent report indicating that UL33 interacts with the UL31/UL34 complex of the viral tegument and this interaction is highly conserved throughout the herpesviruses; suggesting a role for UL33 at later times during packaging (73). However, UL33 has been shown to associate with viral capsids independently of UL28 and UL15; therefore it is possible that UL33 performs numerous functions, with terminase-associated UL33 functioning in encapsidation, while capsid-associated UL33 molecules play a role during tegumentation and egress.

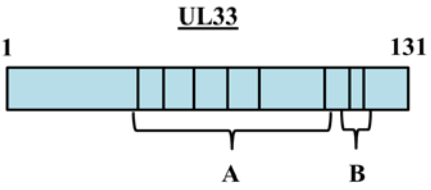

Mutation Region	Cleavage & Packaging	Complex Formation
A	-	-
B	-	+

Figure 11. UL33 protein domain mutations affecting terminase activity.

1.5.2 Model of terminase activity

Based upon empirical evidence and considering the DNA encapsidation process in dsDNA bacteriophage, the following is a model for HSV-1 terminase formation and function. During infection the UL15, UL28, and UL33 proteins are translated within the cytoplasm of the infected cell. An initial interaction occurs between the UL28 and UL33 proteins, protecting UL33 from degradation (104, 267). The UL15 protein then interacts with UL28, and this interaction is enhanced by UL33 (104, 267, 269). The assembled terminase complex of UL15, UL28, and UL33 localizes to replication centers within the nucleus via the NLS of UL15 (91, 268). The UL28 protein binds the replicated viral DNA concatemer and scans the DNA for specific sequences (5, 22). Upon encountering a *pac2* site in the correct orientation, the endonuclease activity of UL15 is triggered and cleaves the DNA within an upstream DR1 element (92, 142, 199, 241). This cleavage generates a free L-terminus for packaging that contains a truncated DR1 element containing a one nucleotide 3' overhang (139). The terminase, with bound viral DNA, docks at the UL6 portal of assembled procapsids in an orientation that positions UL15 in close proximity to the portal (16, 258, 263, 270). This interaction activates the DNA translocation function of UL15 which begins packaging the free L-terminus into the viral capsid in an ATP-dependent manner (51, 148, 273). DNA packaging also triggers protease activation and subsequent cleavage of the scaffold protein, resulting in procapsid maturation to the mature, polyhedral form (39, 90, 151, 170). DNA translocation continues from the L-component, through the junction, and into the S-component (148). As packaging nears completion, single-stranded regions within the *a* sequence of the S-component are extruded and the *pac1* motif is recognized by the UL28 subunit (5). This triggers the second DNA cleavage by UL15, producing an S-terminus containing a single *a* sequence followed by a one nucleotide extension

of the DR1 element (92, 139, 142, 199, 241). The freed genome end is packaged and the terminase components subsequently disassociate from the viral capsid, to possibly act in additional rounds of cleavage and packaging (16, 204, 223, 274).

1.6 SPECIFIC AIMS AND RATIONALE

The goal of this research is to examine the role of the UL28 protein in the formation and function of the HSV-1 terminase complex. The endogenous terminase will be isolated from HSV-1-infected cells via tandem affinity purification (TAP) of the UL28 protein to allow for physical characterization of the complex and biochemical analysis using *in vitro* functional assays. Genetic analysis of UL28 by deletion and site-directed mutagenesis will elucidate protein domains that are critical for biochemical activity, and the interaction with other terminase subunits and viral DNA. TAP of UL28 complexes from cells infected with HSV-1 UL28 domain mutants followed by *in vitro* functional assays will determine the effect of these mutations on terminase activity. Completion of this research will further elucidate the protein composition and function of the HSV-1 terminase complex.

1.6.1 Specific aim I: Purification and *in vitro* analysis of the HSV-1 terminase complex

Biochemical analysis of the HSV-1 terminase complex has been hampered, due largely to the inability to effectively purify the terminase proteins. In this study, HSV-1 recombinants were generated that express a TAP tag fused to the N-terminus of the UL28 protein. TAP of the UL28 protein from infected cells demonstrated the successful purification of the UL15 and UL33

terminase components. Isolated complexes were further characterized by sucrose gradient centrifugation and mass spectrometry, which identified several novel interacting proteins of viral and cellular origin. Biochemical analysis demonstrated the purified complexes possessed sequence-specific nuclease activity that is dependent upon the presence of Mn^{2+} ions.

1.6.2 Specific aim II: Analysis of UL28 protein domains critical in terminase complex assembly and function

The UL28 and UL15 terminase subunits contain amino acid domains that are conserved between the herpesviruses and phage, and have been shown to be important for the cleavage and packaging of viral DNA. Using a bacterial artificial chromosome system, a panel of HSV-1 recombinants were generated that encode site-specific mutations or deletions of the nuclease domain of UL15 or the metal-binding domain of UL28, and each virus expresses the NTAP-UL28 protein under CMV promoter control for purification purposes. For each recombinant virus, phenotypic analysis combined with the identification of terminase complex subunits isolated by TAP, revealed those protein domains required for terminase complex assembly, or implicated to function during viral DNA cleavage and packaging.

2.0 AFFINITY PURIFICATION OF THE HERPES SIMPLEX VIRUS TYPE I TERMINASE COMPLEX

2.1 ABSTRACT

During productive lytic infection, herpes simplex virus 1 (HSV-1) assembles empty procapsids that are subsequently packaged with the viral genome by means of a protein complex called the terminase. Several lines of genetic evidence indicate that the viral UL15, UL28, and UL33 proteins compose the terminase; however biochemical analysis of these proteins has been hampered by the inability to purify the intact complex. In this study, terminase complexes were isolated by tandem affinity purification (TAP) using recombinant viruses expressing either a full-length NTAP-UL28 fusion protein (vFH476) or a C-terminally truncated NTAP-UL28 fusion protein (vFH499). TAP of UL28 from vFH476-infected cells followed by silver staining, Western blotting, and mass spectrometry identified the UL15, UL28, and UL33 subunits, while TAP from vFH499-infected cells confirmed previous findings that the C-terminus of UL28 is required for the interaction of UL28 with both UL33 and UL15. Analysis of the purified complexes by sucrose density gradient ultracentrifugation revealed that the terminase exists as a heterotrimeric complex of the three proteins. Biochemical assays demonstrated that the complex possesses HSV-1 *a* sequence-specific nuclease activity in the presence of manganese (Mn^{2+}) ions. A proteomics approach was utilized to profile the host and viral protein interactions

following TAP from Vero cells infected with the vFH476, vFH499, or KOS viruses. There were 198 proteins isolated from the vFH476 and vFH499 TAP samples that were not observed with the KOS control. Of the 198 proteins, 22 were identified as HSV-1 proteins, while the remaining 176 were of host cell origin, and these were classified into groups based on cellular location or function. Several interactions were confirmed by Western blot analysis including the terminase interaction with DNA damage-binding protein 1 (DDB1), which is of particular interest as it has been shown to interact with proteins from numerous viruses. These results demonstrate that TAP is an effective method for the purification of the terminase complex, and will allow for further biochemical analysis of proposed complex functions such as ATPase and DNA-binding activity.

2.2 INTRODUCTION

A critical step during productive HSV-1 infection is the cleavage and packaging of replicated, concatemeric viral DNA into preformed capsids. This process has been shown to require the products of seven viral genes; UL6, UL15, UL17, UL25, UL28, UL32, and UL33 (3, 4, 6, 10, 33, 116, 117, 132, 165, 166, 173, 195, 198, 205, 206, 225, 256, 272). Many of these genes have been assigned putative functions based upon similarities between HSV-1 and double-stranded DNA (dsDNA) bacteriophage cleavage and packaging systems (32), with many of these assigned functions being supported by a growing body of genetic, biochemical, and microscopic evidence. The UL6 protein forms a dodecameric complex at one of the twelve capsid vertices and functions as a portal through which viral DNA can enter or exit the capsid (30, 35, 155, 235). The UL17 and UL25 proteins have recently been shown to form a heterodimeric complex termed

the capsid vertex-specific component that functions at each of the penton vertices to stabilize DNA-filled capsids (41, 232, 236). The UL32 protein is not well-characterized, but may play a role in localizing capsids to sites of DNA packaging (36, 116). The UL15, UL28, and UL33 proteins are thought to form the viral terminase complex, responsible for the initial cleavage of the replicated viral DNA concatemer, transportation of the DNA to the capsid portal, DNA translocation into the capsid via an ATP-dependent mechanism, and a final DNA cleavage once a complete viral genome has been packaged (46).

Although numerous dsDNA bacteriophage cleavage and packaging systems encode for terminase complexes consisting of one large and one small subunit, biochemical and genetic studies suggest that HSV-1 encodes a three subunit complex composed of the UL15, UL28, and UL33 gene products (1, 17, 32, 91, 104, 112, 179, 258, 267, 268, 271). UL15 is the most well-conserved gene among the herpesviruses and contains sequence similarity to the large terminase subunit, gp17, of bacteriophage T4 (52, 273). The UL15 protein possesses conserved Walker A and B sequences that are thought to encode for the proposed ATPase activity of the terminase complex, and these sequences have been shown to contain key residues required for the cleavage and packaging of viral DNA (52, 67, 178, 249, 273). The UL15 protein also contains a nuclear localization signal required for transport of interacting UL28 subunits to the infected cell nucleus, and once there, UL15 has been proposed to localize the terminase to sites of DNA replication and packaging (91, 268). Furthermore, a fragment of the UL15 homolog in human cytomegalovirus (HCMV), UL89, was shown to possess sequence-specific nuclease activity that was dependent on the presence of Mn^{2+} ions (142). The crystal structure of this UL89 protein fragment was resolved and revealed specific Mn^{2+} coordinating amino acids that are conserved among the herpesviruses. The UL28 protein has been shown to interact with specific HSV-1

DNA sequences that are required for cleavage and packaging of viral DNA (5). Furthermore, the UL28 homolog in HCMV, UL56, has also been shown to possess DNA-binding and nuclease activity that is specific for HCMV sequences required for cleavage and packaging of HCMV DNA (22). Interestingly, several small organic molecules have been described that inhibit HCMV replication by targeting the UL56 protein (83, 114, 238). These compounds have been shown to block the processing and encapsidation of viral DNA demonstrating the validity of targeting the cleavage and packaging complex for therapeutic intervention. The final terminase subunit, UL33, is the least well-characterized but may be required for correct assembly of the terminase complex, or may act to regulate the enzymatic activity of the other subunits during complex function (104, 267, 269).

Although a great deal of information has been obtained from genetic studies of the HSV-1 cleavage and packaging genes, these proteins have proven difficult to isolate for biochemical and structural studies. The goal of the following studies was to isolate a functional terminase complex from HSV-1-infected cells by affinity chromatography using a virus expressing a UL28-TAP fusion protein. The TAP procedure resulted in the isolation of soluble UL28-complexes containing the UL15 and UL33 proteins. Isolated complexes were characterized using genetic, biochemical, and proteomic approaches to determine the stoichiometry and composition of the HSV-1 terminase. We view these studies as a critical step in understanding how the terminase complex functions in the context of productive HSV-1 infection.

2.3 MATERIALS AND METHODS

2.3.1 Cells and Viruses

African green monkey kidney cells (Vero) were maintained in Dulbecco's modified Eagle's medium supplemented with 5% newborn calf serum, 100 U penicillin per ml, and 100 μg streptomycin per ml (growth medium). UL28-complementing (CV28) cells were maintained exactly as Vero cells but supplemented with 10% newborn calf serum (267). MRC-5 cells (ATCC, Manassas, VA) were cultured per ATCC instructions. The KOS strain of HSV-1 was used as the wild-type virus. The vNTAP-UL25 and vUL17-CTAP viruses were previously described (41, 232).

2.3.2 Construction of recombinant viruses

The NTAP-UL28 (vFH475) and CMV-NTAP-UL28 (vFH476) mutant viruses were generated by recombination of a KOS genome maintained within a bacterial artificial chromosome (BAC) (81). The KOS BAC clone was transferred to GS1783 bacteria (gift from G. Smith) and mutagenesis was performed using the two-step bacteriophage Red-mediated homologous recombination system (231), as previously described (42). The CMV-NTAP-UL28-741s (vFH499) mutant virus was generated by the same methods, but through recombination of a vFH476-BAC that was transformed into GS1783 bacteria. Primers and template plasmid DNA used to amplify the kanamycin resistance construct are listed in Table 5. Plasmids p-EP-TAP-in and p-EP-Kan-S were a kind gift from Dr. Paul Kinchington (University of Pittsburgh). The UL28 reverse primer (vFH475, vFH476) was designed in such a way that recombination resulted

in the loss of the first 3 nucleotides (start ATG) of the UL28 open reading frame (ORF). BAC DNA was transfected into Vero (vFH475, vFH476) or UL28-complementing CV28 cells (vFH499) and recombinant viruses were harvested from cell lysates and plaque purified on Vero (vFH475, vFH476) or UL28-complementing CV28 cells (vFH499). Insertion of the CMV promoter and/or TAP tag in recombinant UL28 viruses was confirmed by PCR amplification of purified viral DNA using the following primers that flank the UL28 ORF: 5' – GGATGACCCGTTTGGGGAGG – 3' and 5' – TTGTACGGGGCGATGTTCTCC – 3'. The 3,436 (vFH475), 4,044 (vFH476), and 4056 (vFH499) bp PCR products (vFH475 vFH476, respectively) were extracted from agarose gels and used for restriction fragment length polymorphism analysis using KpnI and sequencing analysis using the following primers: 5' – GAATAGAGCAGAAACGCA – 3' (CMV and/or TAP); 5' – TCTTCTTCGGTTTCGGGT – 3' (CMV and/or TAP); and 5' – ATACAAGGCTGTTAGAGA – 3' (vFH499-741s insertion).

Table 5. PCR primers for generation of recombinant viruses

Primer	Sequence[a]	Template	Recombinant Virus
UL28-NTAP Forward	CGGTCCACCGCATACTCCGGCCGCGGTACAGATCGGCGCCGC GAG ATGAAGCGACGATGGAAAAAG	p-EP-TAP-in	vFH475
UL28-CMV-NTAP Forward	CGGTCCACCGCATACTCCGGCCGCGGTACAGATCGGCGCCGC GAG CATTAGTTATTAATAGTAATC	p-EP-TAP-in	vFH476
UL28 Reverse	*TAACAACTTTTGACGGGCCACGGTGGGCTCGGACACCGGGGCGG C* GCCCAGCTTGCAGCCGCCGGA	p-EP-TAP-in	vFH475, vFH476
UL28-741s Forward	CCGCCCGGCGTATATCTCACGTACGAC **TCCGACTGTCCGCTGGTGGCCATCGTCGCGAGATCCTAG** TAGGGATAACAGGGTAATCGATTT	p-EP-Kan-S	vFH499
UL28-741s Reverse	*GCCGATACAGCCGTCGGGGGCGCTCTC* **CTAGGATCTCGCGACGATGGCCACCAGCGGACAGTCGGA** GCCAGTGTTACAACCAATTAACC	p-EP-Kan-S	vFH499

[a]Underlined sequences are complementary for the indicated plasmid template. Italicized, bold, and normal-type sequences are different UL28 sequences. Sequences in the same type within primer pairs are complementary.

2.3.3 TAP

The TAP protocol was performed by infecting 5 x 10^8 Vero cells with KOS, vFH476, or vFH499 virus at an MOI of 10 PFU/cell. The infection was allowed to proceed for 18 h at 37°C, after which the cells were harvested and pelleted via centrifugation at 5,000 rpm for 10 min at 4°C. All remaining steps were performed at 4°C. The cells were washed in a total volume of 50ml 1 x PBS, and the final cell pellet was resuspended in 24 ml of streptavidin binding buffer (SBB) (300 mM KCl, 40 mM Tris-HCl [pH 7.5], 2 mM EDTA, 0.1% NP-40 substitute, and 5 mM β-mercaptoethanol) containing protease inhibitors (Roche 1 697 498). The cells were lysed by sonication using a probe sonicator. The cell suspension was sonicated 4 times for 10 s each at an output of 6 W with chilling on ice between each sonication step. Benzonase (1,500 U; Novagen, 71205-3) was added to the samples and left at 4°C for 30 min. The extract was then clarified via centrifugation at 12,000 rpm in a Sorvall SS-34 rotor for 20 min at 4°C. The supernatant was transferred to a new tube, 1.5 ml of streptavidin resin (0.75 ml packed volume) (Pierce, 53117) was added, and the samples were rotated at 4°C for 2 h. The resin was pelleted by centrifugation at 3,500 rpm for 5 min, and the supernatant was removed. The resin was washed three times by being resuspended in 5 ml of SBB followed by centrifugation at 3,500 rpm for 5 min. Protein was eluted from the resin by adding 3 ml of streptavidin elution buffer (300 mM KCl, 40 mM Tris-HCl [pH 7.5], 2 mM EDTA, 0.1% NP-40 substitute, 5 mM β-mercaptoethanol, 2 mM D-biotin [Sigma, 47868]) containing Roche protease inhibitors, and the sample was rotated at 4°C for 30 min. The protein-resin mixture was spun down at 7,000 rpm in a microcentrifuge for 2 min, and the supernatant was collected as the streptavidin eluate. Twelve milliliters of calmodulin binding buffer (CBB) (150 mM NaCl, 10 mM Tris-HCl [pH 7.5], 1 mM magnesium

acetate, 1 mM imidazole, 2 mM $CaCl_2$, 0.1% NP-40 substitute, 10 mM β-mercaptoethanol) containing Roche protease inhibitors was added to the streptavidin eluate. An additional 11.25 μl of 1 M $CaCl_2$ was added to the mixture along with 1.2 ml of calmodulin resin (0.6 ml packed volume) (Agilent Technologies, 214303-52), and samples were rotated at 4°C for 2 h. The resin was pelleted by centrifugation at 3,500 rpm for 5 min, and the supernatant was removed. The resin was washed three times by resuspension in 5 ml of CBB followed by centrifugation at 3,500 rpm for 5 min. Protein was eluted from the resin by adding 3 ml of calmodulin elution buffer (150 mM NaCl, 10 mM Tris-HCl [pH 7.5], 1 mM magnesium acetate, 1 mM imidazole, 0.1% NP-40 substitute, 10 mM β-mercaptoethanol, 2 mM EGTA), and the sample was rotated at 4°C for 30 min. The protein-resin mixture was spun down at 7,000 rpm in a microcentrifuge for 2 min, and the supernatant was collected as the final (calmodulin) eluate.

2.3.4 Sucrose gradient ultracentrifugation

UL28 protein complexes were purified from vFH476-infected Vero cells by a partial TAP procedure whereby proteins were collected after elution from the streptavidin resin. The eluted protein sample was concentrated 10-fold by column centrifugation (Pierce, 89884A). Concentrated proteins were separated by centrifugation on 2.5 to 20% sucrose (in 1X PBS) gradients (SW50.1 rotor at 35,000 rpm for 18 hr). Fractions were collected from the bottom to the top of the gradient using a Beckman fraction recovery system (Beckman, 34890). A total of 33 fractions (130 μL each) were collected and protein was precipitated by adding an equal volume of 16% trichloroacetic acid. Proteins were pelleted by centrifugation at 13,000 rpm for 10 min and pellets were resuspended in 30 μL 2x PAGE loading buffer (Invitrogen)

supplemented with 0.4 M Tris-base. Odd numbered protein fractions were resolved on a 4 to 12% SDS-polyacrylamide gel and visualized by Western blot analysis using anti-UL28, UL15, or UL33 antibodies. Molecular weight control proteins, aldolase and BSA (GE Healthcare Life Sciences), were processed in the same manner, but were visualized by staining with Imperial protein stain (Thermo Scientific, 24615).

2.3.5 Mass spectrometry

TAP-purified proteins from vFH476-infected cells were resolved on a 4 to 12% SDS-polyacrylamide gel and stained with either Imperial protein stain or SYPRO Ruby protein gel stain (Invitrogen, S-12000). Stained gels were sent to Dr. Lisa Jones (Washington University in St. Louis, St. Louis, MO) who performed the remaining mass spectrometry analysis by the following methods. The in-gel digest was performed as previously described (154). Briefly, gel plugs were washed with acetonitrile (Sigma, St. Louis, MO) in a 96 well plate and rocked for 10 min twice. The samples were dried in a speed vac for 10 minutes. A 0.2 µg/µl stock of trypsin (Sigma, St. Louis, MO) was made up in 100 µL of 1 mM triethyl ammoniumbicarbonate pH 8.2. Trypsin, 5 µL, was added to each dried gel plug. The plate was incubated at 58 °C for 30 min. After digestion, 1 µL of 1% acetonitrile with 1% formic acid was added to each gel plug. The plate was incubated at 37 °C for 1 hr. The solution from each well plate was transferred to autosampler vials and centrifuged at 10,000 rpm for 40 min. To reduce keratin contamination, the in-gel digest was performed in a laminar flow hood. Digested samples were loaded onto a 100 µm x 2 cm Acclaim PepMap100 C18 nano trap column (5 µm, 100 Å) (Thermo Scientific, Pittsburgh, PA) with an Ultimate 3000 liquid chromatograph (Thermo Scientific, Pittsburgh, PA) at 8 µL/min. The peptides were separated on a silica capillary column that was custom-packed

with C18 reverse phase material (Magic, 0.075 mm x 150 mm, 5μu, 120 Å, Michrom Bioresources, Inc., Auburn, CA). The gradient was pumped at 260 nL/min from 0-80% solvent B (20% water, 80% acetonitrile, 0.1% formic acid) for 60 min, then to 80% solvent B for 7 min, and re-equilibrated to solvent A (water, 0.1% formic acid) for 10 min. The mass spectrometry was performed on an LTQ-FT-ICR Ultra (Thermo-Fisher, Pittsburgh, PA). The mass spectrometer was operated in data-dependent acquisition mode controlled by the Xcalbur 2.0.7 software. Peptide mass spectra were acquired from an m/z range of 350-2000 at high mass resolving power. The top six most abundant multiply charged ions with minimum signal intensity at 800 counts were subjected to collision-induced dissociation (CID) in the linear ion trap. Charge state rejection of +1 ions was employed. Precursor activation was performed with an isolation width of 2 Da and an activation time of 30 ms. The raw data were aligned and converted into a centroided peaklist file by Progenesis LC-MS (Nonlinear Dynamics, Durham, NC) (167). The files were search using MASCOT 2.2.06 (Matrix Science, London, U.K.). The enzyme specificity was set to trypsin with 2 missed cleavages. The mass tolerance for precursor and fragment ions was 12 ppm and 0.6 Da, respectively. Oxidation of methionine was specified in Mascot as a variable modification. The data was searched against the NCBI 20120108 database. A threshold of 5% probability that protein identification is incorrect was implemented. Scaffold_3_00_08 (Proteome Software Inc., Portland, OR) was used to validate MS/MS based peptide and protein identifications. Peptide identifications were accepted if they could be established at greater than 95.0% probability as specified by the Peptide Prophet algorithm (109). Protein identifications were accepted if they could be established at greater than 99.0% probability and contained at least 2 identified peptides. Protein probabilities were assigned by the Protein Prophet algorithm (146).

The TAP samples (KOS, vFH476, and vFH499) eluted from the calmodulin resin were sent to MS Bioworks (Ann Arbor, MI; www.msbioworks.com) and TCA precipitated according to the protocol from Rahim et.al (105). The pellets were resuspended in 50µL of 1X LDS PAGE loading buffer and 25µL per sample was separated approximately1.5cm on a 10% Bis-Tris Novex mini-gel (Invitrogen) using the MES buffer system. The gel was stained with Coomassie blue and excised into ten equally sized segments. Gel segments were processed using a robot (ProGest, DigiLab) with the following protocol. The gel segments were washed with 25mM ammonium bicarbonate followed by acetonitrile and reduced with 10mM dithiothreitol at 60°C followed by alkylation with 50mM iodoacetamide at room temperature. The samples were then digested with trypsin (Promega) at 37°C for 4h, quenched with formic acid and the supernatant was analyzed directly without further processing. Mass spectrometry of each gel digest was analyzed by nano LC/MS/MS with a Waters NanoAcquity HPLC system interfaced to a ThermoFisher Orbitrap Velos Pro. Peptides were loaded on a trapping column and eluted over a 75µm analytical column at 350nL/min; both columns were packed with Jupiter Proteo resin (Phenomenex). The mass spectrometer was operated in data-dependent mode, with MS performed in the Orbitrap at 60,000 FWHM resolution and MS/MS performed in the Velos. The fifteen most abundant ions were selected for MS/MS. The data were analyzed and searched against both Uniprot *Macaca mulatta* + Uniprot *HHV1 Strain* using Mascot search engines. Mascot DAT files were parsed into the Scaffold software for validation, filtering, and to create a nonredundant list per sample. Data were filtered using a minimum protein value of 90%, a minimum peptide value of 50% (Prophet scores) and requiring at least two unique peptides per protein.

2.3.6 Western blotting

Protein samples were separated on a 4 to 12% SDS-polyacrylamide gel, and transferred to nitrocellulose. The nitrocellulose was washed twice in Tris-buffered saline (TBS) and incubated overnight in Rockland Near Infra-Red blocking buffer (Rockland Immunochemicals, MB-070-003). Primary antibodies used (dilution in parenthesis) include: UL28 rabbit polyclonal antibody UL28-GST (1:1000) (17), VP5 rabbit polyclonal antibody NC1 (1:5000) (47), rabbit monoclonal Anti-Calmodulin Binding Protein Epitope Tag Antibody, clone C16T (1:3000) (Millipore, 05-932), UL15 rabbit polyclonal antibody UL15-GST(1-104) (1:1000) (196), UL33 rabbit polyclonal antibody UL33-GST (1:500) (179), rabbit polyclonal DDB1 Antibody (1:5000) (Bethyl Laboratories, Inc., A300-462A), and rabbit monoclonal AIF Antibody (1:2500) (Abgent, AJ1021a). The blocked nitrocellulose was reacted with the diluted antibodies for 2 h at room temperature, washed five times in TBS with 0.5% Tween 20, and incubated with IRDye 800-conjugated goat anti-rabbit secondary antibody (Rockland Immunochemicals) diluted 1:15,000 in Rockland Near Infra-Red blocking buffer with 0.1% Tween 20. The blots were washed and scanned using an Odyssey system (Li-Cor, Lincoln, NE). Integrated intensity values were obtained using Odyssey software, Version 3.0 (Li-Cor, Lincoln, NE).

2.3.7 Nuclease assays

Assays were performed essentially as described by Nadal et al. (142) with the following modifications. Protein complexes purified by TAP were incubated in a reaction mixture containing 30mM Tris-HCl (pH8.0), 50mM NaCl, and linearized (HindIII digested) plasmid DNA at 37^{o}C for 18 hr. Metal ion requirement was examined by the addition of $CaCl_2$, $MgCl_2$,

or $MnCl_2$ to the reaction mixture (3mM final concentration). Reactions were stopped by the addition of EDTA (pH 8.0) to a final concentration of 30mM. Samples were resolved on a 1% agarose/1X TAE gel containing 1ug/mL ethidium bromide. The gel was viewed and photographed over UV-light.

2.4 RESULTS

Existing evidence indicates that the HSV-1 terminase consists of a heterotrimeric complex of the proteins encoded by the HSV-1 UL15, UL28, and UL33 genes (46). In this study, we used tandem affinity purification (TAP) to isolate the terminase complex from infected cells. Biochemical studies were performed to confirm the protein composition and determine the stoichiometry of the complex, and to measure the associated nuclease activity. Mass spectrometry was utilized to identify viral and cellular proteins that associate with the complex during infection.

2.4.1 Characterization of NTAP-UL28 virus

Previous studies have shown that the amino terminus of UL28 is not essential for virus growth and can tolerate the insertion of foreign epitopes (104). Therefore, the TAP tag was inserted at the amino terminus of UL28. The 78 amino acid TAP tag used for these studies has been previously described (232), and consists of a streptavidin-binding peptide and a calmodulin-binding peptide. The TAP-tag was inserted at the N-terminus of the UL28 open reading frame

through manipulation of an HSV-1 (KOS) genome maintained within a recombinant bacterial artificial chromosome (BAC) (Figure 12).

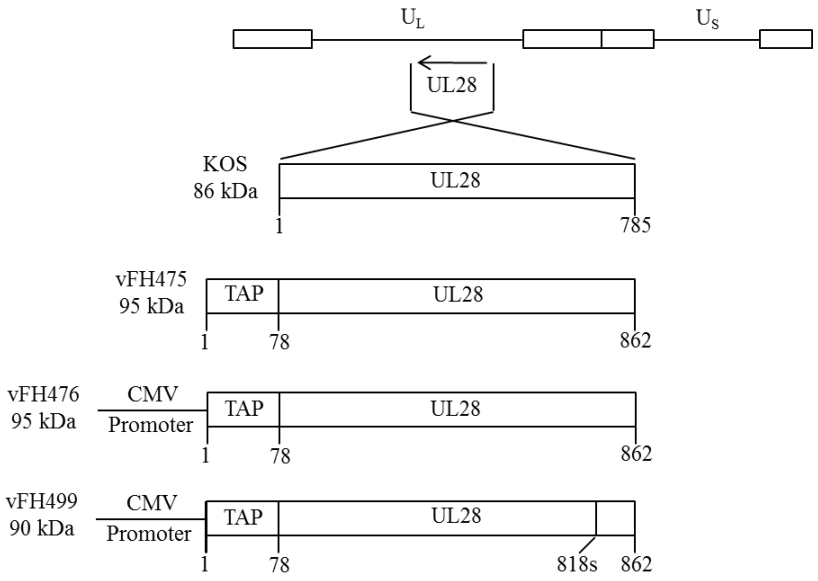

Figure 12. Recombinant UL28 virus constructs. The HSV-1 genome is shown at the top with the long and short unique regions represented as U_L and U_S, respectively. The UL28 open reading frame from wild-type KOS or each recombinant virus is expanded below, with virus names and protein sizes indicated to the left of each construct. Amino acid numbers below each construct indicate protein length. The vFH499 virus contains a nonsense mutation of amino acid 818.

The BAC was transfected into Vero cells and the recovered virus, vFH475, was plaque purified on Vero cells. Two additional HSV-1 UL28 recombinant viruses, vFH476 and vFH499, were generated in the same manner. vFH476 expresses an NTAP-UL28 gene under the transcriptional control of the cytomegalovirus (CMV) immediate early promoter and vFH499 expresses a C-terminally truncated NTAP-UL28 protein under CMV promoter control (Figure 12). The truncation in vFH499 is the result of an insertion of a linker sequence containing an in-frame stop codon after amino acid 741 of UL28 and this truncation has been previously shown to preclude the interaction of both the UL15 and UL33 proteins with UL28 (104).

The recovered viruses were plaque purified on Vero (vFH475 and vFH476) or UL28-complementing CV28 (vFH499) cells and virus stocks were prepared and titrated. The vFH475 and vFH476 viruses yielded similar titers on Vero and CV28 cells while the vFH499 virus, which expresses a nonfunctional UL28 protein, formed plaques only on CV28 cells (Table 6).

Table 6. Viral stock titers: NTAP-UL28 fusion mutants

Virus	Plating efficiency (PFU/mL) in:	
	Vero cells	CV-28 cells
KOS	5.9×10^9	9.8×10^8
vFH475	3.1×10^9	3.8×10^8
vFH476	2.8×10^{10}	2.1×10^9
vFH499	< 1000	2.9×10^9

Intracellular replication of each recombinant virus was compared to wild-type KOS virus by establishing single-step growth curves in Vero and CV28 cells. Cells were infected with each virus at an MOI of 1, harvested at 0, 2, 4, 7, 10, 22, and 30 h postinfection (hpi), and assayed for infectious virus by plaque assay on CV28 cells (Figure 13). When grown on Vero or CV28 cells the vFH475 and vFH476 virus titers were reduced (1- to 2-logs) compared to KOS. The vFH499 virus failed to produce virus on Vero cells, but grew to near wild-type levels on CV28 cells. Taken together, these results demonstrate that the vFH475 and vFH476 viruses grow on noncomplementing cells, but addition of the fusion protein and/or expression from the CMV promoter reduces the overall virus yield.

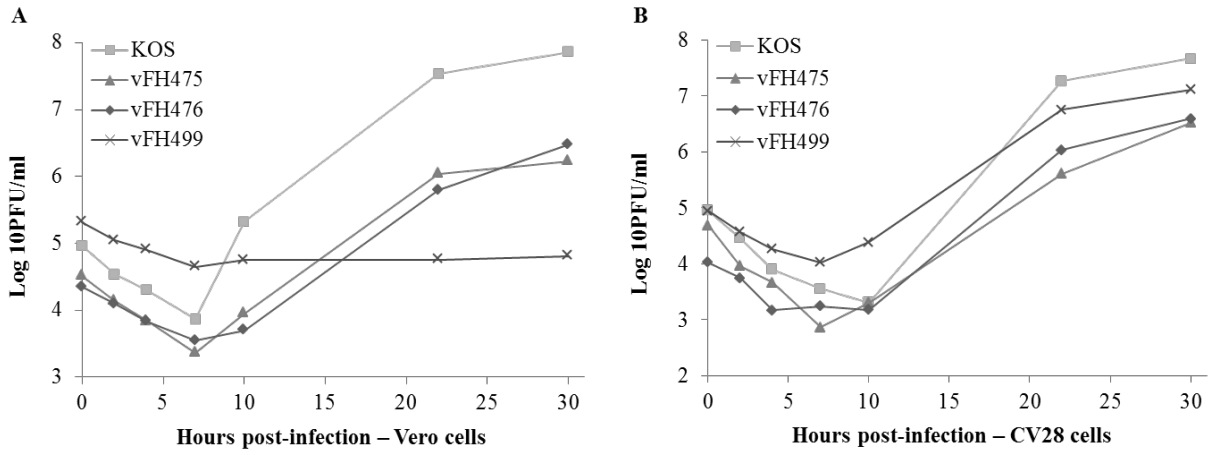

Figure 13. Recombinant NTAP-UL28 virus single-step growth curves Vero (A) or CV28 (B) cells were infected with the indicated HSV-1 recombinant viruses or with wild-type (KOS) virus at an MOI of 1 at 4°C for 1 h and incubated at 37°C. The cultures were harvested at the indicated times post-infection, freeze-thawed, and the virus yield at each time point was determined by plaque titer on CV28 cells.

NTAP-UL28 protein expression was examined for vFH475, vFH476, and vFH499 by Western blotting and compared to UL28 protein expression from the wild-type KOS virus. Infected Vero cell lysates were isolated at 18 hpi and probed with a UL28 antibody (Figure 14). The UL28 protein expressed by KOS resolved in SDS-PAGE with an apparent molecular mass of 86 kDa, and each recombinant virus expressed a UL28 protein with mobility corresponding to the expected molecular weight. NTAP-UL28 proteins expressed by vFH475 and vFH476 exhibited slightly lower mobility compared to KOS, corresponding to the additional 78 amino acids (approximately 8.6 kDa) of the TAP-tag, while the NTAP-UL28 protein expressed from vFH499 was slightly smaller than from vFH475 and vFH476 due to the truncation of 44 amino acids from the UL28 C-terminus.

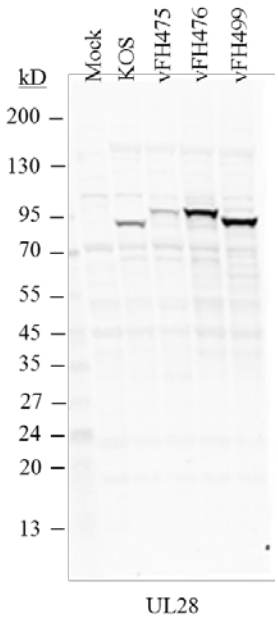

Figure 14. Recombinant NTAP-UL28 fusion protein expression. Vero cells were infected with wild-type (KOS) virus or the indicated HSV-1 recombinant viruses at an MOI of 10. At 18 h post-infection cell lysates were harvested, resolved by SDS-PAGE, and Western blots were probed with a UL28 antibody.

Total cell extracts from KOS-, vFH475-, vFH476-, and vFH499-infected Vero cells were prepared at various times postinfection, and expression of the UL28 gene product was analyzed by Western blot analysis (Figure 15). In KOS-infected Vero cells, the 86 kDa UL28 protein was first detected at 8 hpi, and the intensity of this band showed a moderate increase at later times postinfection. The recombinant viruses expressing the 95 kDa (vFH475 and vFH476) and 90 kDa (vFH499) NTAP-UL28 fusion proteins, showed a similar pattern of expression as the KOS UL28 protein. However, expression of the NTAP-UL28 gene from the CMV promoter (vFH476 and vFH499) resulted in increased levels of the UL28 fusion protein compared to KOS and vFH475. The blots were stripped and probed for the major capsid protein VP5, demonstrating that similar amounts of cell extracts were loaded in each lane. These results demonstrate that

placing the NTAP-UL28 fusion under CMV promoter control resulted in an increase in UL28 protein levels without altering the kinetics of expression. Since the goal of these studies was to isolate and characterize the HSV-1 terminase complex via affinity purification of the NTAP-UL28 protein, the recombinant viruses expressing NTAP-UL28 under CMV promoter control were utilized for the remainder of these studies.

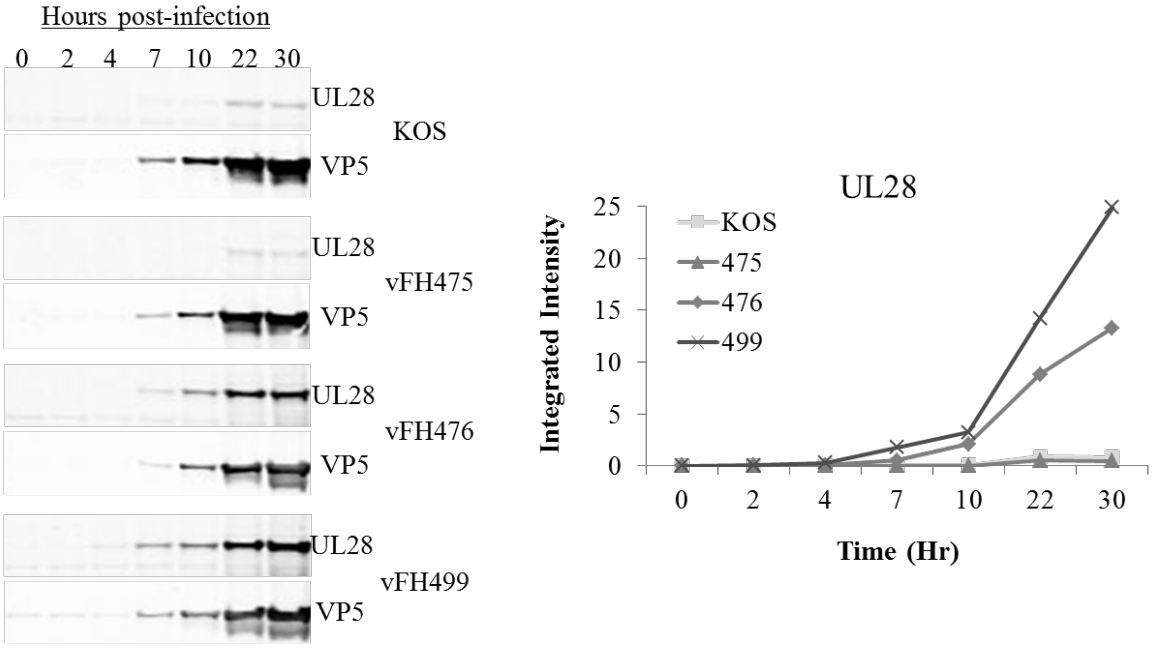

Figure 15. Recombinant NTAP-UL28 fusion protein expression time course. (A) Vero cells were infected with the indicated HSV-1 recombinant viruses or with wild-type (KOS) virus at an MOI of 1 at 4°C for 1 h and incubated at 37°C. Infected cell lysates were harvested at the indicated times post-infection, resolved by SDS-PAGE, and Western blots were probed with UL28 and VP5 antibodies. VP5 is the major capsid protein and serves to show even loading between samples. (B) Integrated intensity values were obtained for each UL28 band in (A) using Odyssey software, Version 3.0 (Li-Cor, Lincoln, NE) and plotted versus time.

2.4.2 Tandem affinity purification of NTAP-UL28 protein complexes

Tandem affinity purification is a dual purification procedure that allows for efficient isolation of protein complexes under native conditions (183). The TAP procedure was utilized to isolate the putative HSV-1 terminase complex of UL15, UL28, and UL33 from infected cells via the NTAP-UL28 fusion protein. Vero cells were infected with NTAP-UL28 viruses or KOS at an MOI of 10 and cell extracts were harvested at 18 hpi and applied to the TAP procedure (Figure 16). The TAP tag utilized in these studies encodes a calmodulin-binding domain and a streptavidin-binding domain (Stratagene-Interplay). Infected cell extracts were incubated with streptavidin resin and interacting complexes were eluted with biotin, then incubated with calmodulin resin in the presence of calcium, and eluted with EGTA. Silver stain of the final calmodulin-eluted samples revealed a major band at approximately 95 kDa in the vFH476 lane, corresponding to the full-length NTAP-UL28 fusion protein, and a band at 90 kDa in the vFH499 lane which corresponds to the truncated NTAP-UL28 protein (Figure 16A). Bands observed in the KOS lane represent background proteins that interact nonspecifically throughout the TAP procedure. The additional bands in the vFH476 and vFH499 lanes represent proteins that copurify with the tagged complex and were identified by Western blot analysis (Figure 16B). The putative terminase subunits, UL15 and UL33, were observed in complexes containing the full-length UL28 protein, but as expected, not from complexes containing the UL28-741s truncation mutant. Note that both the UL15 and UL33 proteins were also readily observed by silver stain from vFH476-infected cells. Blots for UL28 and the calmodulin-binding peptide confirmed each major band observed by silver stain contained the NTAP-UL28 protein in both the vFH476 and vFH499 lanes and additional bands at approximately 63, 50, and 43 kDa were observed that may represent cleavage or degradation products of the UL28 protein. In summary,

these results indicate that TAP of the UL28 protein is an effective method for the efficient isolation of the putative terminase complex of UL28, UL15, and UL33.

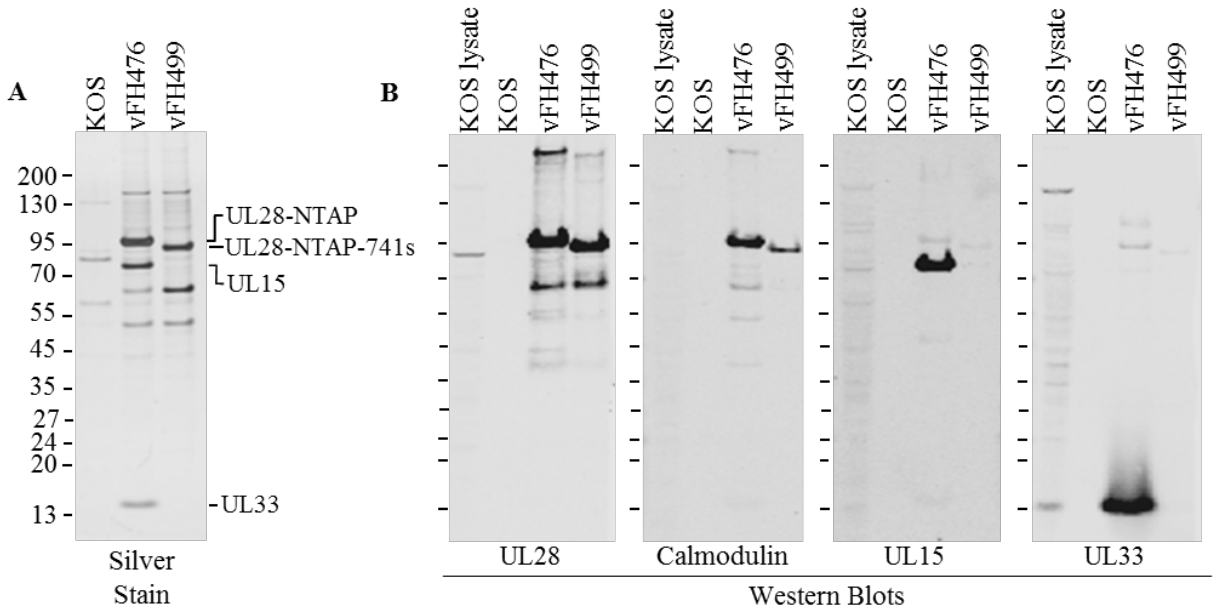

Figure 16. TAP of NTAP-UL28 fusion proteins. Vero cells were infected with the indicated HSV-1 recombinant viruses or with wild-type (KOS) virus. (A) After TAP, proteins eluted from the calmodulin column were resolved by SDS-PAGE and identified by silver staining. (B) Immunoblots (antibodies listed below each blot) demonstrating the presence of each TAP-tagged protein. Protein standards (kDa) are shown to the left of each gel or blot.

2.4.3 Oligomeric state of TAP-purified terminase components

The oligomeric state of TAP-purified terminase components was examined by sucrose density gradient ultracentrifugation (Figure 17). A partial TAP procedure was performed where UL28 complexes were isolated from vFH476-infected cells using only the initial streptavidin-binding and elution steps. Purified proteins were separated on 2.5-20% sucrose gradients, and fractions were collected from the bottom to the top of the gradient. A total of 33 fractions were collected

and analyzed by SDS-PAGE and Western blotting for the UL15, UL28 and UL33 proteins (Figure 17B). Molecular weight control proteins, aldolase and BSA (158 and 66 kDa respectively), were subjected to identical centrifugation and fractionation conditions and their relative positions in each gradient were determined by SDS-PAGE and Coomassie staining (data not shown). Immunoblots were analyzed by densitometry and the values obtained for each fraction were plotted onto the same graph, revealing three distinct peaks in intensity: i) the UL15, UL28, and UL33 proteins in fraction 11, ii) the UL28 and UL33 proteins in fraction 17, and iii) the UL33 protein alone in fraction 27 (Figure 17A). In fraction 11, a protein complex composed of the UL15, UL28, and UL33 proteins in a 1:1:1 ratio would be expected to possess a molecular mass of approximately 190 kDa, while in fraction 17 a 1:1 complex of UL28 and UL33 would be approximately 109 kDa. The proposed size of each complex is consistent with the relative migration of the molecular weight standards. The observation of the UL33 protein alone in fraction 27 may suggest that this protein possesses a weaker affinity for UL28 and readily dissociates from the complex. Taken together, sucrose gradient centrifugation of UL28 complexes purified by TAP from vFH476-infected cells revealed a complex composed of the UL15, UL28 and UL33 proteins.

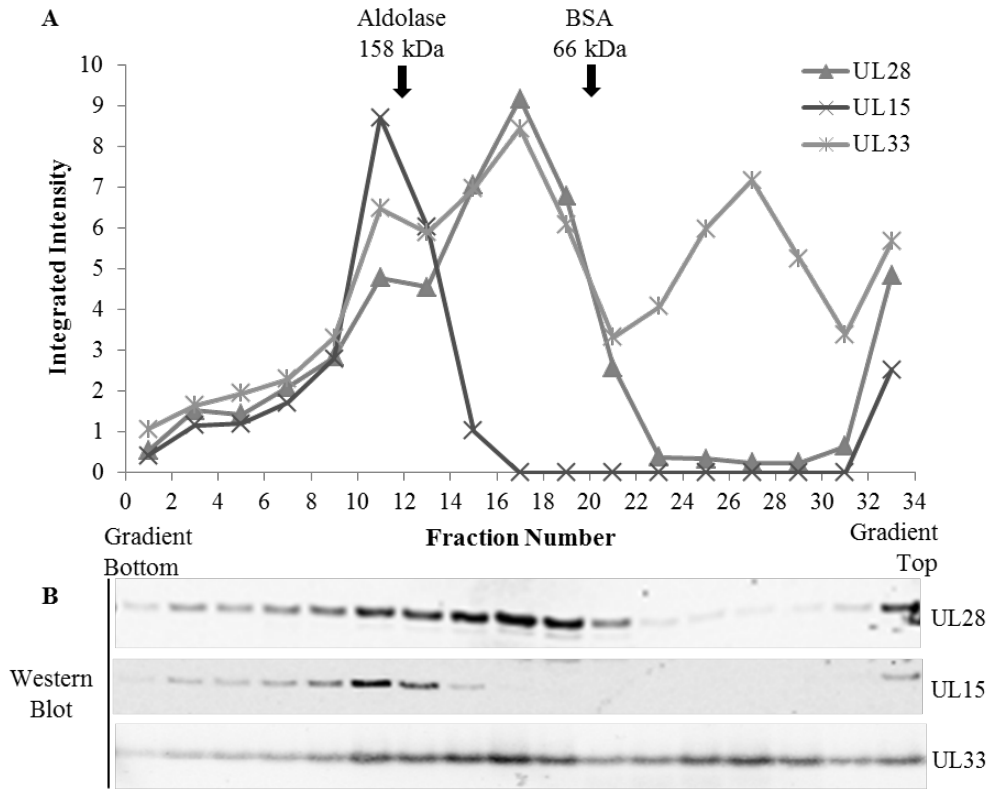

Figure 17. Sedimentation velocity analysis of TAP-purified UL28 complexes. Complexes from vFH476-infected Vero cells were purified through the initial streptavidin column, layered onto a 2.5-20% sucrose gradient, and centrifuged at 35K RPM at 4°C for 18 hours. The gradient was fractionated and individual fractions were resolved by SDS-PAGE, followed by immunoblotting (antibodies listed beside each blot) (B) and densitometry (A). Integrated intensity values (A) were obtained for each band using Odyssey software, Version 3.0 (Li-Cor, Lincoln, NE). Control proteins, aldolase and BSA, were subjected to identical centrifugation and fractionation conditions and their relative positions in each gradient , indicated in (A), were determined by SDS-PAGE and staining (data not shown).

2.4.4 Mass spectrometry analysis of UL28 complexes

Numerous protein bands were observed that copurify with UL28 complexes by TAP (Figure 16). One goal of this study was to characterize the viral (and possibly cellular) proteins that participate in terminase complex assembly and function during the course of infection. In order to identify those proteins, TAP-purified UL28 complexes were resolved by SDS-PAGE, stained,

and bands were analyzed by LC/MS/MS by two distinct approaches, as described in Materials and Methods.

In the first approach, specific protein bands of particular interest were isolated and examined. UL28 complexes were purified from vFH476-infected Vero cells or MRC-5 cells, a human epithelial lung cell line. The MRC-5 cell line was utilized to examine terminase subunits isolated from a physiologically relevant human cell line. The purified protein complexes were resolved by SDS-PAGE, stained, and bands corresponding to the NTAP-UL28, UL15, and UL33 proteins were isolated and confirmed by LC/MS/MS (Figure 18, Table 7). Also of particular interest were those bands corresponding to sizes of approximately 150, 63, and 50 kDa (unknowns 1-3 respectively) which were also observed as predominant bands by silver staining in Figure 16. In both cell types, LC/MS/MS analysis determined unknown 1 to be the VP5 major capsid protein while unknowns 2 and 3 consisted of peptides from UL28. Due to the interaction between the terminase and capsid during the encapsidation process (15, 16, 204, 274), it is not surprising that some VP5 copurifies with UL28 during TAP. However, it is interesting that unknowns 2 and 3 consisted mainly of peptides from UL28, and this result may suggest that the UL28 protein is cleaved during encapsidation. However whether these fragments represent degraded proteins or specific cleavages that play a vital function during encapsidation remains to be elucidated.

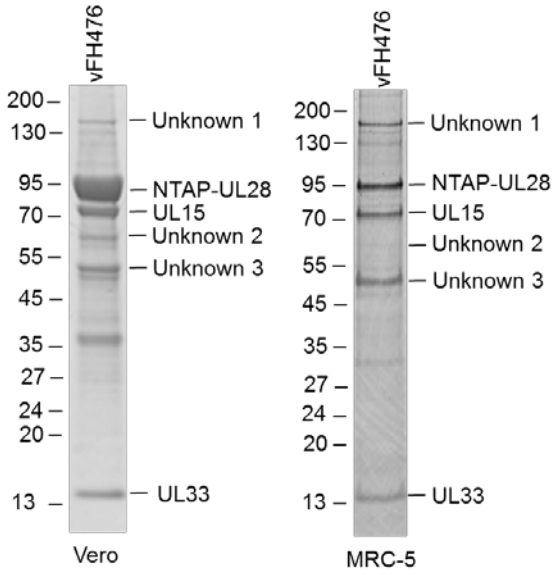

Figure 18. NTAP-UL28 fusion complexes isolated from primate and human cell lines. Vero or MRC-5 cells were infected with vFH476 and at 18 hpi, UL28 complexes were purified by TAP. Isolated complexes were resolved by SDS-PAGE and stained using either Imperial stain (Vero) or SYPRO Ruby stain (MRC-5).

Table 7. Mass spectrometry confirmation and analysis of specific interacting proteins

Band	Protein	MW[a]	No. of unique peptides	% coverage
Vero				
NTAP-UL28	UL28	95	7	17
UL15	UL15	81	16	44
UL33	UL33	15	9	82
Unknown 1	UL19	149	3	3.6
Unknown 2	UL28	86	8	11.2
Unknown 3	UL28	86	21	30.7
MRC-5				
NTAP-UL28	UL28	95	31	37
UL15	UL15	81	61	76
UL33	UL33	15	4	35
Unknown 1	UL19	149	45	40
Unknown 2	UL28	86	4	7
Unknown 3	UL28	86	29	36

[a]MW, (kDa)

A second LC/MS/MS analysis consisted of purifying UL28 complexes from Vero cells infected with vFH476, vFH499, or KOS viruses. The isolated proteins were resolved by SDS-PAGE, stained, and the entire lane, containing all isolated proteins, was analyzed by LC/MS/MS for each sample. This approach, although less specific, was more comprehensive in that comparison of the identified proteins between each virus allowed for the elimination of background proteins (KOS vs. vFH476 and vFH499) and the identification of proteins requiring the C-terminal 44 amino acids of UL28 for interaction (vFH476 vs. vFH499). A total of 888 *Macaca mulatta* plus *HHV1 Strain 17* proteins were detected (across all three samples). The criteria used to determine if a protein specifically interacted with NTAP-UL28 proteins were: i) the protein had at least 5 spectral counts in the vFH476 or vFH499 samples; ii) the protein was

not detected in the control KOS sample; or iii) the protein was detected with a 4-fold or more increase based on dividing the spectral count values. Based on these criteria, it was found that 198 proteins were unique or four-fold higher in both the vFH476 and vFH499 samples compared to the KOS control. Of the 198 proteins, 22 were identified as HSV-1 proteins (Table 8 and Appendix A, Table 12), while the remaining 176 were of host cell origin (Table 9 and Appendix A, Table 13).

Table 8. HSV-1 interacting proteins

Protein group[a]	Protein	MW[b]	No. of unique peptides			% Coverage			Spectral counts		
			476	499	KOS	476	499	KOS	476	499	KOS
Capsid/Packaging											
UL15	Terminase	81	82	31	6	97	50	6.4	1714	69	7
UL19	VP5	149	84	84	52	76	77	50	623	807	120
UL28	Terminase	86	110	89	25	98	89	27	3499	2072	138
UL33	Terminase	14	17	-	-	78	-	-	70	-	-
Tegument											
RS1	ICP4	133	19	16	-	17	14	-	37	29	-
UL36	ICP1/2	336	117	123	21	44	47	8.2	283	342	23
UL50	dUTPase	39	16	10	7	37	18	13	42	14	7
Envelope											
UL44	gC	55	11	11	-	32	31	-	70	72	-
UL1	gL	25	13	14	3	41	45	13	34	37	4

[a]Only proteins meeting the following criteria are shown: i) ≥ 30 spectral counts in the vFH476 or vFH499 samples; ii) no spectral counts in the KOS sample; or iii) 5-fold or higher spectral counts in vFH476 versus KOS. See Appendix A, Table 12 for the complete list of proteins.

[b]MW, (kDa)

Examination of the identified viral proteins further confirmed that the UL15, UL28 and UL33 proteins were purified by TAP from cells infected with the full-length NTAP-UL28 fusion (vFH476) (Table 8). Interestingly, peptides identified as UL15 were associated with complexes isolated using the UL28 C-terminal truncation mutant, vFH499. This may suggest that the UL15

protein possesses additional UL28 interaction domains, or is indirectly associating with UL28 through another protein such as VP5. On the other hand, the UL33 protein was not copurified with vFH499 further confirming that UL33 requires the C-terminus of UL28 for interaction. The major capsid protein, VP5, was also identified further supporting the previous mass spectrometry analysis of unknown 1 (Figure 18, Table 7).

Examination of the 176 potential interacting cellular proteins (see Appendix A, Table 13) led to their classification into groups based largely upon cellular location or function (Table 9). Of these groups, there are several that we find to be of particular interest including proteins of the cytoskeleton. It is well-established that HSV-1 relies heavily upon the host cytoskeleton for capsid transport during its initial travel to the nucleus and final egress and envelopment stages (65, 135, 187). Therefore it is not surprising that proteins such as dynein and tubulin were identified, and typically with very high spectral count values. Of further interest are those proteins that function in DNA repair. HSV-1 DNA is replicated as a branched concatemer and successful encapsidation requires the resolution of these branched structures into linear molecules (246). Therefore, DNA repair proteins functioning in such processes as recombination or endonuclease cleavage appear as likely targets to be utilized by HSV-1 during productive infection. One such protein identified by LC/MS/MS was DNA damage-binding protein 1 (DDB1) (Table 9). In uninfected cells, DDB1 functions as a component of numerous multiprotein complexes that are typically involved in various aspects of DNA repair (103). However, DDB1 has also been shown to interact with viral proteins from numerous viruses including hepatitis B and C viruses, human immunodeficiency virus, murine cytomegalovirus, and the closely related alphaherpesvirus, bovine herpesvirus type 1 (93, 108, 193, 233, 242).

Table 9. Interacting cellular proteins

Protein group[a]	MW[b]	No. of unique peptides			% coverage			Spectral counts		
		476	499	KOS	476	499	KOS	476	499	KOS
Cytoskeletal										
cytoplasmic dynein 1 heavy chain 1	531	203	186	42	42	36	7.8	381	385	57
tubulin beta-2A chain[c]	50	5	4	-	68	60	-	269	280	-
myosin light chain kinase 2, skeletal/cardiac muscle	62	4	4	-	2.2	3.3	-	61	45	-
keratin, type I cytoskeletal 28	53	3	2	-	13	11	-	44	48	-
utrophin	395	39	52	5	13	17	1.1	42	61	6
filamin-C isoform b	284	38	45	6	18	19	2.8	41	47	6
Ribosomal										
40S ribosomal protein S18	18	25	24	10	75	75	51	73	46	13
40S ribosomal protein S14	18	13	11	5	44	38	29	56	26	8
40S ribosomal protein S4, X isoform	28	19	15	7	48	49	22	35	22	7
60S ribosomal protein L23	15	10	9	2	58	54	14	32	19	2
Enzymes										
E3 ubiquitin-protein ligase UBR5	309	61	10	-	27	3.4	-	89	14	-
UDP-glucose:glycoprotein glucosyltransferase 1 precursor	175	2	-	-	1.8	-	-	42	-	-
serine palmitoyltransferase 1 isoform a	53	18	19	-	29	37	-	42	30	-
Chaperones										
60 kDa heat shock protein, mitochondrial	61	3	4	-	71	72	-	247	662	-
midasin	460	54	21	-	11	5.2	-	80	23	-
heat shock protein beta-1	23	16	17	6	68	68	33	42	39	6
DNA repair										
DNA-dependent protein kinase catalytic subunit isoform 1	469	168	149	29	39	36	7.4	291	252	39
DNA damage-binding protein 1	124	34	22	2	36	21	1.9	40	25	2
structural maintenance of chromosomes protein 1A	143	28	40	-	23	31	-	34	53	-
Misc.										
RING finger protein 213 isoform 3	373	77	52	-	24	17	-	129	71	-
CAD protein	246	41	47	12	19	22	6.1	75	101	14
mitochondrial import inner membrane translocase subunit TIM50	50	17	18	6	28	33	16	44	35	7
AIF-1	66	23	24	-	35	41	-	43	43	-
protein KIAA1967	103	16	5	3	19	5.7	3.1	35	5	3

[a]Only proteins meeting the following criteria are shown: i) ≥ 30 spectral counts in the vFH476 or vFH499 samples; ii) no spectral counts in the KOS sample; or iii) 5-fold or higher spectral counts in vFH476 versus KOS. See Appendix A, Table 13 for the complete list of proteins.

[b]MW, (kDa)

[c]Only a representative tubulin protein (1/8) is shown. See Appendix A, Table 13 for the complete list.

In order to confirm the proposed interaction of DDB1 with purified UL28 complexes, proteins were isolated by TAP from KOS-, vFH476-, or vFH499-infected cells, resolved by

SDS-PAGE, and Western blot analysis was performed using anti-DDB1 antibodies (Figure 19). The approximately125 kDa DDB1 protein was clearly detected in uninfected Vero cells and cells infected with KOS or each recombinant virus. However, DDB1 was not observed in TAP-purified eluates from KOS-infected cells, but found in eluates from vFH476-infected cells, confirming the LC/MS/MS data (Table 9). DDB1 is also seen in TAP-purified eluates from vFH499-infected cells but diminished in signal compared to vFH476, which correlates well with the number of spectral counts determined by LC/MS/MS from each purified sample (Table 9). Apoptosis-inducing factor-1 (AIF-1), a known effector of caspase-independent apoptosis (86, 160), was also confirmed to interact by Western blot analysis (Figure 19). Several other potential interacting proteins of interest remain to be confirmed by Western blot analysis, and although we have confirmed the interactions of DDB1 and AIF-1; that they play a role critical to the proper assembly or functioning of the terminase during the course of productive HSV-1 infection remains to be elucidated.

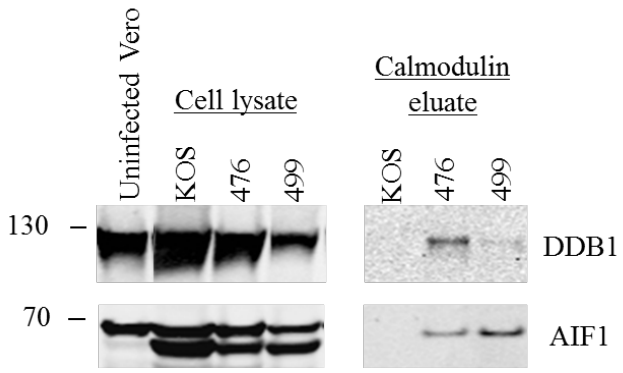

Figure 19. Confirmation of associated cellular proteins. Vero cells were infected with the indicated HSV-1 recombinant viruses or with wild-type (KOS) virus, harvested, and UL28 complexes were purified by TAP. Infected cell lysates or purified proteins were resolved by SDS-PAGE and analyzed by Western using anti-DDB1 or anti-AIF-1 antibodies. Protein standards (kDa) are shown to the left of each gel or blot.

2.4.5 Nuclease activity of the purified terminase complex

The UL15 subunit of the viral terminase is thought to encode for complex nuclease activity and contains a conserved ATPase domain that is required for cleavage and packaging of HSV-1 DNA. It has also been shown that a purified C-terminal fragment of UL89, the UL15 homolog in HCMV, possesses nuclease activity that is dependent upon the presence of Mn^{2+} ions. In order to determine if UL28 complexes isolated by TAP possess nuclease activity, an *in vitro* assay was performed. Purified proteins from vFH476-infected Vero cells were incubated with linearized plasmid DNA and $CaCl_2$, $MgCl_2$, or $MnCl_2$ was added to each reaction to determine if metal ions were required for activity (Figure 20A). The plasmid DNAs used either contained HSV-1 *a* sequence DNA, specific viral sequences that are essential for the cleavage and packaging of DNA, or did not contain specific sequences. When incubated with either plasmid DNA, purified UL28 complexes showed robust nuclease activity in the presence of Mn^{2+} ions. Complexes also possessed activity in magnesium (Mg^{2+}) that was more pronounced with *a* sequence specific DNA versus nonspecific plasmid sequences. In calcium, complexes showed only slight activity with *a* sequence-containing DNA and little to no activity with nonspecific DNA. Comparison of nuclease activity from proteins purified from KOS-infected cells to input plasmid DNA indicated that little to no DNA degradation was due to contaminating nucleases purified by TAP.

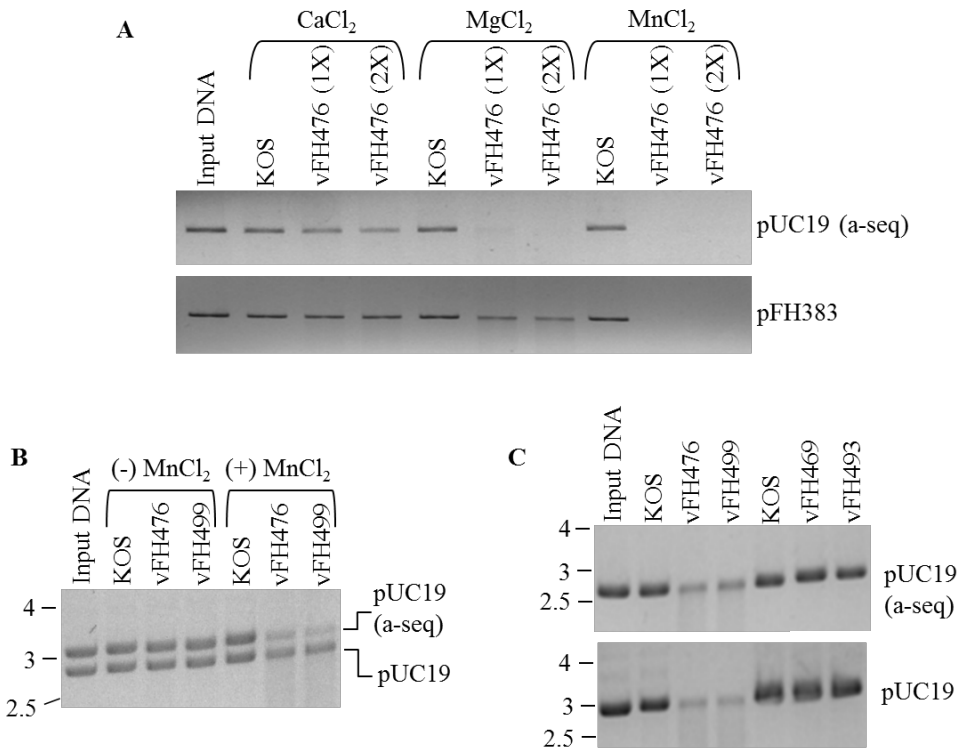

Figure 20. Nuclease activity of purified UL28 complexes. Complexes purified by TAP from each of the indicated viruses were incubated in a reaction mixture containing 30mM Tris-HCl (pH8.0), 50mM NaCl, the indicated metal ion (3mM), and the indicated linearized plasmid DNA(s) at 37°C for 18 h, and then resolved by agarose gel electrophoresis. Each assay demonstrates (A) metal ion requirements, (B) DNA sequence specificity, or (C) protein specificity.

The observed DNA specificity was further tested by incubation of complexes purified from vFH476- and vFH499-infected cells with equal amounts of *a* sequence-containing and nonspecific linear plasmid DNA in the presence or absence of Mn^{2+} ions (Figure 20B). Complexes isolated using full-length UL28 (vFH476) again showed increased activity for *a* sequence-containing DNA but only in presence of Mn^{2+}. Surprisingly however, complexes isolated using the UL28 C-terminal truncation mutant (vFH499) also showed nuclease activity that was specific for *a* sequence DNA and only with Mn^{2+}, possibly suggesting that UL28 alone possesses nuclease activity. However, mass spectrometry analysis indicated that the UL15

subunit could still interact with the UL28 C-terminal truncation mutant, although in greatly decreased amounts, therefore this interaction may be the basis for the existing nuclease activity displayed by these complexes.

In order to demonstrate that nuclease activity was specific for terminase components, protein complexes were purified by TAP from an NTAP-UL25 virus (vFH469) and a CTAP-UL17 virus (vFH493). Both viruses have been previously described and encode tagged proteins that are essential for HSV-1 cleavage and packaging but are not implicated to possess nuclease activity (41, 232). Protein complexes were incubated with either *a* sequence-containing DNA or nonspecific DNA in the presence of Mn^{2+} ions (Figure 20C). Complexes purified from both vFH476- and vFH499-infected cells again displayed increased activity in the presence of *a* sequence-containing DNA. However, complexes purified from KOS-, vFH469-, or vFH493-infected cells did not display nuclease activity supporting that the observed activity seen with UL28 complexes is due to terminase components. Taken together, the data suggests that the isolated UL28 complexes possess a robust nuclease activity in the presence of Mn^{2+} and Mg^{2+} ions that is specific for viral *a* sequence DNA, and appears to be encoded by terminase complex subunits.

2.5 DISCUSSION

A productive HSV-1 infection requires the UL28, UL15, and UL33 gene products for cleavage and packaging of replicated, concatemeric viral DNA into capsids, and it has long been proposed that these proteins comprise a viral terminase complex similar in function to those utilized by dsDNA bacteriophage (32, 46). However, biochemical analysis of the terminase has proven

difficult due to the inability to purify the terminase complex subunits, particularly UL15 and UL28. In this study, we have demonstrated the effective purification of the terminase complex from cells infected with HSV-1 recombinants expressing the UL28 protein fused to an N-terminal tandem affinity purification tag. The isolation of endogenous complexes allowed for the analysis of complex stoichiometry, characterization by proteomic methods, and preliminary biochemical analysis of complex nuclease activity.

Addition of the TAP tag to the N-terminus of UL28 (vFH475) did not alter UL28 protein expression kinetics, but reduced virus growth by approximately 1 log compared to wild-type KOS virus. Western blot of vFH475-infected cell lysates revealed relatively low level UL28 protein expression similar to that observed with wild-type KOS virus. Therefore, a second recombinant virus, vFH476, was constructed which expresses the NTAP-UL28 fusion protein under the transcriptional control of the human cytomegalovirus (CMV) immediate-early gene promoter in order to increase UL28 expression levels for higher yield purification. Compared to vFH475 or wild-type KOS, the vFH476 virus expressed NTAP-UL28 fusion proteins in sufficiently larger amounts, more suitable for downstream biochemical and proteomic analysis. One consideration was that the overexpression of UL28 may result in a deleterious effect on HSV-1 proliferation, possibly through the formation of a large subset of terminase complexes with improper stoichiometry (i.e. UL28 complexes lacking UL15, UL33, or both subunits). However, single-step growth curve analysis of vFH476 revealed a small decrease in virus titer (approximately 1 log) versus wild-type KOS, similar to that observed with vFH475, suggesting that the reduction in growth was due only to the addition of the TAP tag and that the CMV promoter caused no observable growth defect. It is not known why the addition of the TAP tag reduced growth of vFH475 and vFH476 relative to KOS virus growth, although it is possible that

the addition of 78 amino acids to the N-terminus of UL28 (the TAP tag) results in a steric hindrance to complex assembly or function (i.e. the terminase interaction with replicated viral DNA). The final generated recombinant virus, vFH499, is identical to vFH476 but encodes a nonsense mutation within UL28 resulting in the expression of a protein missing the C-terminal 44 amino acids. These amino acids have been previously shown to be essential for the interaction of UL15 and UL33 with UL28 (104, 267), and as expected, this virus only replicated to high titers on a UL28-complementing cell line.

TAP of UL28 complexes from vFH476- or vFH499-infected cells followed by Western blotting confirmed that the UL33 and UL15 proteins were only copurified in the presence of the full-length UL28 protein. Mass spectrometry analysis of specific SDS-PAGE bands confirmed the presence of the UL15, UL28, and UL33 proteins in purified UL28 complexes from vFH476-infected cells. This analysis also revealed that two unknown proteins, migrating in SDS-PAGE at approximately 63 and 50 kDa respectively, were composed of UL28 peptides. These bands were also detected by Western blot of TAP-purified complexes from vFH476- and vFH499-infected cells using antibodies against UL28 and the calmodulin-binding domain located within the N-terminal TAP tag of UL28, suggesting the missing amino acids are from the C-terminus. Furthermore, the truncated bands seen with vFH476 are identical in size to those observed with vFH499; indicating that the amino acids must be removed from the C-terminus. This is the first report of truncated forms of UL28, and it is unclear whether these proteins represent specific cleavage products that play a function during infection or are degraded proteins that arise during the TAP procedure.

Silver stain analysis of purified complexes revealed the presence of several unknown proteins that interact with the full-length and/or truncated forms of UL28. A comprehensive

proteomic analysis was performed using complexes purified from vFH476-, vFH499-, or wild-type KOS-infected cells. Mass spectrometry analysis identified 198 proteins unique to the vFH476 and vFH499 TAP samples compared to the KOS control. Of the 198 proteins, 22 were identified as HSV-1 proteins, while the remaining 176 were of host cell origin, and these were classified into groups based on cellular location or function. It is important to note that although the current mass spectrometry approach allowed for the elimination of nonspecific interactors (proteins identified in KOS sample), a large number of proteins (198) were identified as significantly interacting with UL28 complexes. This may be due to the purification of entire capsids by TAP, as the terminase associates with capsids during the DNA encapsidation process (46). The identification of the major capsid protein, VP5, in complexes from both recombinant viruses supports this notion and may also explain the identification of several tegument and envelope proteins which would likely copurify with the VP5 capsid surface to which they are indirectly (or directly) associated. Therefore it is likely that many of the 198 identified proteins interact indirectly with the viral terminase and do not represent complex components that play a role in terminase assembly or function during the cleavage and packaging of viral DNA, and additional rounds of mass spectrometry analysis will need to be performed in order to further validate each of the proposed interactions.

Examination of the interacting viral proteins further confirmed the association of the UL28, UL15 and UL33 subunits and the importance of the C-terminal 44 amino acids of UL28 for the association of these proteins. Interestingly, the UL15 protein was identified in the sample expressing the C-terminally truncated UL28 (vFH499), albeit at significantly lower counts compared to amounts copurified with the full-length UL28 protein (vFH476), while the UL33 protein was only copurified with the full-length UL28 protein. These results suggest that UL15

can either interact with a domain outside of the C-terminal 44 amino acids of UL28 or can interact indirectly with UL28 via another protein (i.e. VP5).

Examination of the interacting cellular proteins allowed for their classification into groups based upon cellular location and/or function, revealing several interesting observations. Numerous protein components of the host cytoskeleton were identified and displayed high spectral counts. Studies have indicated that HSV-1 utilizes microtubule-based transport during viral entry and egress (65, 135, 187) and the current data may suggest that once formed in the cytoplasm, the terminase utilizes host cytoskeletal elements for localization to the nucleus. Other proteins of interest include those involved in host DNA repair and recombination, which could possibly be utilized during HSV-1 infection for the resolution of branched, concatemeric viral DNA structures during the cleavage and packaging process. The interactions of apoptosis-inducing factor 1 (AIF-1) and DNA damage-binding protein 1 (DDB1) with UL28 complexes purified from vFH476- or vFH499-infected cells were confirmed by Western blotting using antibodies against AIF-1 or DDB1. Within uninfected cells DDB1 acts as a component of several multiprotein complexes that function in processes including DNA repair, transcriptional regulation, and protein ubiquitination (103), while AIF-1 functions as a mitochondrial protein but in times of stress, can cause caspase-independent apoptosis (86, 160). DDB1 has also been shown to perform a range of essential functions during the infectious cycle of several viruses (93, 108, 119, 193), and has recently been determined to interact with the VP8 protein (HSV-1 VP13/14 homolog) of the closely related alphaherpesvirus, bovine herpesvirus-1 (242). In the current study, the HSV-1 VP13/14 tegument proteins were not identified by mass spectrometry analysis suggesting that DDB1 does not indirectly interact with UL28 through an interaction with VP13/14. AIF-1 has been shown to translocate to the nucleus of HSV-1 infected cells but

apoptosis was not observed to occur (277), and the results of the current analysis may suggest that UL28 or another component the terminase complex bind AIF-1 before it can effectively initiate apoptosis. Overall, that AIF-1 and DDB1 were copurified with the viral terminase complex is intriguing because no host cell proteins have been implicated in the cleavage and packaging process. Clearly, further experimentation is required to determine if these proteins play a functional role during HSV-1 infection.

Purification of NTAP-UL28 complexes allowed for the further characterization of terminase complex stoichiometry. Sucrose density gradient ultracentrifugation of purified complexes followed by fractionation and Western blotting for the UL28, UL15, and the UL33 proteins revealed significant amounts of each protein comigrating in a gradient fraction corresponding to a size range greater than 158 kDa. This size range is consistent with a 1:1:1 complex of UL28, UL15, and UL33 and possessing an approximate molecular mass of 190 kDa. This data is in agreement with a previous study demonstrating that interacting UL15 and UL28 subunits purified from HSV-1 infected cells comigrate through a sucrose gradient to a position consistent with a 1:1 heterodimer of both proteins (112). It is important to note that, at the time of this study the UL33 protein was not yet implicated as a terminase subunit and therefore was not blotted for. Without immunoblot confirmation, the presence or absence of UL33 (Mr ~19 kDa) is not easily distinguished by size estimations based upon complex migration relative to standard proteins; therefore the association of UL33 in this study cannot be ruled out. Two additional gradient fractions of interest were determined to contain UL28 and UL33, or the UL33 protein alone. This observation combined with the lack of complexes containing only UL15 and UL28 lend support to previous studies suggesting that the UL28/UL33 interaction enhances the interaction of UL15 with UL28 and increases the number of properly formed complexes (104,

267, 269). Taken together these results may suggest that within infected cells terminase complex formation occurs in an ordered fashion, with the UL28 and UL33 proteins interacting before UL15 is added to the complex. Furthermore, the UL15 subunit encodes the signal for terminase nuclear translocation; therefore, the addition of UL15 as the final subunit may serve to prevent premature nuclear localization of incomplete complexes. The observation of monomeric UL33 may indicate that the UL28/UL33 interaction is of low affinity and the identification of far fewer UL33 peptides, relative to UL15 peptides, by mass spectrometry is consistent with this notion.

Although the results of this study clearly demonstrate the interaction between the UL15, UL28, and UL33 terminase subunits, the oligomeric status of the terminase is not known. Terminase complexes utilized by dsDNA bacteriophage consist of interacting small and large subunits and the functional terminase holoenzyme is a multimeric complex of these proteins (72). Therefore, it appears likely that the HSV-1 terminase complex would also form a higher-order structure at the capsid portal, although further experiments must be performed to validate this proposition.

UL28 complexes isolated by TAP were shown to possess sequence-specific nuclease activity in the presence of Mn^{2+} ions, similar to the activity observed with a purified fragment of the UL89 protein (UL15 homolog) of HCMV (142). Interestingly, complexes purified using the C-terminally truncated NTAP-UL28 fusion (vFH499), which precludes the interaction of the UL15 and UL33 subunits, displayed nuclease activity similar to that observed with complete terminase complexes (vFH476). This may suggest that the UL28 protein encodes for nuclease activity, and previous reports have demonstrated that the UL28 homolog in HCMV, UL56, can cleave HCMV DNA (22). However, mass spectrometry revealed that small amounts of UL15 are copurified from vFH499-infected cells, which may suggest that UL28 does not necessarily

possess nuclease activity. It is also interesting that the observed nuclease activity resulted in DNA degradation as opposed to a single (or possibly double) cleavage that is thought to generate free genome ends during DNA packaging within infected cells. This degradation has also been observed in nuclease assays examining the purified UL89 protein (UL15 homolog) of HCMV (142, 199), and may suggest that terminase nuclease activity *in vitro* is nonspecific. The observed specificity for *a* sequence-containing DNA may be due to UL28 preferentially interacting with a region of the viral *a* sequence in a manner consistent with the proposed DNA-binding function of UL28 during packaging. However, once bound the terminase nuclease activity may not be specific, and one possible explanation is that complex stoichiometry affects specificity. As mentioned previously, analogy with terminase complexes of dsDNA bacteriophage suggests that the HSV-1 terminase functions as a multimeric complex at the portal vertex of capsids. It is possible that the terminase complexes isolated and examined in this study are not complete multimeric complexes and/or are not assembled at the capsid portal, and in the absence of these protein interactions regulation of nuclease activity is absent, resulting in terminase DNA degradation as opposed to specific cleavage events.

The results of these studies have demonstrated that TAP is an effective method for the purification of UL28 complexes from HSV-1-infected cells. This method will allow for further biochemical analysis of purified complexes and demonstration of the proposed cleavage and packaging functions. The ability to purify endogenous terminase complexes is novel to the field and represents a critical step toward establishing an *in vitro* HSV-1 cleavage and packaging system.

3.0 MUTATIONAL ANALYSIS OF ESSENTIAL RESIDUES WITHIN THE HERPES SIMPLEX VIRUS TYPE I UL15 AND UL28 TERMINASE SUBUNITS

3.1 ABSTRACT

Productive infection with herpes simplex virus type 1 (HSV-1) requires the cleavage of replicated viral DNA concatemers into linear, monomeric genomes that are packaged into preformed viral capsids. Analogy with the cleavage and packaging systems of double-stranded DNA bacteriophage, combined with limited empirical evidence, suggests that the HSV-1 UL15, UL28, and UL33 proteins form the viral terminase complex that performs the essential cleavage and packaging functions. The UL15 and UL28 proteins contain conserved amino acid residues that have been shown to be critical for terminase activity in the closely related herpesvirus, human cytomegalovirus. In order to assess the importance of these residues, recombinant viruses encoding either a deletion of the putative metal-binding domain of UL28 (vFH505) or mutation of amino acids within the proposed UL15 nuclease domain (vFH506, vFH507) were generated. Mutations were introduced into the genome of an HSV-1 virus (vFH476) that expressed a tandem affinity purification (TAP) tagged protein. The TAP tag fused to the N-terminus of UL28 (NTAP-UL28) allowed for the direct assessment of purified terminase complexes encoding domain mutations. A final virus (vFH510) was generated by deletion of the putative UL28 metal-binding domain within the genome of a previously described HSV-1

recombinant (vFH499) encoding an NTAP-UL28 fusion protein with a C-terminal truncation of 44 amino acids required for terminase complex formation. Each domain mutant virus replicated to high titers only on complementing cell lines and produced only B-capsids, indicating that each mutated protein was nonfunctional. TAP of UL28 complexes from cells infected with each domain mutant followed by immunoblotting for the terminase subunits revealed that only vFH510 did not copurify UL15 or UL33, due to the C-terminal truncation of UL28. Viral DNA replication levels were not significantly affected in cells infected with vFH505, vFH506, or vFH507 but each virus was deficient in the cleavage and packaging of replicated viral DNA. Taken together, these results suggest that the putative UL28 metal-binding domain and conserved amino acids within the UL15 nuclease domain are not essential for terminase complex formation, but are required for the cleavage and packaging functions of the viral terminase.

3.2 INTRODUCTION

HSV-1 proliferation requires the cleavage of replicated, concatemeric viral DNA into linear, monomeric genomes that are subsequently packaged into preformed capsids for further viral assembly. Numerous studies have identified seven viral proteins that are essential for the DNA cleavage and encapsidation process: UL6, UL15, UL17, UL25, UL28, UL32, and UL33 (3, 4, 6, 10, 33, 116, 117, 132, 165, 166, 173, 195, 198, 205, 206, 225, 256, 272). At a unique vertex of the capsid, twelve copies of the UL6 protein form the portal through which DNA enters and exits the capsid (30, 35, 155, 235). Recent cryo-electron microscopy (cryo-EM) experiments have revealed that the UL17 and UL25 proteins form a heterodimeric complex that assembles around the capsid vertices, termed the capsid vertex specific component, that is thought to stabilize the

capsid during and after DNA packaging (41, 232, 236). The function of the UL32 protein is largely unknown but it may play a role in the transport of assembled capsids to sites for DNA encapsidation (36, 116). The remaining three proteins, UL15, UL28, and UL33, form a complex within infected cells that is thought to function as the viral terminase (46).

By analogy to double-stranded DNA (dsDNA) bacteriophage systems, it is thought that the HSV-1 terminase binds replicated viral DNA concatemers, cleaves the DNA into unit length monomers, transports the DNA to preformed procapsids, docks at the portal complex, packages the DNA into capsid, makes a final cleavage upon packaging a complete genome, and dissociates from the capsid (32). Difficulties with the purification of the terminase proteins and the lack of an *in vitro* cleavage and packaging system in HSV-1 has hampered studies on the role of the UL15, UL28, and UL33 proteins in the DNA packaging reaction. However, cryo-EM and genetic studies have provided several lines of evidence demonstrating that these proteins function as the HSV-1 terminase. These include studies demonstrating that: i) viral DNA is not cleaved in HSV-1 mutants encoding mutations that preclude the interaction of UL15 or UL33 with UL28 (18, 104, 225, 267, 269); ii) HSV-1 recombinants with mutations in the UL6 portal that interfere with the terminase/portal interaction are also deficient in cleavage and packaging of replicated viral DNA (270); iii) the transient association of UL15 and UL28 with viral capsids is also observed with dsDNA bacteriophage terminases (16, 32, 204, 223, 274); iv) human cytomegalovirus (HCMV) strains displaying resistance to inhibitors of viral DNA cleavage possess mutations within protein homologs of UL15 and UL28 (114, 238); and v) the UL15 and UL28 proteins encode multiple conserved domains that are essential for cleavage and packaging of viral DNA (4, 9, 10, 33, 104, 114, 142, 173, 178, 225, 238, 268, 269, 271-273).

UL15 is the most conserved gene within the family *Herpesviridae* and expresses a protein encoded within two exons of a spliced transcript (49). Exon I and the N-terminal region of exon II contain domains typically encoded by proteins that function in ATP metabolism, suggesting these regions provide the motor function for DNA translocation into the capsid (52, 67, 249, 273). Specifically the Walker A and B box motifs are conserved in homologs of the UL15 protein found in dsDNA bacteriophages, and are essential for viral DNA cleavage and packaging (52, 178, 249, 273). A recent study demonstrated that a purified, soluble fragment of exon II of the HCMV UL89 protein (UL15 homolog) possessed nuclease activity in the presence of manganese (Mn^{2+}) ions (142). The crystal structure of this fragment was resolved and identified three Mn^{2+} coordinating amino acids that are conserved within exon II of the HSV-1 UL15 protein. The UL28 protein has been shown to bind specific HSV-1 DNA sequences which are required for cleavage and packaging and this function has also been observed within HCMV (5, 22). Furthermore, UL28 encodes a putative metal-binding domain which was discovered in HCMV and shown to contain residues that are conserved among the herpesviruses (114). HCMV strains that were resistant to an inhibitor of viral DNA cleavage possessed a one-residue mutation within this domain, suggesting its importance in mediating terminase function.

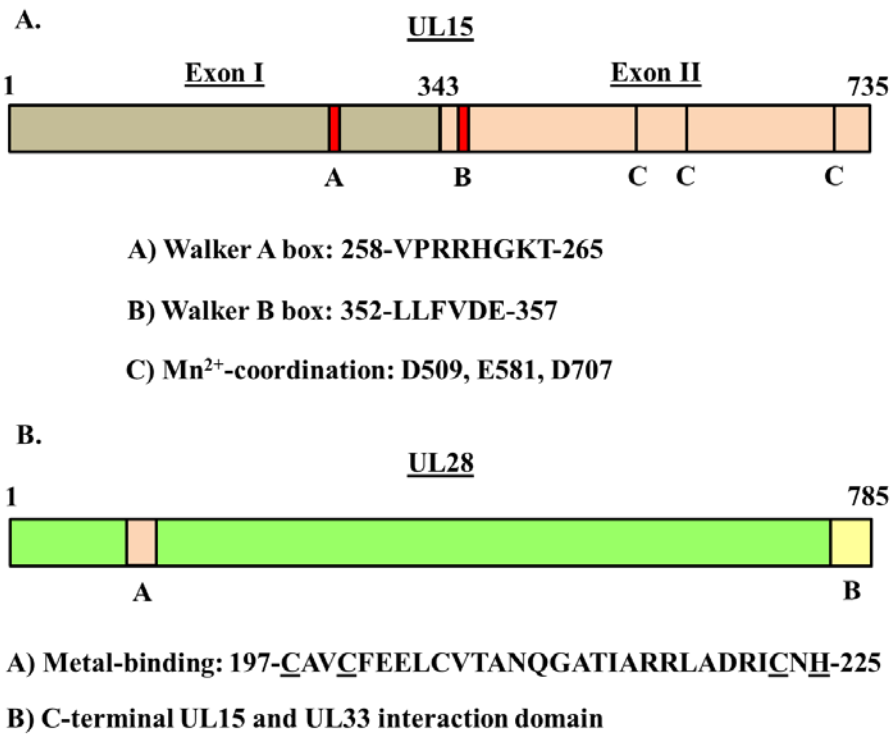

Figure 21. Conserved amino acid domains within the (A) UL15 and (B) UL28 proteins.

Previously (Section 2.0), we have demonstrated a method for the efficient purification of terminase complexes from HSV-1-infected cells by TAP of the UL28 protein encoding an N-terminal TAP tag fusion. In this chapter, mutations or deletions within the nuclease domain of UL15 or the metal-binding domain of UL28 were introduced into the genome of the NTAP-UL28 fusion virus. Characterization of these viruses followed by the isolation of terminase complexes revealed that the domain mutations did not preclude complex formation but each virus was deficient in viral DNA cleavage.

3.3 MATERIALS AND METHODS

3.3.1 Cells and Viruses

African green monkey kidney (Vero) and UL15-complementing (C2) cell lines were maintained in Dulbecco's modified Eagle's medium supplemented with 5% newborn calf serum, 100 U penicillin per ml, and 100 μg streptomycin per ml (growth medium) (272). UL28-complementing (CV28) cells were maintained exactly as Vero cells but supplemented with 10% newborn calf serum (267). The KOS strain of HSV-1 was used as the wild-type virus. The NTAP-UL28 (vFH475), CMV-NTAP-UL28 (vFH476), and CMV-NTAP-UL28-741s (vFH499) mutant viruses were described previously (Section 2.3.2). The GCB virus, containing a 1881 bp deletion within the UL28 open reading frame, was described previously (225).

3.3.2 Construction of recombinant viruses

The CMV-NTAP-UL28(Δ197-225) (vFH505), CMV-NTAP-UL28, UL15(D706A, D707A) (vFH506), and CMV-NTAP-UL28, UL15(D509A) (vFH507) viruses were generated by recombination of a vFH476 (Section 2.3.2) genome maintained within a bacterial artificial chromosome (BAC) (81). The vFH476 BAC clone was transferred to GS1783 bacteria (gift from G. Smith) and mutagenesis was performed using the two-step bacteriophage Red-mediated homologous recombination system (231), as previously described (42). The CMV-NTAP-UL28(Δ197-225)-741s (vFH510) mutant virus was generated by the same methods, but through recombination of a vFH499-BAC (Section 2.3.2) that was transformed into GS1783 bacteria. Primers and template plasmid DNA used to amplify the kanamycin resistance construct are listed

in Table 10. Plasmid p-EP-Kan-S was a kind gift from Dr. Paul Kinchington (University of Pittsburgh). BAC DNA was transfected into Vero and UL15-complementing C2 (vFH506, vFH507) or UL28-complementing CV28 (vFH505, vFH510) cells and recombinant viruses were harvested from cell lysates and plaque purified on C2 (vFH506, vFH507) or CV28 (vFH505, vFH510) cells. Base pair changes in the UL15 ORF of vFH506 and vFH507 were confirmed by PCR amplification of purified viral DNA using the following primers that flank the UL15 ORF: 5' – TCACGAGACGCGTGTGATAGG – 3' and 5' – AACGTTATCCGAGGCCAGGACTTTAAC – 3'. The 1182 bp PCR products were extracted from agarose gels and used for restriction fragment length polymorphism analysis using NarI (vFH506) or BamHI (vFH507) and sequencing analysis using the following primers: 5' – TCACGAGACGCGTGTGATAGG – 3' (vFH506) and 5' – AGTGCTCCAGGGCGAAGATG – 3' (vFH507). Deletion of the metal-binding domain from the UL28 ORF of vFH505 and vFH510 was confirmed by PCR amplification of purified viral DNA using the following primers that flank the UL28 ORF: 5' – TTTCTCACCCCGCTGTCGG – 3' and 5' – AACAGCGCCAGTTCCACG – 3'. The 764 bp PCR products were extracted from agarose gels and used for restriction fragment length polymorphism analysis using PvuI and sequencing analysis using the following primer: 5' – ATGAAGCAGCTAAACTACTGCCACCTC – 3' (vFH505 and vFH510).

Table 10. PCR primers for generation of recombinant domain mutant viruses

Primer	Sequence[a]	Template	Recombinant Virus
UL28 (Δ197-225) Forward	TCGGGCCTTATCGTCCCCCCGGAGCTT **AGCGACCCGTCCCACCCCGTCACCCAGCAGGCGCAG** TAGGGATAACAGGGTAATCGATTT	p-EP-Kan-S	vFH505, vFH510
UL28 (Δ197-225) Reverse	*CCGCAGCTCGTTGGCGTCCAGCCGCAC* **CTGCGCCTGCTGGGTGACGGGGTGGGACGGGTCGCT** GCCAGTGTTACAACCAATTAACC	p-EP-Kan-S	vFH505, vFH510
UL15 (D706A, D707A) Forward	GACGTCCGTACGTATTCC **GGAAAACGGAACGGCGCATCGGCTGCCCTTATGGTCGCC GTC** TAGGGATAACAGGGTAATCGATTT	p-EP-Kan-S	vFH506
UL15 (D706A, D707A) Reverse	*GAGGTAGATGGCCATAAT* **GACGGCGACCATAAGGGCAGCCGATGCGCCGTTCCGTTTT CC** GCCAGTGTTACAACCAATTAACC	p-EP-Kan-S	vFH506
UL15 (D509A) Forward	CTCATGGCC **CCCGATTTGTACGTGTACGTGGCTCCCGCGTTCACGGCCA ACACC** TAGGGATAACAGGGTAATCGATTT	p-EP-Kan-S	vFH507
UL15 (D509A) Reverse	*GGAGGCTCG* **GGTGTTGGCCGTGAACGCGGGAGCCACGTACACGTACAA ATCGGG** GCCAGTGTTACAACCAATTAACC	p-EP-Kan-S	vFH507

[a]Underlined sequences are complementary for the indicated plasmid template. Italicized, bold, and normal-type sequences are different UL28 or UL15 sequences. Individual underlined base-pairs represent mutations. Sequences in the same type within primer pairs are complementary.The individual double-underlined base-pair indicates a silent mutation to disrupt a *NarI* restriction site.

3.3.3 Capsid purification

Capsids were purified by sucrose gradient centrifugation as previously described (42). Briefly, Vero cells (1.5×10^8) were infected at an MOI of 5 PFU/cell and incubated at 37°C. At 18 h pot-infection the infected cells were harvested by scraping, rinsed with phosphate-buffered saline (PBS), resuspended in 20 mM Tris (pH 7.5) containing protease inhibitors (Roche), adjusted to 1% Triton X-100, and incubated for 30 min on ice. The resulting isolated nuclei were harvested by low-speed centrifugation, resuspended in 10 ml of TNE buffer (500 mM NaCl, 10 mM Tris, 1 mM EDTA [pH 7.5]), and sonicated to lyse the nuclei. The nuclear lysate was then resolved by low-speed centrifugation, and the supernatant was layered onto the top of 20 to 50% sucrose (in TNE buffer) gradients. Centrifugation was performed in an SW41 rotor at 24,000 rpm for 1 h.

The positions of A, B, and C capsids were observed as light-scattering bands, with A capsids found at a higher position (least dense) on the gradients and C capsids being found at a lower position (most dense) on the gradients.

3.3.4 TAP

The TAP protocol was performed by infecting 5 x 10^8 Vero cells with virus at an MOI of 10 PFU/cell. The infection was allowed to proceed for 18 h at 37°C, after which the cells were harvested and pelleted via centrifugation at 5,000 rpm for 10 min at 4°C. All remaining steps were performed at 4°C. The cells were washed in a total volume of 50ml 1 x PBS, and the final cell pellet was resuspended in 24 ml of streptavidin binding buffer (SBB) (300 mM KCl, 40 mM Tris-HCl [pH 7.5], 2 mM EDTA, 0.1% NP-40 substitute, and 5 mM β-mercaptoethanol) containing protease inhibitors (Roche 1 697 498). The cells were lysed by sonication using a probe sonicator. The cell suspension was sonicated 4 times for 10 s each at an output of 6 W with chilling on ice between each sonication step. Benzonase (1,500 U; Novagen, 71205-3) was added to the samples and left at 4°C for 30 min. The extract was then clarified via centrifugation at 12,000 rpm in a Sorvall SS-34 rotor for 20 min at 4°C. The supernatant was transferred to a new tube, 1.5 ml of streptavidin resin (0.75 ml packed volume) (Pierce, 53117) was added, and the samples were rotated at 4°C for 2 h. The resin was pelleted by centrifugation at 3,500 rpm for 5 min, and the supernatant was removed. The resin was washed three times by being resuspended in 5 ml of SBB followed by centrifugation at 3,500 rpm for 5 min. Protein was eluted from the resin by adding 3 ml of streptavidin elution buffer (300 mM KCl, 40 mM Tris-HCl [pH 7.5], 2 mM EDTA, 0.1% NP-40 substitute, 5 mM β-mercaptoethanol, 2 mM D-biotin [Sigma, 47868]) containing Roche protease inhibitors, and the sample was rotated at 4°C for 30 min. The protein-

resin mixture was spun down at 7,000 rpm in a microcentrifuge for 2 min, and the supernatant was collected as the streptavidin eluate. Twelve milliliters of calmodulin binding buffer (CBB) (150 mM NaCl, 10 mM Tris-HCl [pH 7.5], 1 mM magnesium acetate, 1 mM imidazole, 2 mM $CaCl_2$, 0.1% NP-40 substitute, 10 mM β-mercaptoethanol) containing Roche protease inhibitors was added to the streptavidin eluate. An additional 11.25 μl of 1 M $CaCl_2$ was added to the mixture along with 1.2 ml of calmodulin resin (0.6 ml packed volume) (Agilent Technologies, 214303-52), and samples were rotated at 4°C for 2 h. The resin was pelleted by centrifugation at 3,500 rpm for 5 min, and the supernatant was removed. The resin was washed three times by resuspension in 5 ml of CBB followed by centrifugation at 3,500 rpm for 5 min. Protein was eluted from the resin by adding 3 ml of calmodulin elution buffer (150 mM NaCl, 10 mM Tris-HCl [pH 7.5], 1 mM magnesium acetate, 1 mM imidazole, 0.1% NP-40 substitute, 10 mM β-mercaptoethanol, 2 mM EGTA), and the sample was rotated at 4°C for 30 min. The protein-resin mixture was spun down at 7,000 rpm in a microcentrifuge for 2 min, and the supernatant was collected as the final (calmodulin) eluate.

3.3.5 Western blotting

Protein samples were separated on a 4 to 12% SDS-polyacrylamide gel, and transferred to nitrocellulose. The nitrocellulose was washed twice in Tris-buffered saline (TBS) and incubated overnight in Rockland Near Infra-Red blocking buffer (Rockland Immunochemicals, MB-070-003). Primary antibodies used (dilution in parenthesis) include: UL28 rabbit polyclonal antibody UL28-GST (1:1000) (17), rabbit monoclonal Anti-Calmodulin Binding Protein Epitope Tag Antibody, clone C16T (1:3000) (Millipore, 05-932), UL15 rabbit polyclonal antibody UL15-GST(1-104) (1:1000) (196), and UL33 rabbit polyclonal antibody UL33-GST (1:500) (179).

The blocked nitrocellulose was reacted with the diluted antibodies for 2 h at room temperature, washed five times in TBS with 0.5% Tween 20, and incubated with IRDye 800-conjugated goat anti-rabbit secondary antibody (Rockland Immunochemicals) diluted 1:15,000 in Rockland Near Infra-Red blocking buffer with 0.1% Tween 20. The blots were washed and scanned using an Odyssey system (Li-Cor, Lincoln, NE).

3.3.6 Southern blotting

T-175 flasks (3 x10^7 cells per flask) of Vero, CV28, or C2 cells were infected with virus at an MOI of 5 PFU per cell. At 18 h postinfection, the medium was removed and the cells were washed in 1 X phosphate-buffered saline. Cells were harvested by scraping from the plate and pelleted. The cells were lysed and total cell DNA or DNase-resistant DNA samples were prepared as previously described (96, 217). The final DNA was digested with BamHI to assess the cleavage of viral DNA. DNA was separated by agarose gel electrophoreses, transferred to a nylon membrane, and hybridized as previously described (96). Southern blots were scanned with a Storm 840 PhosphorImager.

3.3.7 Real-time PCR

60 mm plates (4 x10^6 cells per plate) of Vero, CV28, or C2 cells were infected with virus at an MOI of 5 PFU per cell. Each infection was performed in triplicate. At 18 h postinfection, the medium was removed and the cells were washed in 1 X phosphate-buffered saline. Cells were harvested by scraping from the plate and pelleted. The cells were lysed and total cell DNA was prepared as previously described (96). Each reaction was set up such that the PCR mixture

contained 7.5 µl 2 X Power SYBR® Green PCR Master Mix (Applied Biosystems, 4367659), 0.375 µl of each primer (stock concentration, 10 µM, see below), and 3 µl isolated DNA in a total volume of 12 µl. Purified KOS virus DNA was also included in each plate in a standard curve of 1:10 dilutions from 3 x 10^7 to 30 copies per well, which covers the threshold cycle values for the DNA samples tested. Each reaction for the standard curve was performed in triplicate. The reactions were carried out in a Step One Plus real-time PCR machine from Applied Biosystems under the following conditions: 95°C for 10 min, followed by 40 cycles of 95°C for 15 s and 60°C for 1 min. A melt curve was also included under the following conditions: 95°C for 15 s and 60°C for 1 min, followed by +0.3°C to 95°C for 15 min. The results were analyzed using the SDS 2.3 software from Applied Biosystems. Each isolated DNA sample was amplified using primers for the viral TK gene (forward: 5' – ACCCGCTTAACAGCGTCAACA – 3'; reverse: 5' – CCAAAGAGGTGCGGGAGTTT – 3') to measure genome copies, and primers for the cellular GAPDH gene (forward: 5' – TTCGACAGTCAGCCGCATCTTCTT – 3'; reverse: 5' – CAGGCGCCCAATACGACCAAATC – 3') for normalization of cell number. The KOS standard curve was amplified only with viral TK primers.

3.4 RESULTS

3.4.1 Characterization of NTAP-UL28 viruses possessing UL15 and UL28 domain mutations

Previous studies (Section 2.0) have demonstrated that the terminase complex of UL15, UL28, and UL33 can be isolated from cells infected with a recombinant HSV-1 expressing an NTAP-UL28 fusion protein under cytomegalovirus (CMV) promoter control. The recombinant virus used in these studies, vFH476, was generated through manipulation of an HSV-1 (KOS) genome maintained within a recombinant bacterial artificial chromosome (BAC). In order to utilize TAP for the isolation of terminase complexes possessing mutations within the nuclease domain of the UL15 subunit or the putative metal-binding domain of the UL28 subunit, mutations were introduced into the genome of the vFH476 BAC (Figure 22).

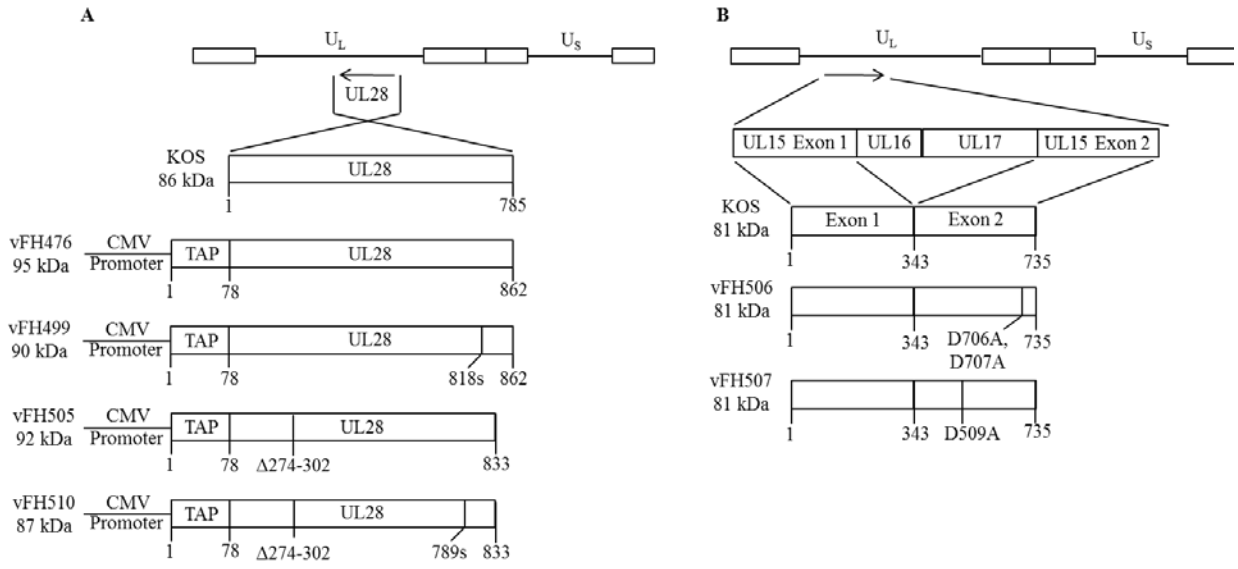

Figure 22. Recombinant UL28 and UL15 virus constructs. The HSV-1 genome is shown at the top with the long and short unique regions represented as U_L and U_S, respectively. The expressed UL28 (A) or UL15 (B) protein from wild-type HSV-1 KOS or each recombinant virus is expanded below, with virus names and protein sizes indicated to the left of each construct. Amino acid numbers below each construct indicate: deletion of the indicated amino acids (Δ), a nonsense mutation of the indicated amino acid (s), and mutation of the indicated amino acid (ie. D509A), or protein length (number alone)

The putative UL28 metal-binding domain, located at residues 197-228 of the UL28 ORF, was deleted from the vFH476 BAC. The resulting vFH505 BAC (NTAP-UL28(Δ197-225)) was transfected into Vero and UL28-complementing CV28 cells. Virus was recovered only on the complementing cell line, indicating that the mutated UL28 protein was nonfunctional. Two additional viruses with site-specific mutations of conserved amino acids within the UL15 nuclease domain were generated in the same manner. vFH506 (NTAP-UL28, UL15(D706A, D707A)) contains the mutation of a conserved aspartic acid residue at position 707 to alanine and a second aspartic acid to alanine mutation at residue 706, while vFH507 (NTAP-UL28, UL15(D509A)) contains the mutation of a conserved aspartic acid at position 509 to alanine. Both viruses could only be recovered on UL15-complementing C2 cells, suggesting that the amino acid changes resulted in expression of nonfunctional UL15 proteins. A final recombinant

virus was created through manipulation of the previously described vFH499 BAC, which encodes a C-terminally truncated NTAP-UL28 gene under CMV promoter control (Figure 22, see also Section 2.0). The UL28 protein expressed by vFH499 is missing the C-terminal 44 amino acids which are required for the interaction of UL15 and UL33 with UL28 (104). The putative UL28 metal-binding domain was also deleted in the vFH499 BAC and the resulting virus, vFH510 (NTAP-UL28(Δ197-225)-741s), was recovered only on UL28-complementing CV28 cells.

The recovered viruses were plaque purified on UL28-complementing CV28 (vFH505, vFH510) cells or UL15-complementing C2 (vFH506, vFH507) cells and virus stocks were prepared and titrated. Each of the recombinant viruses only grew to high titers on the respective complementing cell line, suggesting that each recombinant virus expressed a nonfunctional UL15 or UL28 protein (Table 11).

Table 11. Viral stock titers: UL15 and UL28 domain mutants.

Virus	Virus plating efficiency (PFU/mL) in[a]:		
	Vero cells	CV-28 cells	C2 cells
KOS	5.9×10^9	9.8×10^8	6.7×10^9
vFH476	2.8×10^{10}	2.1×10^9	ND
vFH499	< 1000	2.9×10^9	ND
vFH505	< 1000	3.1×10^8	ND
vFH506	5×10^4	ND	7×10^8
vFH507	< 1000	ND	1.75×10^9
vFH510	< 1000	1.7×10^8	ND

[a]ND, not determined

Viral capsids were isolated from cells infected with wild-type KOS virus, the parental vFH476 or vFH499 viruses, or each domain mutant virus at 18hpi (Figure 23). The results

clearly show that only KOS and the vFH476 virus, which encodes a full-length UL28 protein, produce viral C-capsids. As expected vFH499 virus produced only B-capsids, as did each domain mutant virus. These results further suggest that each domain mutant virus expresses a nonfunctional UL15 or UL28 protein.

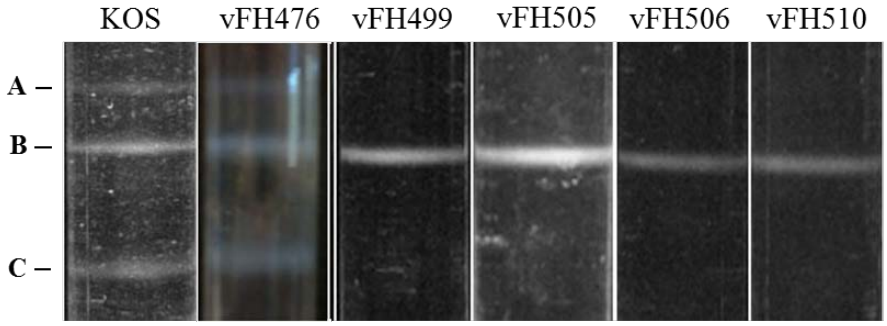

Figure 23. Capsid formation by UL15 and UL28 domain mutant viruses. Viral capsids were isolated from the nuclei of cells infected with the indicated viruses. Capsids were layered onto a 20-50% sucrose gradient, and centrifuged at 24K RPM at 4°C for 1 h. The positions of A-, B-, and C-capsid bands observed by light-scattering are indicated. A-capsids are the least dense and found at a higher position on the gradients, while C-capsids are the densest and migrate to a lower gradient position.

3.4.2 TAP of UL28 protein complexes from cells infected with UL15 and UL28 domain mutant viruses

The TAP tag used for these studies has been previously described (232), and consists of a streptavidin-, and calmodulin-binding peptide (Stratagene-Interplay) which allows for the dual purification of protein complexes eluted under native conditions (183). Vero cells were infected with either the wild-type KOS virus, the parental NTAP-UL28 viruses (vFH476, vFH499), or the UL28 (vFH505, vFH510) and UL15 (vFH506, vFH507) domain mutant viruses at an MOI of 10. At 18 hpi, cell extracts were harvested and applied to the TAP procedure (Figure 24). Infected

cell extracts were first incubated with streptavidin resin and interacting complexes were eluted with biotin. In the second purification the eluted complexes were incubated with calmodulin resin in the presence of calcium and eluted with EGTA. Western blot of the final calmodulin-eluted samples using antibodies against UL28 revealed the full-length 95 kDa NTAP-UL28 protein in lanes containing the NTAP-UL28 virus (vFH476) and the UL15 domain mutants (vFH506, vFH507), which also express a full-length NTAP-UL28 protein (Figure 24). The viruses expressing mutated forms of the UL28 protein revealed proteins of the expected size at 90, 92, and 87 kDa, corresponding to the C-terminal truncated NTAP-UL28 (vFH499), deletion of the putative metal-binding domain of NTAP-UL28 (vFH505), and combined C-terminal truncation and metal-binding domain deletion of NTAP-UL28 (vFH510) within UL28, respectively. Blots were also probed for the UL15 and UL33 proteins to determine if the domain mutations affected terminase complex formation. As previously observed (Section 2.4.2), both UL15 and UL33 were copurified using the full-length NTAP-UL28 virus (vFH476) but were not isolated by TAP using the C-terminally truncated NTAP-UL28 fusion virus (vFH499) The mutated UL15 proteins encoded by vFH506 and vFH507 were shown to copurify with UL28 complexes, as well as the UL33 protein. The UL15 and UL33 proteins were also associated with purified complexes containing the deletion of the putative metal-binding domain within the NTAP-UL28 fusion (vFH505). As observed with the C-terminally truncated NTAP-UL28 fusion virus (vFH499), UL15 and UL33 were not associated with the NTAP-UL28 mutant encoding both the truncation and metal-binding domain deletion (vFH510). Also of note, no terminase subunits were purified from lysates of KOS-infected cells, confirming the specificity of the TAP procedure. These results determined that each recombinant virus expresses a mutated UL15 or UL28 protein of expected molecular weight. It was also demonstrated that the

UL15 and UL33 proteins copurify with UL28 in all samples except for those where the NTAP-UL28 fusion protein lacks the final 44 amino acids; suggesting that the mutations introduced within the nuclease domain of UL15 or the metal-binding domain of UL28 do not affect terminase complex formation.

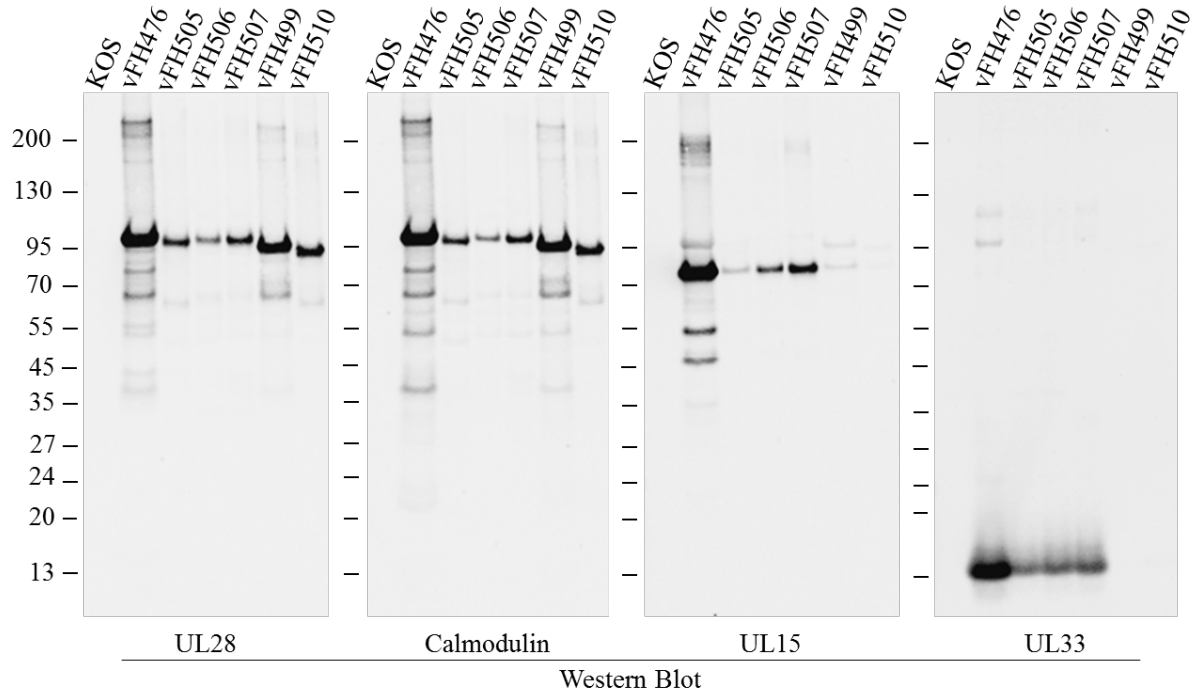

Figure 24. TAP and immunoblot of UL28 complexes purified from UL15 and UL28 domain mutant viruses. Vero cells were infected with the indicated HSV-1 recombinant viruses or with wild-type (KOS) virus. After TAP, proteins eluted from the calmodulin column were resolved by SDS-PAGE and identified by Western blot (antibodies listed below each blot). Protein standards (kDa) are shown to the left of each blot

Previously, Western blot analysis of UL28 complexes purified by TAP revealed the purification of several truncated forms of UL28 (Section 2.4.2), and mass spectrometry confirmed that fragments migrating in SDS-PAGE at approximately 63 and 50 kDa were composed of UL28 peptides (Section 2.4.4). In the current analysis, blotting for UL28 or the

calmodulin-binding peptide demonstrated the presence of the same truncated forms of the NTAP-UL28 protein with the viruses expressing altered UL15 proteins (vFH506, vFH507). In contrast, the vFH505 and vFH510 viruses express smaller truncated NTAP-UL28 proteins of approximately 60 kDa due to the 29 amino acid deletion of the putative metal-binding domain of UL28. The detection of these proteins in each sample using the calmodulin-binding antibody demonstrated that the 63 and 60 kDa NTAP-UL28 proteins are the result of the loss of approximately 30-35 kDa (~300 amino acids) from the C-terminus of UL28.

3.4.3 UL15 and UL28 domain mutations preclude cleavage and packaging of replicated viral DNA in infected cells

The UL15 nuclease domain mutant viruses (vFH506, vFH507) and the UL28 metal-binding domain deletion virus (vFH505) were not deficient in terminase complex formation; therefore, in order to determine if these mutations affected terminase complex function, the ability of each domain mutant virus to cleave and package viral DNA during infection was examined. Replicated viral DNA concatemers are essentially endless, containing relatively few free genome ends, while cleaved and packaged viral DNA contains free L and S component termini. Southern blot analysis of infected cell DNA digested with BamHI can differentiate cleaved genomic termini from “endless” concatemeric DNA. The BamHI K fragment spans the junction linking the L and S components of the viral genome, while DNA cleavage generates BamHI S and Q fragments representing the free L and S genome termini respectively (Figure 25). Therefore, a Southern blot BamHI K fragment probe detects only L-S junctions within uncleaved DNA, but will detect the Q and S terminal fragments and L-S junction of cleaved monomeric genomes.

Vero cells were infected with the UL15 nuclease domain mutants (vFH506 or vFH507), the UL28 metal-binding domain mutants (vFH505 or vFH510), the full-length NTAP-UL28 fusion (vFH476), or the C-terminally truncated NTAP-UL28 fusion (vFH499) viruses. Infection with wild-type KOS virus served as a positive control, while GCB, a previously described UL28-null virus deficient in cleavage and packaging (225), served as the negative control. Cell lysates were treated with DNaseI before DNA isolation, in order to degrade any unpackaged viral and cellular DNA. Southern blot analysis of DNaseI-protected DNA digested with BamHI and probed with the BamHI K or Q fragments revealed that only the wild-type KOS virus and the full-length NTAP-UL28 fusion virus were capable of successfully cleaving and packaging viral DNA into capsids, as indicated by the detection of the joint (K) and terminal (Q and S) DNA fragments (Figure 25). Infection of UL15-complementing C2 cells (vFH506, vFH507) or UL28-complementing CV28 cells (GCB, vFH499, vFH505, vFH510) restored the ability of each recombinant virus to cleave and package viral DNA, indicating that the observed defects in DNA cleavage and packaging are due to the mutations within UL15 or UL28. Specifically, deletion of the putative metal-binding domain of UL28 (vFH505) or mutation of amino acids within the UL15 nuclease domain (vFH506, vFH507) was not shown to preclude terminase complex formation, but these viruses were deficient in cleavage and packaging, indicating that the putative metal-binding domain of UL28 and amino acids 509, and 706-707 of UL15 are required for the cleavage and packaging functions of the viral terminase.

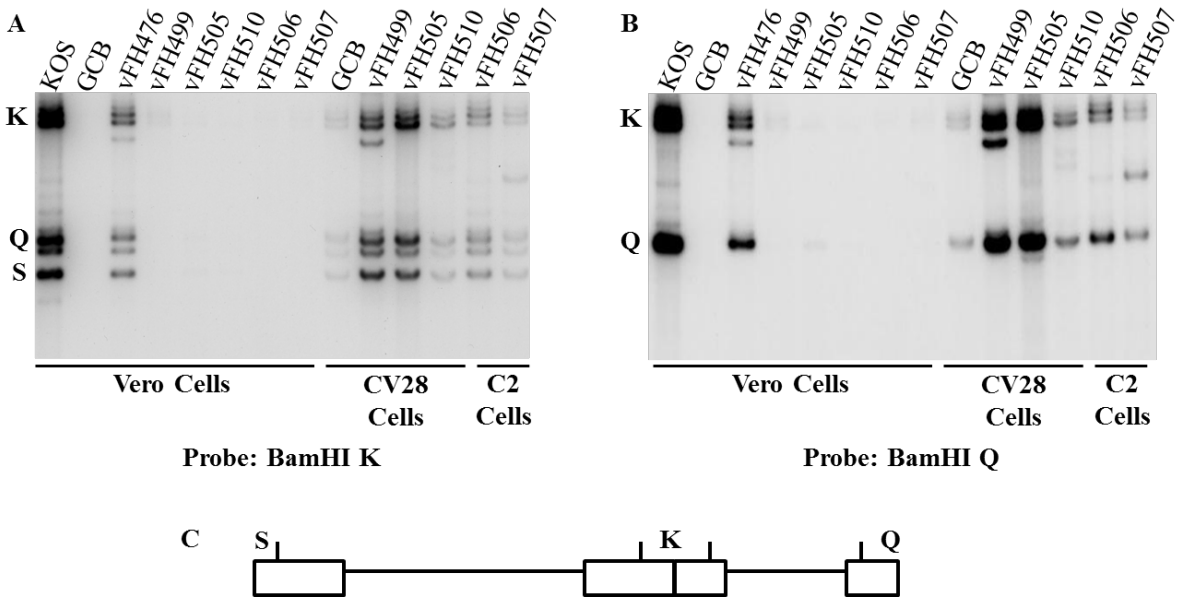

Figure 25. Analysis of viral DNA packaging. Vero, CV28, or C2 cells were infected with the indicated virus at an MOI of 5 PFU per cell. At 18 hpi, DNaseI-protected, total infected cell DNA was isolated, digested with BamHI, and subjected to Southern blot analysis using the (A) BamHI K fragment (32P labeled) or (B) BamHI Q fragment (32P labeled) as a probe (C) The locations of the BamHI K joint-spanning fragment and the two end fragments, BamHI-Q and -S, in the HSV-1 genome.

3.4.4 UL15 and UL28 domain mutations do not affect viral genome replication

Southern blots demonstrating the cleavage and packaging activity of the UL15 and UL28 domain mutant viruses on UL15- or UL28-complementing cell lines also revealed that the overall levels of viral DNA appeared to be significantly lower in the domain mutant viruses compared to wild-type KOS virus. Quantitative real-time PCR (qRT-PCR) was utilized to measure viral genome replication levels in cells infected with the UL15 nuclease domain mutants (vFH506 or vFH507), the UL28 metal-binding domain mutants (vFH505 or vFH510), the full-length or C-terminally truncated NTAP-UL28 fusion viruses (vFH476 or vFH499), or the UL28-null GCB virus. For all viruses, viral genome replication was measured in noncomplementing Vero cells and UL15-complementing C2 cells (vFH506, vFH507) or UL28-complementing CV28 cells (GCB,

vFH499, vFH505, vFH510) and compared to replication by wild-type KOS virus. The results indicate that each recombinant virus did not replicate viral genomes as well as wild-type KOS, but the difference only appears significant (greater than 1 log) with vFH510 replication in Vero and CV28 cells, and GCB replication in UL28-complementing CV28 cells. However, a comparison of replication levels between KOS and vFH510-infected Vero cells over time did not reveal a significant difference in the number of genomes produced by both viruses at any specific time point (Figure 27). Taken together, these results suggest that deletion of the putative metal-binding domain of UL28 (vFH505) or mutation of amino acids within the UL15 nuclease domain (vFH506, vFH507) does not significantly reduce viral genome replication relative to what is observed during wild-type KOS infection.

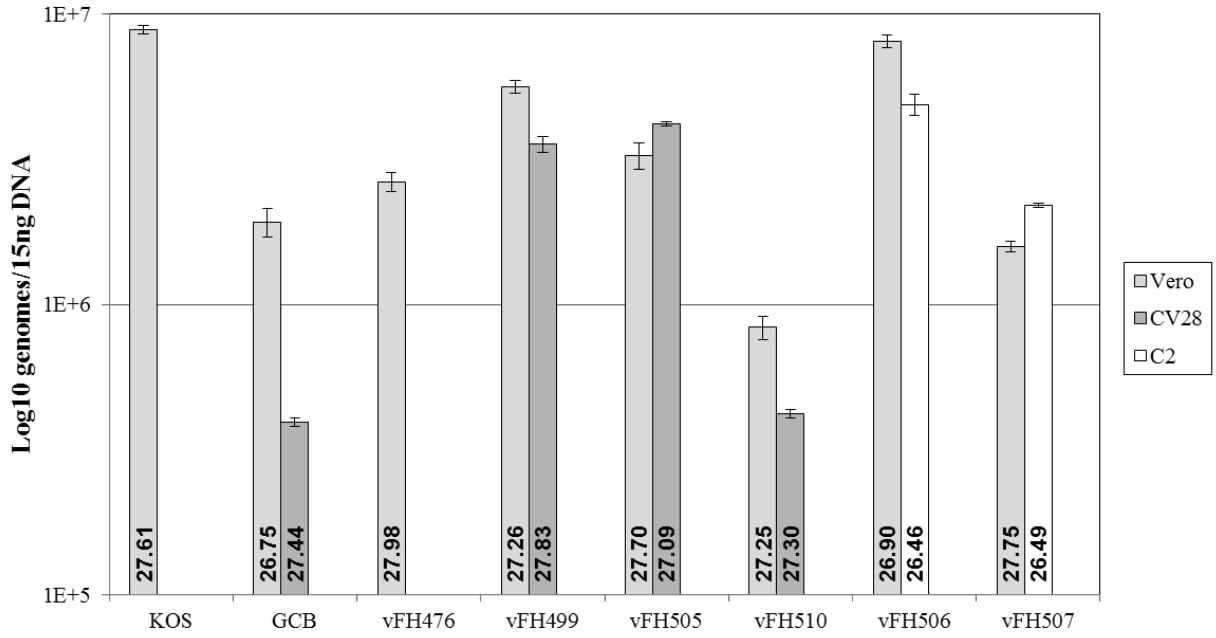

Figure 26. qRT-PCR analysis of viral genome replication. Genome isolation and qRT-PCR for the viral TK gene were performed as described in Materials and Methods. The procedure for creating standard curves for quantification is also described in Materials and Methods. The graphs indicate the number of viral DNA genomes per 15ng DNA at 18 hpi in Vero, CV28, or C2 cells. Numbers at the base of each bar indicate amplification (Ct) of the cellular GAPDH gene to ensure equal amounts of cells were examined. The error bars represent standard deviations from triplicate experiments.

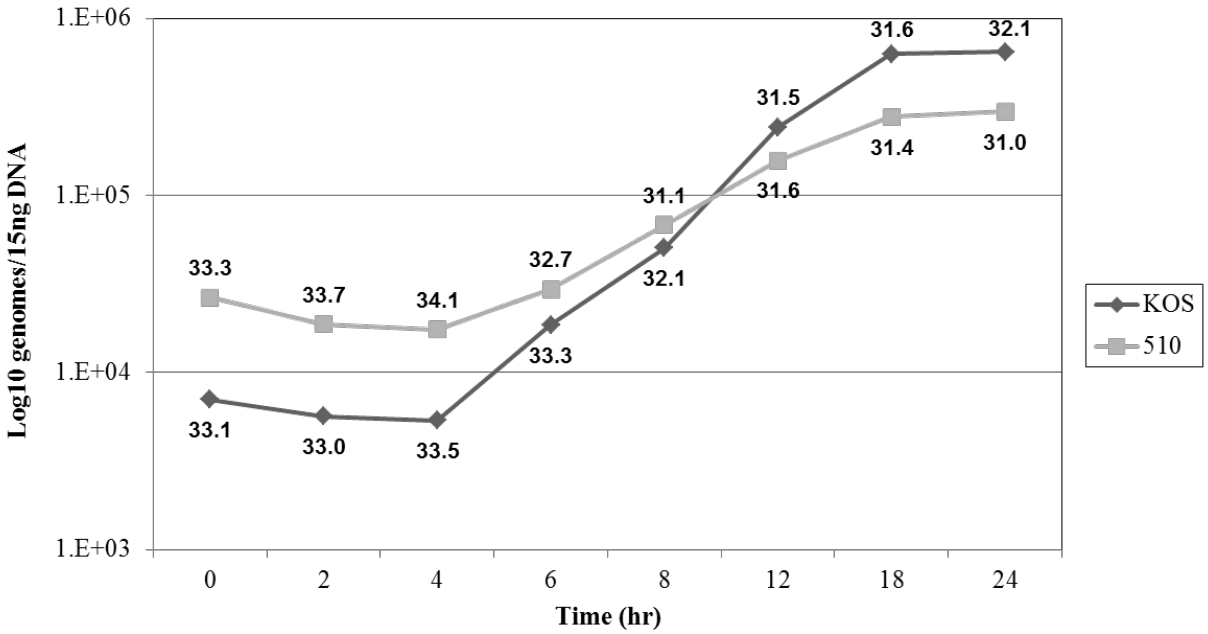

Figure 27. Time course comparing wild-type KOS and vFH510 viral genome replication. Genome isolation and qRT-PCR for the viral TK gene were performed as described in Materials and Methods. The procedure for creating standard curves for quantification is also described in Materials and Methods. The graph indicates the number of viral DNA genomes per 15ng DNA at the indicate time (hpi) in Vero cells. Numbers above or below each time point indicate amplification (Ct) of the cellular GAPDH gene to ensure equal amounts of cells were examined. Each time point was performed in triplicate.

3.5 DISCUSSION

Similar to double-stranded DNA bacteriophage, HSV-1 is thought to encode for a viral terminase complex that cleaves and packages replicated viral DNA into capsids; a process required for productive lytic HSV-1 infection (32). Numerous studies have indicated that the UL15, UL28, and UL33 proteins form the proposed HSV-1 terminase complex and homologs of these proteins appear to form terminases in several other herpesviruses such as HCMV and varicella zoster virus (25, 46, 226, 243-245, 250). Several amino acid domains implicated to mediate terminase complex formation and function(s) have been identified within the UL15 and UL28 subunits and these domains are conserved across the herpesviruses (52, 54, 114, 142). This study was

performed to analyze the effect of mutations introduced within a conserved putative metal-binding motif of UL28 or within the nuclease domain of UL15, in order to determine the importance of these regions in terminase complex formation and function during HSV-1 infection.

Previous studies (Section 2.0) have determined that the HSV-1 terminase complex of interacting UL15, UL28, and UL33 subunits can be isolated by tandem affinity purification (TAP) via fusion of the TAP tag to the N-terminus of UL28. In order to examine the effect of domain mutations on purified terminase complexes, amino acid changes were introduced into the genome of the full-length NTAP-UL28 fusion virus (vFH476) or a second, previously described, NTAP-UL28 fusion virus (vFH499, Section 2.0) that encodes a truncated UL28 protein lacking C-terminal residues required for the interaction of UL15 and UL33 with UL28. A deletion of the putative UL28 metal-binding domain, located at residues 197-228 of the UL28 ORF, was introduced into the genomes of the full-length and C-terminally truncated NTAP-UL28 fusion viruses, generating vFH505 and vFH510 respectively. Site-specific mutations of conserved amino acids within the UL15 nuclease domain were introduced into the genome of the full-length NTAP-UL28 fusion virus, to generate two additional viruses. vFH506 contains the mutation of a conserved aspartic acid residue at position 707 to alanine and a second aspartic acid to alanine mutation at residue 706, while vFH507 also contains the mutation of a conserved aspartic acid at position 509 to alanine. Each of the recombinant domain mutant viruses grew only on UL28- or UL15-complementing cell lines indicating that each mutation resulted in the expression of a nonfunctional UL15 or UL28 protein. Furthermore, only viral B-capsids could be isolated from infected cells suggesting that these proteins were deficient in some aspect of the cleavage and packaging pathway.

TAP of UL28 complexes from cells infected with each of the domain mutant viruses, followed by immunoblotting for the terminase subunits revealed several interesting results. First, only vFH510, which encodes for the deletion of the putative UL28 metal-binding domain and a truncation of the UL28 C-terminus, did not copurify the UL33 protein or significant amounts of the UL15 protein. These results provide further support that the C-terminus of UL28 is essential for terminase complex formation (104, 267), and suggest that the domain mutations within vFH505, vFH506, and vFH507 affect an aspect of terminase complex function. Second, the observation of low level UL15 copurification in vFH510-infected cells supports previous mass spectrometry results, which identified a small number UL15 peptides in complexes purified from cells infected with the C-terminally truncated NTAP-UL28 fusion virus (vFH499), and may suggest that UL15 can interact at a second location internal to the C-terminal 44 amino acids of UL28, but this interaction appears to be of much lower affinity. Finally, previously observed truncated forms of UL28 were observed to copurify with UL28 complexes isolated from cells infected with each of the domain mutant viruses. Also as seen previously, each truncated band was detected when blots were probed with an antibody against the calmodulin-binding peptide located within the N-terminal TAP tag, suggesting that amino acids are missing from the C-terminus of UL28. Further confirmation of a loss of C-terminal amino acids is observed when comparing the mutants encoding the UL28 metal-binding domain deletion (vFH505 and vFH510). Compared to all other virus lanes, the truncated UL28 bands for vFH505 and vFH510 are approximately 3 kDa smaller due to the domain deletion, but when directly compared, the truncated bands are of equal size even though vFH510 also encodes for a 44 amino acid truncation of UL28, and this phenomenon is also observed with vFH499 (NTAP-UL28-741s). It is not known whether these bands are indicative of protein degradation during purification or are

specific cleavage events that perform a viral function. However, it is possible that cleavage of the UL28 C-terminus may function in the dissociation of the terminase from viral capsids upon the completion of packaging. The UL28 and UL15 proteins are not observed to associate with packaged viral capsids or mature virions (16, 126, 204, 223, 274), whereas UL33 associates with each capsid type independently of UL15 or UL28 (15, 179). Therefore, once packaging has completed, cleavage of a large region of the UL28 C-terminus, which is essential for the interaction of UL15 and UL33 with UL28 (104, 267), may function to disrupt the terminase complex or liberate the UL15 and UL28 subunits from UL33 which remains capsid associated.

Southern blot analysis of DNaseI-protected DNA revealed that the UL28 and UL15 mutations resulted in a block in viral DNA cleavage and packaging during the infection of noncomplementing Vero cells. Successful cleavage and packaging of replicated viral DNA was restored within UL15- or UL28-complementing cell lines, indicating that the defect in cleavage and packaging is due to the specific domain mutation. The levels of DNA isolated from each mutant appeared to be lower than with wild-type KOS infection, possibly suggesting lower packaging efficiency or lower levels of viral DNA replication by the mutant viruses. Real-time PCR measurement of viral DNA replication determined that although each recombinant virus did not replicate to wild-type KOS virus levels on noncomplementing or complementing cell lines, the difference was not significant; suggesting that the lower levels of packaged DNA observed with the mutant viruses are not due to a defect in viral DNA replication.

It is important to note that very little is known regarding the oligomeric status of the HSV-1 terminase complex at the capsid portal during the cleavage and packaging process. The functional terminase holoenzyme of dsDNA bacteriophages is a multimer of interacting small and large terminase subunits (72); therefore it appears likely that the HSV-1 terminase would

also function as a multimer. Considering this, it is difficult to exclude the possibility that the UL28 metal-binding domain and UL15 nuclease domain mutations examined in the current study affect the formation of higher order complexes at the capsid portal. However, the observation of what may be reduced DNA packaging efficiency with each of the domain mutant viruses within complementing cell lines may argue that complex formation is occurring. It is possible that each domain mutation results in a dominant-negative effect, with nonfunctional oligomeric terminase complexes forming at the capsid portal that contain mutated and wild-type terminase proteins, although this remains to be further elucidated.

Taken together the results presented in this study suggest that the putative metal-binding domain of UL28 and amino acids 509, and 706-707 of UL15 are not required for terminase complex formation, but are essential for the cleavage and packaging functions of the viral terminase. That deletion of the putative UL28 metal-binding domain alone (vFH505) did not affect complex formation, but precluded viral DNA cleavage and packaging is in agreement with a previous study demonstrating the same phenotype with recombinant viruses possessing amino acid insertions within this domain (104). A previous mutational analysis of the conserved amino acids within the UL15 nuclease domain was performed with the UL15 homolog in HCMV, UL89 (142). This study demonstrated that these conserved amino acids coordinated an interaction with Mn^{2+} ions that is essential for *in vitro* nuclease activity of UL89, and that mutation of the residues to alanine abolished nuclease activity. Therefore it seems highly likely that both UL15 domain mutant viruses used in this study (vFH506 and vFH507) are specifically deficient in nuclease activity, and further experiments will include examining the *in vitro* nuclease activity of purified complexes. Furthermore, these results indicate that the TAP procedure can effectively purify terminase complexes encoding mutations within specific

domains, which will allow for the direct biochemical assessment of the role that each conserved domain may play during HSV-1 infection.

4.0 SUMMARY AND CONCLUSIONS

Productive herpes simplex virus type 1 (HSV-1) infection requires the cleavage of branched, replicated viral DNA concatemers into linear, monomeric genomes that are subsequently packaged into preformed capsids. Gene products of the viral UL6, UL15, UL17, UL25, UL28, UL32, and UL33 genes are essential for DNA encapsidation, and viruses expressing a nonfunctional protein from any of these seven genes are deficient in growth; accumulating replicated concatemeric viral DNA and unpackaged capsid forms within the infected cell nucleus (3, 4, 6, 10, 33, 116, 117, 132, 165, 166, 173, 195, 198, 205, 206, 225, 256, 272). The UL15, UL28, and UL33 proteins form a complex within infected cells that is thought to function similarly to the terminase complexes of double-stranded DNA (dsDNA) bacteriophage (46). The proposed functions of the HSV-1 terminase include: i) binding to replicated viral DNA; ii) cleavage of replicated DNA concatemers into linear, genome-length monomers; iii) association with the immature capsids at a unique portal vertex; and iv) translocation of cleaved, replicated viral DNA into the capsid.

In vitro demonstration of the proposed terminase functions has been hampered by the inability to purify the UL15 and UL28 subunits. However, several genetic and electron microscopy experiments have provided indirect evidence suggesting that the complex of UL15, UL28, and UL33 functions as the HSV-1 terminase (46). Studies have determined that complex formation is essential for function, as viruses encoding mutations that preclude the interaction

UL28 with UL15 or UL33 do not cleave or package replicated viral DNA during infection (18, 104, 225, 267, 269). Cleavage and packaging is also deficient during infection with recombinant viruses encoding mutations within the UL6 portal protein that preclude the interaction of the terminase with the portal complex (270). Studies have shown that the UL15 and UL28 proteins are not associated with packaged C-capsids but are observed on the other capsid forms; suggesting a transient association with unpackaged capsids that is similar to what is observed with terminases of dsDNA bacteriophage (16, 32, 204, 223, 274). Evidence has also come from closely related herpesviruses such as human cytomegalovirus, where strains displaying resistance to inhibitors of viral DNA cleavage were shown to possess mutations within UL89 and UL56, homologs of the HSV-1 UL15 and UL28 proteins respectively (114, 238).

The UL15, UL28, and UL33 proteins are members of a group of approximately 40 genes that are conserved throughout the family *Herpesviridae* (54), and within these proteins several conserved domains have been identified that are implicated in terminase activity (4, 6, 9, 10, 18, 33, 104, 114, 142, 173, 178, 225, 238, 268, 269, 271-273). UL15 is the most highly conserved gene throughout the herpesviruses and is implicated to encode for the nuclease and ATPase activities of the terminase complex (52, 67, 104, 142, 178, 238, 268, 269, 271, 273). The amino acid sequence of UL15 contains Walker A and B box motifs typically found in proteins that metabolize ATP and these residues are conserved within the large terminase subunit of bacteriophage T4 (52, 67, 249, 273). Mutations within, or in close proximity to, these domains preclude cleavage and packaging of viral DNA during infection (178, 273). A C-terminal fragment of the UL15 homolog in human cytomegalovirus (HCMV), UL89, was shown to possess sequence-specific nuclease activity that was dependent on manganese (Mn^{2+}) ions (142). Analysis of the crystal structure of this C-terminal UL89 fragment revealed three amino acid

residues that coordinate Mn^{2+} within the active site that are conserved among the herpesviruses. Further studies using HCMV determined that a mutation within UL56, the homolog of HSV-1 UL28, provided resistance to an inhibitor of viral DNA cleavage (114). This mutation occurred within a stretch of amino acids conserved throughout the *Herpesviridae* and resembles a canonical metal-binding domain.

As previously mentioned, there is limited biochemical data regarding the proposed activities of the terminase subunits. In the only study for HSV-1, the UL28 protein was purified from *E. coli* and shown to specifically bind *pac1*-sequence-containing DNA, which was manipulated to adopt novel confirmations and single-stranded regions. Slightly, more data has been generated using the HCMV UL89 and UL56 terminase subunits (UL15 and UL28 homologs respectively). The UL89 protein has been demonstrated to possess sequence-specific nuclease activity that is enhanced upon the interaction with UL56 (142, 199), while UL56 has been shown to bind specific HCMV DNA sequences (22), and unlike UL28, also encodes for ATPase activity (200).

Fusion of a tandem affinity purification (TAP) tag to the N-terminus of UL28 allows for the isolation of terminase complexes composed of interacting UL15, UL28, and UL33 subunits that are suitable for downstream biochemical analysis. In order to purify endogenous HSV-1 terminase complexes from infected cells, a recombinant virus, vFH475, was generated that expresses a UL28 protein fused to an N-terminal TAP tag (NTAP-UL28). The addition of the TAP tag to the N-terminus of UL28 resulted in a decrease in virus growth of approximately 1 log compared to wild-type KOS virus. The vFH475 virus expressed an NTAP-UL28 protein of expected size but the expression levels, although identical to wild-type KOS, were deemed too low for purification purposes. Therefore a recombinant virus, vFH476, was

created that expresses the NTAP-UL28 fusion under the transcriptional control of the cytomegalovirus (CMV) immediate early promoter. Growth of vFH476 was decreased approximately 1 log compared to KOS, similar to vFH475, indicating that the addition of the CMV promoter did not affect virus growth. The NTAP-UL28 protein of vFH476 was expressed with similar kinetics as the wild-type UL28 protein but expression levels were significantly increased validating CMV promoter use.

TAP of UL28 complexes from vFH476-infected cells followed by immunoblotting for the terminase subunits resulted in the purification of NTAP-UL28 and the copurification of the UL15 and UL33 proteins, while no terminase subunits were purified by TAP when cells were infected with wild-type KOS virus. Furthermore, mass spectrometry analysis of specific SDS-PAGE bands confirmed the purification of each terminase subunit in the vFH476 sample. Silver staining of vFH476-purified complexes revealed the presence of several unidentified proteins copurifying with UL28 complexes that represent potential novel terminase components of viral or cellular origin. These results demonstrate that TAP of an NTAP-UL28 fusion protein from HSV-1-infected cells is an effective method for the purification of endogenous HSV-1 terminase complexes.

Sucrose gradient ultracentrifugation of complexes purified from vFH476-infected cells revealed three significant regions of the gradient. The first contained significant amounts of the UL15, UL28, and UL33 proteins comigrating at a size range of approximately 190 kDa and consistent with a 1:1:1 heterotrimeric complex of the three proteins. The second was consistent with a 1:1 heterodimer of UL28 and UL33, while the final region contained UL33 alone. It is interesting that no regions contained comigrating UL15 and UL28 subunits, although not entirely surprising. Previous studies have suggested that one role for UL33 may be to enhance the

interaction between UL28 and UL15 during complex formation, and it has been shown that in the absence of UL33, the number of interacting UL15 and UL28 subunits is reduced (104, 267, 269). Taken together these results may suggest that terminase complex formation is an ordered process, with UL33 first interacting with UL28, and UL15 binding last. Furthermore, complex formation in this fashion could act to prevent premature nuclear localization of incomplete terminase complexes, as the signal for translocation to the nucleus resides within UL15 (268).

Previous studies have determined that the C-terminus of UL28 is essential for the interaction of the UL15 and UL33 proteins with UL28 (104, 267). The vFH499 virus was generated, which expresses a C-terminally truncated NTAP-UL28 protein under CMV promoter control. The truncation in vFH499 is the result of the insertion of a linker sequence containing an in-frame stop codon after amino acid 741 of UL28, previously shown to preclude the interaction of UL15 and UL33 with UL28 (104). vFH499 replicated to high titers only on a UL28-complementing cell line, and Western blot analysis of proteins isolated by TAP did not detect UL15 or UL33, further confirming that the C-terminus of UL28 is essential for terminase complex formation and function. However, mass spectrometry analysis did identify a small set of peptides copurifying in the vFH499 sample that corresponded to UL15, possibly suggesting that UL15 can interact at a position internal to the C-terminal 44 amino acids of UL28, but that this interaction is of low affinity.

Interestingly, immunoblotting of purified complexes from vFH476 and vFH499-infected cells revealed several truncated forms of UL28. Proteins of approximately 63 and 50 kDa were confirmed to contain UL28 peptides by mass spectrometry, and these truncated proteins were detected by Western blot using an antibody directed against the calmodulin-binding peptide within the N-terminal TAP tag of UL28, indicating that the missing amino acids must be C-

terminal. In order to generate the observed proteins of roughly 63 and 50 kDa, approximately 300 or 400 amino acids, respectively, must be removed from the C-terminus of UL28. This is the first report of truncated forms of UL28 and it is unknown whether they represent byproducts of protein degradation or specific cleavage fragments that function during HSV-1 infection. Previous studies indicate that UL15 and UL28 are not associated with packaged capsids and as mentioned above, the C-terminus of UL28 is required for terminase complex formation (16, 104, 204, 223, 267, 274). Therefore, removal of a large segment of the UL28 C-terminus may function to dissociate the terminase from the portal complex after packaging has completed. Inherent in this proposed mechanism is that each terminase complex could only package one viral genome before being disrupted, and this is in contrast to terminases of dsDNA bacteriophage, which are thought to perform several rounds of DNA packaging (72).

A comprehensive proteomic analysis was performed using complexes purified from vFH476, vFH499, or wild-type KOS-infected cells, and mass spectrometry identified 198 proteins unique to the vFH476 and vFH499 TAP samples compared to the KOS control. Of the 198 proteins, 22 were identified as HSV-1 proteins, while the remaining 176 were of host cell origin, and these were classified into groups based on cellular location or function. Examination of the interacting viral proteins confirmed the interaction of the UL15, UL28, and, UL33 subunits. Of the remaining viral proteins, none were copurified in amounts significant enough to warrant consideration as components of the viral terminase. Furthermore, several of these proteins are known components of the viral tegument and envelope layers and may be indirectly associated with the viral terminase through the isolation of viral capsids by the TAP procedure. The interacting cellular proteins were classified into groups based upon cellular location and/or function and the results indicated that protein components of the host cytoskeleton displayed the

highest spectral count values of any group, possibly suggesting that the terminase complex utilizes host cytoskeletal elements for localization during viral infection. Two cellular proteins were confirmed to interact by Western blot, apoptosis-inducing factor 1 (AIF-1) and DNA damage-binding protein 1 (DDB1). DDB1 functions as a component of host cell repair pathways and previous studies have shown that DDB1 interacts with proteins of several viruses, including herpesviruses, to perform essential functions during viral infection (93, 103, 108, 193, 233). Recently, DDB1 has been shown to interact with the VP8 tegument protein (HSV-1 VP13/14 homolog) of bovine herpesvirus type-1 (BHV), and initial data suggests the monoubiquitination of VP8 by DDB1 (242). Mass spectrometry did not identify the interaction of VP13/14 with UL28 complexes; therefore it appears likely that DDB1 performs a function different from that in BHV. AIF-1 is an essential mitochondrial protein that can translocate to the nucleus and cause caspase-independent apoptosis in times of stress (86, 160). Within HSV-1-infected cells, AIF-1 was shown to translocate to the nucleus, however apoptosis was not observed to occur (277). The results of the current analysis may suggest that UL28 or another component the terminase complex bind AIF-1 before it can effectively initiate apoptosis. Overall, the interaction of host cell components with the viral terminase complex is intriguing as cellular proteins are implicated in the cleavage and packaging process, and further analysis will help to elucidate the potential role of these proteins during HSV-1 infection.

UL28 complexes isolated by TAP were shown to possess nuclease activity in the presence of Mn^{2+} ions that was specific for HSV-1 *a* sequences, similar to the activity seen with a purified fragment of the HCMV UL89 protein (UL15 homolog) (142). Interestingly, complexes purified using the C-terminally truncated NTAP-UL28 fusion (vFH499), which precludes the interaction of the UL15 and UL33 subunits, displayed nuclease activity similar to

that observed with complete terminase complexes (vFH476). These results suggest that the UL28 protein encodes for nuclease activity, and are supported by previous studies demonstrating that the HCMV UL56 terminase subunit possesses nuclease activity (UL28 homolog) (22). However as previously mentioned, mass spectrometry revealed small amounts of UL15 copurifying with the C-terminal NTAP-UL28 protein, which may indicate that UL28 does not possess nuclease activity. Also interesting is that the observed nuclease activity resulted in DNA degradation similar to that observed in nuclease assays examining the purified UL89 protein (UL15 homolog) of HCMV (142, 199), and may suggest that terminase nuclease activity *in vitro* is nonspecific, possibly due to complex stoichiometry. The terminase complexes isolated and examined in this study may not possess the correct stoichiometry and/or may not be properly assembled at the capsid portal, resulting in terminase DNA degradation as opposed to specific cleavage events.

Mutations within the putative metal-binding domain of UL28 or the nuclease domain of UL15 do not preclude terminase complex formation but are essential for terminase activity. Four HSV-1 recombinant viruses were generated that express the NTAP-UL28 protein under CMV promoter control and also encode for mutations within the putative metal-binding domain of UL28 or nuclease domain of UL15. The vFH505 and vFH510 viruses contain a deletion of the UL28 putative metal-binding domain (residues 197-225), and vFH510 also contains an insertion mutation resulting in the expression of a UL28 truncation of the C-terminal 44 amino acids required for UL15 and UL33 binding. The vFH506 and vFH507 viruses encode site-specific mutations of conserved amino acids within the UL15 nuclease domain. vFH506 contains the mutation of a conserved aspartic acid residue at position 707 to alanine and a second aspartic acid to alanine mutation at residue 706, while vFH507 contains the mutation of

a conserved aspartic acid at position 509 to alanine. Each virus grew to high titers only on UL15 or UL28 complementing cell lines and produced only viral B-capsids during infection, indicating that each mutated UL15 or UL28 protein was nonfunctional.

TAP and Western blotting demonstrated that complexes consisting of interacting UL15, UL28, and UL33 subunits were isolated from cells infected with each mutant virus except for vFH510, which is missing the C-terminal UL28 residues essential for complex formation. These results suggested that for the remaining three viruses, (vFH505-vFH507) the observed defect in virus growth was not due to a defect in terminase complex formation. Western blots also revealed the previously observed truncated forms of UL28. Also as seen previously, the approximately 60 and 50 kDa fragments were detected for each mutant virus (bands were shifted down by ~3 kDa in vFH505 and vFH510 due to the metal-binding domain deletion) using an antibody against the calmodulin-binding peptide of the N-terminal UL28 TAP tag, indicating that amino acids were removed from the C-terminus of UL28.

Southern blot analysis of DNaseI-protected viral DNA isolated from infected cells demonstrated that each domain mutant virus was deficient in cleavage and packaging of replicated viral DNA. Infection of UL15 or UL28 complementing cells restored the ability of each mutant virus to cleave and package DNA, although the amount of packaged DNA was reduced compared to wild-type KOS. Real time PCR measurement of viral genomes replicated during infection of complementing or noncomplementing cells revealed that although replication was not as efficient with each mutant virus as with wild-type KOS, the observed reduction was not significant. These results suggest that the putative metal-binding domain of UL28 and amino acids 509, and 706-707 of UL15 are not required for terminase complex formation, but are essential for the cleavage and packaging functions of the viral terminase.

Ongoing experiments and future directions. The results of the experiments presented herein raise several additional questions regarding the assembly and function of the HSV-1 terminase complex during viral infection. The mass spectrometry, sucrose density gradient centrifugation, and Western blotting analysis all support that the HSV-1 terminase complex consists of interacting UL15, UL28, and UL33 subunits. However, there is the overlying question of complex stoichiometry and whether a multimeric terminase complex is required for biochemical activity. Future experiments could involve attempting to visualize the terminase complex at the portal vertex of isolated capsids by electron microscopy and 3D image reconstruction. However, the difficulty in this method would lie in determining and aligning the portal-containing vertexes of each capsid, which would be required for accurate 3D image reconstruction. It may also be possible to glean information regarding complex stoichiometry from a comparative analysis of terminase protein subunit levels found associated with isolated A-, B-, and C-capsids by Western blot analysis. The use of a standard protein, such as the VP5 major capsid protein, would allow for the quantitation and estimation of terminase subunit levels associated with each capsid type, and this information could be utilized to estimate the copy number of each terminase subunit per capsid relative to the known amount of VP5 that composes each HSV-1 capsid. Critical to this procedure is the purity of the isolated A-, B-, and C-capsid samples, and it is also essential that the terminase subunits are not stripped or dissociate from capsids during the capsid isolation procedure. It would also be interesting to examine isolated A-, B-, and C-capsids by Western blot for the C-terminally truncated forms of the UL28 protein, as the presence or absence of these peptides may provide insight into their potential function during HSV-1 infection.

In discussing the capsid association of the terminase, it should also be noted that it is largely unknown which amino acids of the terminase subunits mediate this interaction(s). Therefore, the association of the terminase subunits with isolated viral A-, B-, and C- capsids should be examined by Western blot for each of the recombinant viruses generated in this study. These results would be of particular interest in regards to the UL28 metal-binding domain mutants (vFH505, vFH510) and the UL15 nuclease domain mutants (vFH506, vFH507) which were deficient in cleavage and packaging of viral DNA. It may be that these mutations preclude or diminish the association of the terminase with the capsid, which would also preclude the DNA encapsidation process.

The mass spectrometry analysis performed in these studies identified the novel interaction of the cellular AIF-1 and DDB1 proteins with the viral terminase, and future experiments will aim to elucidate the role of these proteins during viral infection. Currently experiments are in progress that will examine the effect of siRNA-knockdown of AIF-1 or DDB1 on HSV-1 proliferation. It may also be of benefit to further confirm the interaction between these proteins by colocalization assays performed at various times post-infection. Mass spectrometry analysis also resulted in the identification of several viral and cellular proteins interpreted to be nonspecific or indirectly interacting proteins. Future mass spectrometry experiments could take advantage of recombinant viruses for the further elimination of nonspecific interactors. For example, the inclusion of a virus that encodes a deleted UL15 nuclear localization signal (previously generated in {Yang, 2007 #9}) would allow for the identification and/or elimination of proteins that only interact with the terminase complex in the cytoplasm of the host cell. Another example would be to utilize a virus that is deficient or

diminished in the interaction of the terminase with the viral capsid, which may help to identify and reduce the number of nonspecific tegument and envelope interactions.

The research presented herein has demonstrated that TAP of an NTAP-UL28 fusion protein can be utilized to isolate the endogenous terminase complex from HSV-1-infected cells, greatly expanding the number of biochemical assays available for the study of the terminase proteins. Specifically, it is now possible to examine those biochemical activities attributed to the HSV-1 terminase by analogy with the terminase complexes of dsDNA bacteriophage, such as nuclease, ATPase, and DNA-binding activity. These results have also demonstrated the ability to purify terminase complexes from cells infected with recombinant viruses that encode deletions or mutations of specific conserved amino acids within the terminase subunits, allowing further elucidation of those domains that are essential for terminase complex assembly and function during the context of viral infection. Future experiments will include examining the UL28 metal-binding domain mutants (vFH505, vFH510) and the UL15 nuclease domain mutants (vFH506, vFH507) in the nuclease activity assay to determine those residues of UL15 or UL28 that are required for activity. Current work in the laboratory is focused on generating recombinant viruses that encode site-specific mutations of the conserved histidine and/or cysteine residues within the putative UL28 metal-binding domain. Each recombinant virus could then be utilized in ATPase, DNA-binding, and nuclease assays to examine the effect/importance of these residues during viral DNA cleavage and packaging. Finally, these results suggest that it is now theoretically possible to attempt to recapitulate DNA packaging *in vitro* by combining isolated UL28 complexes, capsids, viral DNA, and ATP and performing Southern blot analysis on each sample for the presence of DNaseI protected DNA.

Model for terminase activity. In conclusion the findings of this study shed new light onto the mechanism of terminase complex formation and function during HSV-1 lytic infection. Based upon these results and previous findings from numerous studies, we propose the following model for terminase activity during DNA encapsidation. Within the cytoplasm of the infected cell the UL28 and UL33 proteins initially interact, then UL15 is added to the complex last. This ordered terminase assembly may serve three functions: i) to protect UL33 from degradation (104, 267); ii) to enhance the interaction between UL15 and UL28 (104, 267, 269); and iii) to prevent the premature nuclear localization of complexes. The assembled complex localizes to replication compartments within the nucleus via the nuclear localization signal (NLS) of UL15 (91, 268), where UL28 binds the replicated viral DNA concatemer and scans for specific sequences (5, 22). Recognition of a *pac2* site in the correct orientation activates the endonuclease activity of UL15, resulting in DNA cleavage within an upstream DR1 element and generating a free L-terminus for packaging (92, 142, 199, 241). The terminase, with bound viral DNA, docks at the UL6 portal of assembled procapsids in an orientation that positions UL15 in close proximity to the portal (16, 258, 263, 270). This interaction activates the ATP-dependent DNA translocation activity of UL15 (51, 148, 273), and DNA packaging triggers protease activation, resulting in scaffold cleavage and procapsid maturation to the icosahedral form (39, 90, 151, 170). DNA translocation begins at the L-component, and continues through the junction and into the S-component (148). As packaging nears completion, UL28 recognizes single-stranded *pac1* sequences within the *a* sequence of the S-component (5), and the second UL15-mediated cleavage occurs (92, 142, 199, 241). Cleavage frees the genome from the concatemer and packaging completes. The terminase components subsequently disassociate from the viral capsid (16, 204, 223, 274), possibly through cleavage of a large C-terminal region of UL28.

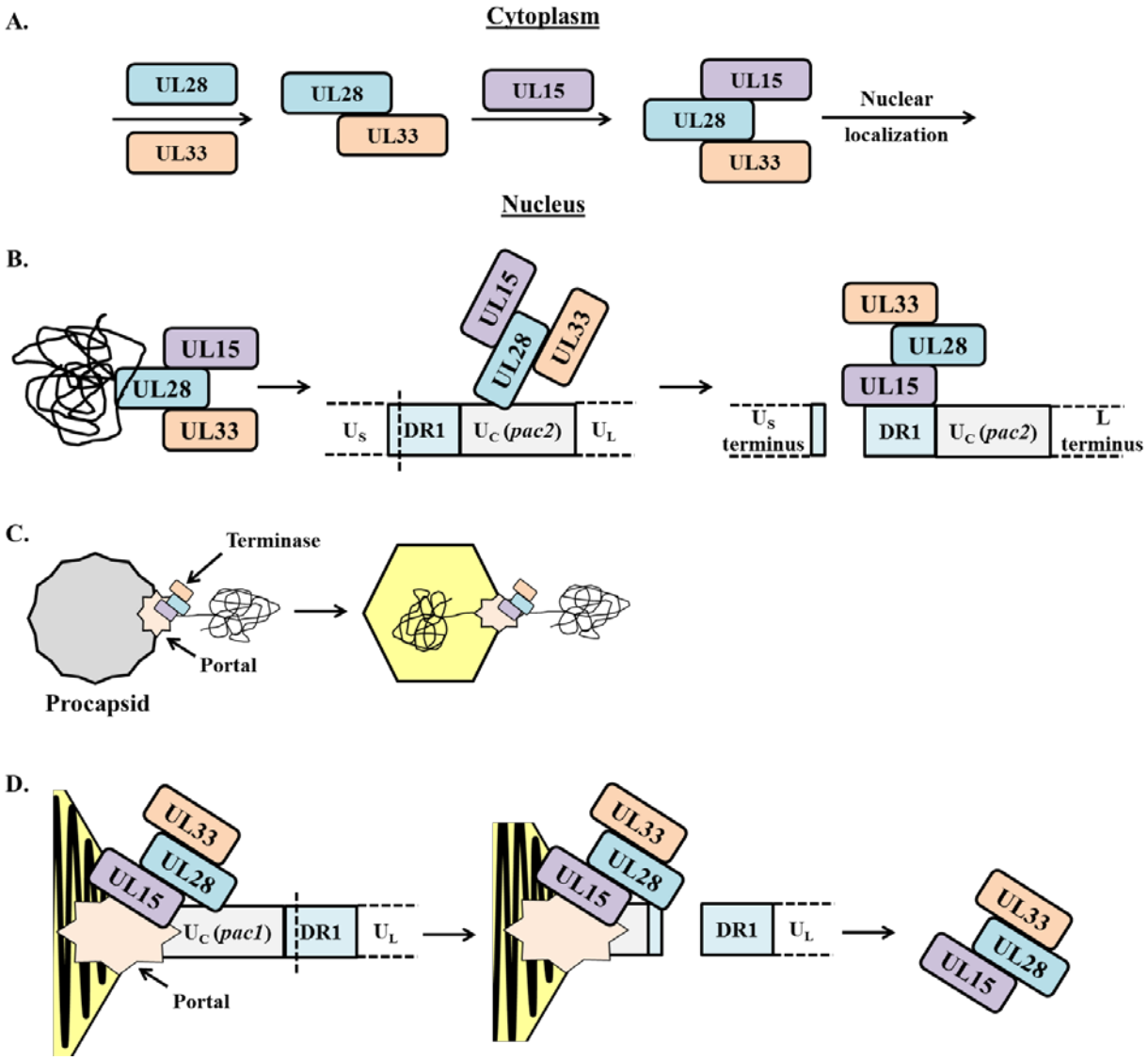

Figure 28. Model of terminase formation and function during HSV-1 infection. (A) Complex formation occurs in the cytoplasm of the infected cell in an ordered fashion with UL28 and UL33 interacting first and UL15 added last. The complex translocates to the nucleus via an NLS within UL15. (B) In the nucleus UL28 binds replicated viral DNA, and when a *pac2* motif is encountered, UL15 cleaves the DNA within an upstream DR1 element, generating a free L-terminus for packaging. (C) The terminase complex with bound DNA docks at the UL6 portal of a procapsid, triggering UL15-mediated DNA translocation that proceeds directionally from the L terminus and into the S component of the viral genome. DNA packaging results in scaffold cleavage and capsid maturation. (D) Upon encountering a *pac1* motif within the S terminus, a second cleavage occurs, and packaging completes. The terminase then dissociates from the portal, possibly through cleavage of the UL28 protein

Taken together, the results of these studies have demonstrated that TAP of a UL28 fusion protein is an effective method for the purification of the endogenous HSV-1 terminase complex

from infected cells. Purification of endogenous terminase complexes is novel to the field and greatly expands the number of available experiments for the analysis of terminase complex formation and function during HSV-1 infection. Most importantly, this method should allow for the direct biochemical analysis of purified complexes and the demonstration of each of the proposed terminase activities which include ATPase, nuclease, and DNA-binding activity. Elucidation of the requirements for each of these activities will greatly aid in the production of novel antivirals to inhibit these terminase functions. Furthermore, the large degree of protein sequence conservation between the herpesviruses suggests that these results should provide data relevant to the treatment of other, more life-threatening, herpesvirus infections, such as those observed with HCMV.

APPENDIX A

SUPPLEMENTARY DATA

Table 12. Interacting HSV-1 protein (complete)

Protein group		Protein	MW[a]	No. of unique peptides			% Coverage			Spectral counts		
				476	499	KOS	476	499	KOS	476	499	KOS
Capsid/Packaging												
	UL6	Portal	74	12	3	-	21	5.3	-	16	3	-
	UL15	Terminase	81	82	31	6	97	50	6.4	1714	69	7
	UL19	VP5	149	84	84	52	76	77	50	623	807	120
	UL25	CVSC	63	22	22	6	46	41	9.5	45	53	11
	UL28	Terminase	86	110	89	25	98	89	27	3499	2072	138
	UL33	Terminase	14	17	-	-	78	-	-	70	-	-
Tegument												
	RL2	ICP0	78	3	-	-	6.7	-	-	6	-	-
	RS1	ICP4	133	19	16	-	17	14	-	37	29	-
	UL13	Protein kinase	57	14	14	3	19	24	8.5	27	28	3
	UL14		24	10	8	3	39	21	12	12	11	3
	UL36	ICP1/2	336	117	123	21	44	47	8.2	283	342	23
	UL49	VP22	32	13	11	-	34	50	-	25	19	-
	UL50	dUTPase	39	16	10	7	37	18	13	42	14	7
	UL51		25	7	7	3	32	44	17	18	17	3
Envelope												
	UL44	gC	55	11	11	-	32	31	-	70	72	-
	US7	gI	41	5	6	-	16	18	-	22	26	-
	UL22	gH	90	10	14	-	13	19	-	15	39	-
	UL53	gK	38	2	4	-	6.8	13	-	5	5	-
	UL1	gL	25	13	14	3	41	45	13	34	37	4
	US6	gD	43	5	6	3	15	18	7.4	18	13	4
	US8	gE	59	16	12	11	31	24	25	68	50	16
Misc.												
	UL5	Helicase-primase	99	10	10	-	6.7	6.7	-	25	20	-

[a]MW, (kDa)

Table 13. Interacting cellular proteins (complete)

Protein	MW[a]	No. of unique peptides			% Coverage			Spectral counts		
		476	499	KOS	476	499	KOS	476	499	KOS
116 kDa U5 small nuclear ribonucleoprotein component isoform b	105	7	2	-	8.6	2.0	-	7	2	-
26S protease regulatory subunit 4	41	3	2	-	11.0	11.0	-	5	5	-
39S ribosomal protein L13, mitochondrial	21	5	-	-	27.0	-	-	5	-	-
40S ribosomal protein S10	19	9	2	2	40.0	11.0	12.0	13	4	2
40S ribosomal protein S14	18	13	11	5	44.0	38.0	29.0	56	26	8
40S ribosomal protein S15	17	6	4	2	23.0	23.0	14.0	11	6	2
40S ribosomal protein S16	16	28	23	11	94.0	82.0	54.0	98	76	24
40S ribosomal protein S17	16	5	5	-	35.0	36.0	-	9	8	-
40S ribosomal protein S18	18	25	24	10	75.0	75.0	51.0	73	46	13
40S ribosomal protein S23	16	13	8	5	57.0	42.0	30.0	21	10	5
40S ribosomal protein S26	13	4	-	-	37.0	-	-	6	-	-
40S ribosomal protein S27	10	9	9	2	50.0	50.0	25.0	24	19	2
40S ribosomal protein S27-like	9	2	2	-	45.0	45.0	-	19	15	-
40S ribosomal protein S29 isoform 1	7	5	3	-	71.0	45.0	-	8	4	-
40S ribosomal protein S4, X isoform X isoform	28	19	15	7	48.0	49.0	22.0	35	22	7
40S ribosomal protein S6	29	12	7	3	29.0	22.0	10.0	23	7	3
60 kDa heat shock protein, mitochondrial	61	3	4	-	71.0	72.0	-	247	662	-
60S acidic ribosomal protein P0	34	6	5	-	18.0	21.0	-	7	6	-
60S ribosomal protein L10a	25	9	7	-	43.0	37.0	-	12	8	-
60S ribosomal protein L10-like	25	11	5	-	43.0	21.0	-	16	8	-
60S ribosomal protein L17 isoform a	23	4	2	-	19.0	10.0	-	5	2	-
60S ribosomal protein L23	15	10	9	2	58.0	54.0	14.0	32	19	2
60S ribosomal protein L24	18	8	3	-	44.0	16.0	-	18	7	-
60S ribosomal protein L37a	10	8	4	-	49.0	26.0	-	9	5	-
60S ribosomal protein L4	48	9	-	-	17.0	-	-	9	-	-
60S ribosomal protein L6	33	9	-	-	34.0	-	-	10	-	-

[a]MW, (kDa)

Table 13. (continued)

Protein	MW[a]	No. of unique peptides			% Coverage			Spectral counts		
		476	499	KOS	476	499	KOS	476	499	KOS
abhydrolase domain-containing protein FAM108B1 isoform 1 precursor	33	7	2	-	20.0	8.5	-	9	2	-
acyl-coenzyme A thioesterase 8	36	6	2	-	21.0	9.4	-	6	2	-
adipocyte plasma membrane-associated protein	47	8	7	-	17.0	16.0	-	9	10	-
ADP-ribosylation factor-like protein 1	16	4	5	-	21.0	35.0	-	9	8	-
ADP-ribosylation factor-like protein 8B	22	4	3	-	15.0	12.0	-	5	3	-
AIF-1	66	23	24	-	35.0	41.0	-	43	43	-
alpha-crystallin B chain	20	12	8	-	54.0	36.0	-	17	9	-
aminoacyl tRNA synthase complex-interacting multifunctional protein 2	33	4	3	-	13.0	8.6	-	5	4	-
baculoviral IAP repeat-containing protein 6	525	6	26	-	1.4	4.8	-	8	37	-
BAG family molecular chaperone regulator 2	24	10	14	-	56.0	64.0	-	21	30	-
CAAX prenyl protease 2 isoform 1	36	4	4	-	13.0	13.0	-	5	4	-
CAD protein	246	41	47	12	19.0	22.0	6.1	75	101	14
carbonyl reductase family member 4	25	13	11	5	45.0	38.0	21.0	21	14	5
cathepsin L1 preproprotein	37	5	3	-	11.0	4.2	-	9	3	-
cation-independent mannose-6-phosphate receptor precursor	267	14	14	-	6.0	6.1	-	14	14	-
CDP-diacylglycerol--inositol 3-phosphatidyltransferase	27	7	6	-	27.0	22.0	-	28	27	-
choline/ethanolaminephosphotransferase 1	47	4	4	-	8.2	10.0	-	10	7	-
complement component 1 Q subcomponent-binding protein, mitochondrial precursor	32	7	6	-	31.0	28.0	-	14	11	-
cytochrome c oxidase subunit II	26	5	4	-	21.0	12.0	-	7	7	-
cytoplasmic dynein 1 heavy chain 1	531	203	186	42	42.0	36.0	7.8	381	385	57
D-beta-hydroxybutyrate dehydrogenase, mitochondrial precursor	38	14	8	3	35.0	21.0	5.0	20	16	4
DNA damage-binding protein 1	124	34	22	2	36.0	21.0	1.9	40	25	2
DNA-dependent protein kinase catalytic subunit isoform 1	469	168	149	29	39.0	36.0	7.4	291	252	39
DNA-directed RNA polymerase II subunit RPB2	134	8	16	-	8.7	13.0	-	8	26	-
dnaJ homolog subfamily A member 2	46	13	14	3	32.0	37.0	6.3	26	27	3
dnaJ homolog subfamily B member 6 isoform b	36	2	2	-	6.1	6.1	-	5	4	-
dolichyl-diphosphooligosaccharide--protein glycosyltransferase subunit 1 precursor	69	5	3	-	8.2	4.9	-	5	5	-
double-strand-break repair protein rad21 homolog	72	5	12	-	6.7	22.0	-	7	15	-
E3 ubiquitin-protein ligase listerin	201	17	22	-	9.6	13.0	-	20	24	-
E3 ubiquitin-protein ligase UBR4	562	8	-	-	1.5	-	-	8	-	-
E3 ubiquitin-protein ligase UBR5	309	61	10	-	27.0	3.4	-	89	14	-
ER lumen protein retaining receptor 2 isoform 1	24	3	3	-	10.0	13.0	-	8	6	-
estradiol 17-beta-dehydrogenase 11 precursor	33	3	5	-	10.0	20.0	-	6	5	-

[a]MW, (kDa)

Table 13. (continued)

Protein	MW[a]	No. of unique peptides			% Coverage			Spectral counts		
		476	499	KOS	476	499	KOS	476	499	KOS
estradiol 17-beta-dehydrogenase 12	35	5	8	-	17.0	24.0	-	10	10	-
extended synaptotagmin-2	99	7	17	-	4.5	17.0	-	11	23	-
fatty acyl-CoA reductase 1	60	8	9	-	16.0	19.0	-	16	12	-
fatty aldehyde dehydrogenase isoform 1	58	11	9	-	24.0	23.0	-	17	13	-
filamin-A isoform 1	276	10	13	-	6.4	7.1	-	13	20	-
filamin-C isoform b	284	38	45	6	18.0	19.0	2.8	41	47	6
galectin-3 isoform 1	27	8	3	-	23.0	16.0	-	11	8	-
general transcription factor II-I isoform 2	110	5	14	-	5.3	18.0	-	5	17	-
glutamate dehydrogenase 1, mitochondrial precursor	62	9	8	-	21.0	18.0	-	11	11	-
glycerol-3-phosphate acyltransferase 3	31	3	2	-	9.8	7.6	-	5	2	-
GTPase HRas isoform 1	21	2	-	-	26.0	-	-	5	-	-
GTP-binding protein Rheb	20	6	4	-	22.0	21.0	-	17	9	-
HEAT repeat-containing protein 1	243	16	20	-	7.9	10.0	-	16	24	-
heat shock protein beta-1	23	16	17	6	68.0	68.0	33.0	42	39	6
heat shock protein HSP 90-alpha isoform 2	58	3	6	-	10.0	19.0	-	10	33	-
heterogeneous nuclear ribonucleoprotein F	46	12	10	3	31.0	31.0	10.0	29	19	7
heterogeneous nuclear ribonucleoprotein U isoform b	84	8	6	2	9.3	6.0	3.0	10	9	2
heterogeneous nuclear ribonucleoproteins C1/C2 isoform b	32	7	5	-	19.0	14.0	-	11	5	-
huntingtin	347	6	4	-	1.8	0.6	-	6	4	-
integrin beta-4 isoform 3 precursor	71	8	13	-	15.0	26.0	-	10	22	-
integrin beta-4 isoform 3 precursor	63	4	7	-	7.6	16.0	-	5	10	-
keratin, type I cytoskeletal 28	53	3	2	-	13.0	11.0	-	44	48	-
L-lactate dehydrogenase B chain	37	2	3	-	13.0	11.0	-	5	5	-
lysophospholipid acyltransferase LPCAT4	57	8	6	-	20.0	19.0	-	13	6	-
microtubule-actin cross-linking factor 1 isoform a	338	23	29	-	9.4	11.0	-	25	39	-
midasin	460	54	21	-	11.0	5.2	-	80	23	-
midasin	55	13	7	-	24.0	14.0	-	21	9	-
mitochondrial dicarboxylate carrier	32	5	5	-	14.0	16.0	-	5	5	-
mitochondrial glutamate carrier 1	35	8	5	-	25.0	13.0	-	8	9	-
mitochondrial import inner membrane translocase subunit TIM50	50	17	18	6	28.0	33.0	16.0	44	35	7
mitochondrial ribonuclease P protein 1	49	10	-	-	29.0	-	-	10	-	-
mitochondrial translocator assembly and maintenance protein 41 homolog precursor	36	4	-	-	14.0	-	-	5	-	-
MLN64 N-terminal domain homolog	25	4	5	-	24.0	31.0	-	5	7	-
myeloid leukemia factor 1 isoform 3	34	5	4	-	20.0	16.0	-	9	6	-
myosin light chain kinase 2, skeletal/cardiac muscle	62	4	4	-	2.2	3.3	-	61	45	-

[a]MW, (kDa)

Table 13. (continued)

Protein	MW[a]	No. of unique peptides			% Coverage			Spectral counts		
		476	499	KOS	476	499	KOS	476	499	KOS
NADH dehydrogenase [ubiquinone] iron-sulfur protein 2, mitochondrial isoform 1 precursor	44	11	10	3	33.0	30.0	7.5	18	18	4
NADH dehydrogenase [ubiquinone] iron-sulfur protein 3, mitochondrial precursor	30	9	11	2	28.0	44.0	9.8	13	18	3
NADH dehydrogenase [ubiquinone] iron-sulfur protein 7, mitochondrial	23	9	5	2	30.0	21.0	11.0	22	13	5
NADH dehydrogenase [ubiquinone] iron-sulfur protein 8, mitochondrial precursor	24	5	-	-	22.0	-	-	6	-	-
nesprin-2 isoform 5	397	21	2	-	6.4	0.7	-	21	2	-
NME1-NME2 protein	30	6	6	-	21.0	24.0	-	11	14	-
nuclear pore complex protein Nup205	228	12	17	-	6.4	9.8	-	12	17	-
nuclear pore membrane glycoprotein 210 precursor	205	5	8	-	2.6	4.2	-	5	8	-
nucleoporin NUP188 homolog	145	11	5	-	9.5	4.4	-	14	7	-
nucleoprotein TPR	79	2	3	-	2.3	3.8	-	6	9	-
nucleoside diphosphate kinase 3 precursor	18	9	11	-	44.0	50.0	-	15	14	-
nucleosome assembly protein 1-like 1	45	5	4	-	15.0	12.0	-	10	5	-
PDZ and LIM domain protein 7 isoform 2	34	4	4	-	19.0	19.0	-	6	6	-
peroxiredoxin-6	25	5	6	-	27.0	21.0	-	6	6	-
pre-mRNA-processing-splicing factor 8	268	19	-	-	3.9	-	-	27	-	-
probable dimethyladenosine transferase	36	12	4	3	33.0	12.0	8.9	12	6	3
probable E3 ubiquitin-protein ligase HERC1	532	11	-	-	2.2	-	-	14	-	-
probable phospholipid-transporting ATPase IB	133	2	-	-	0.8	-	-	5	-	-
probable ubiquitin carboxyl-terminal hydrolase FAF-X isoform 3	291	7	3	-	2.4	1.2	-	7	3	-
prohibitin-2 isoform 2	34	5	5	-	18.0	14.0	-	5	6	-
proliferating cell nuclear antigen	29	11	8	-	39.0	24.0	-	15	14	-
protein disulfide-isomerase TMX3 precursor	52	6	3	-	8.8	5.3	-	6	4	-
protein KIAA1967	103	16	5	3	19.0	5.7	3.1	35	5	3
protein SCO2 homolog, mitochondrial precursor	30	4	4	-	18.0	18.0	-	5	4	-
protein SON isoform F	160	5	-	-	3.9	-	-	5	-	-
protein transport protein Sec16A	231	15	13	-	7.2	5.2	-	24	22	-
protein transport protein Sec61 subunit alpha isoform 1	46	12	13	-	23.0	24.0	-	28	24	-
ras-related protein Rab-1B	22	2	-	-	32.0	-	-	11	-	-
ras-related protein Rab-39A	25	7	5	-	43.0	33.0	-	9	10	-
ras-related protein Rab-5A	24	2	3	-	20.0	27.0	-	6	6	-
ras-related protein Rab-5C isoform a	23	9	5	2	49.0	21.0	11.0	10	6	2
ras-related protein Rab-6A isoform b	23	3	3	-	23.0	19.0	-	5	7	-
ras-related protein Rab-7L1 isoform 1	23	20	15	-	70.0	69.0	-	24	25	-
ras-related protein Rab-9A	23	5	3	-	29.0	23.0	-	6	4	-

[a]MW, (kDa)

Table 13. (continued)

Protein	MW[a]	No. of unique peptides			% Coverage			Spectral counts		
		476	499	KOS	476	499	KOS	476	499	KOS
reticulocalbin-2 precursor	37	4	4	-	12.0	15.0	-	7	9	-
ribonuclease inhibitor	49	7	-	-	18.0	-	-	7	-	-
RING finger protein 213 isoform 3	373	77	52	-	24.0	17.0	-	129	71	-
RING finger protein 213 isoform 3	19	3	2	-	23.0	12.0	-	6	2	-
RNA-binding protein Raly isoform 2	30	6	-	-	20.0	-	-	9	-	-
rRNA 2'-O-methyltransferase fibrillarin	34	5	4	-	15.0	16.0	-	8	4	-
ruvB-like 1	50	3	11	-	5.9	27.0	-	5	13	-
sarcoplasmic/endoplasmic reticulum calcium ATPase 2 isoform b	111	12	16	-	11.0	15.0	-	18	28	-
serine palmitoyltransferase 1 isoform a	53	18	19	-	29.0	37.0	-	42	30	-
serine palmitoyltransferase 2	58	6	6	-	11.0	9.4	-	7	6	-
serine/threonine-protein phosphatase 6 catalytic subunit isoform b	35	5	5	-	15.0	11.0	-	8	5	-
serine/threonine-protein phosphatase PP1-beta catalytic subunit isoform 1	36	4	2	-	34.0	40.0	-	10	10	-
serine-protein kinase ATM	338	6	-	-	1.9	-	-	6	-	-
serpin B3	45	5	-	-	9.5	-	-	8	-	-
serum paraoxonase/arylesterase 2 isoform 1	41	10	9	-	42.0	30.0	-	21	29	-
short/branched chain specific acyl-CoA dehydrogenase, mitochondrial precursor	46	5	9	-	16.0	26.0	-	5	10	-
stromal cell-derived factor 2-like protein 1 precursor	23	4	3	-	32.0	21.0	-	6	5	-
structural maintenance of chromosomes protein 1A	143	28	40	-	23.0	31.0	-	34	53	-
structural maintenance of chromosomes protein 3	142	15	46	-	9.9	40.0	-	21	56	-
succinyl-CoA ligase [ADP-forming] subunit beta, mitochondrial precursor	49	11	8	-	20.0	15.0	-	14	12	-
tail-anchored protein insertion receptor WRB isoform 1	20	3	5	-	18.0	37.0	-	6	8	-
TBC1 domain family member 8B isoform a	134	6	5	-	6.1	5.0	-	6	6	-
T-complex protein 1 subunit alpha isoform a	60	6	7	-	11.0	15.0	-	8	10	-
titin isoform novex-2	2284	4	6	-	0.1	0.1	-	9	6	-
transcription elongation factor SPT6	199	3	-	-	1.3	-	-	6	-	-
translational activator GCN1	293	23	24	-	10.0	10.0	-	26	26	-
translocon-associated protein subunit delta isoform 2 precursor	19	9	9	-	44.0	44.0	-	18	18	-
tubulin alpha-1C chain	50	34	38	15	73.0	74.0	45.0	237	273	35
tubulin alpha-1C chain	50	2	2	-	73.0	74.0	-	230	258	-
tubulin alpha-1C chain	50	2	4	-	53.0	58.0	-	167	191	-
tubulin alpha-4A chain	50	4	6	-	60.0	66.0	-	183	209	-
tubulin beta chain	50	7	7	5	86.0	78.0	48.0	332	363	48

[a]MW, (kDa)

Table 13. (continued)

Protein	MW[a]	No. of unique peptides			% Coverage			Spectral counts		
		476	499	KOS	476	499	KOS	476	499	KOS
tubulin beta-2A chain	50	5	4	-	68.0	60.0	-	269	280	-
tubulin beta-3 chain isoform 1	50	2	3	-	42.0	44.0	-	168	190	-
tubulin beta-4B chain	50	38	40	23	86.0	77.0	48.0	309	327	41
tubulin beta-6 chain	44	16	19	4	73.0	71.0	28.0	151	159	20
tubulin-specific chaperone D	133	9	-	-	8.0	-	-	9	-	-
U5 small nuclear ribonucleoprotein 200 kDa helicase	244	22	4	-	11.0	1.9	-	24	4	-
UDP-glucose:glycoprotein glucosyltransferase 1 precursor	175	2	-	-	1.8	-	-	42	-	-
uncharacterized protein C2orf47, mitochondrial precursor	32	10	9	-	30.0	25.0	-	15	17	-
uncharacterized protein C4orf49	30	3	3	-	23.0	23.0	-	9	6	-
uncharacterized protein C7orf44	16	4	3	-	20.0	19.0	-	5	3	-
uncharacterized protein KIAA0564 isoform a precursor	162	10	8	-	8.6	6.7	-	10	8	-
uncharacterized protein KIAA0564 isoform a precursor	106	2	3	-	9.3	9.1	-	8	8	-
UPF0670 protein C8orf55 precursor	11	5	5	-	51.0	43.0	-	7	10	-
utrophin	395	39	52	5	13.0	17.0	1.1	42	61	6
vacuolar protein sorting-associated protein 13A isoform A	360	5	-	-	0.9	-	-	6	-	-
vacuolar protein sorting-associated protein 13C isoform 2B	423	9	4	-	3.2	0.7	-	9	5	-

[a]MW, (kDa)

BIBLIOGRAPHY

1. **Abbotts, A. P., V. G. Preston, M. Hughes, A. H. Patel, and N. D. Stow.** 2000. Interaction of the herpes simplex virus type 1 packaging protein UL15 with full-length and deleted forms of the UL28 protein. J Gen Virol **81:**2999-3009.
2. **Adams, M. J., and E. B. Carstens.** 2012. Ratification vote on taxonomic proposals to the International Committee on Taxonomy of Viruses (2012). Arch Virol **157:**1411-22.
3. **Addison, C., F. J. Rixon, J. W. Palfreyman, M. O'Hara, and V. G. Preston.** 1984. Characterisation of a herpes simplex virus type 1 mutant which has a temperature-sensitive defect in penetration of cells and assembly of capsids. Virology **138:**246-59.
4. **Addison, C., F. J. Rixon, and V. G. Preston.** 1990. Herpes simplex virus type 1 UL28 gene product is important for the formation of mature capsids. J Gen Virol **71 (Pt 10):**2377-84.
5. **Adelman, K., B. Salmon, and J. D. Baines.** 2001. Herpes simplex virus DNA packaging sequences adopt novel structures that are specifically recognized by a component of the cleavage and packaging machinery. Proc Natl Acad Sci U S A **98:**3086-91.
6. **al-Kobaisi, M. F., F. J. Rixon, I. McDougall, and V. G. Preston.** 1991. The herpes simplex virus UL33 gene product is required for the assembly of full capsids. Virology **180:**380-8.
7. **Albright, B. S., J. Nellissery, R. Szczepaniak, and S. K. Weller.** 2011. Disulfide bond formation in the herpes simplex virus 1 UL6 protein is required for portal ring formation and genome encapsidation. J Virol **85:**8616-24.
8. **Alwine, J. C., W. L. Steinhart, and C. W. Hill.** 1974. Transcription of herpes simplex type 1 DNA in nuclei isolated from infected HEp-2 and KB cells. Virology **60:**302-7.
9. **Baines, J. D., C. Cunningham, D. Nalwanga, and A. Davison.** 1997. The U(L)15 gene of herpes simplex virus type 1 contains within its second exon a novel open reading frame that is translated in frame with the U(L)15 gene product. J Virol **71:**2666-73.
10. **Baines, J. D., A. P. Poon, J. Rovnak, and B. Roizman.** 1994. The herpes simplex virus 1 UL15 gene encodes two proteins and is required for cleavage of genomic viral DNA. J Virol **68:**8118-24.
11. **Baines, J. D., and K. L. Roberts.** 2011. Nuclear Egress and Envelopment of HSV, p. 195-206. *In* S. K. Weller (ed.), Alphaherpesviruses: Molecular Virology. Caister Academic Press, Norfolk, UK.
12. **Baines, J. D., and S. K. Weller.** 2005. Cleavage and Packaging of Herpes Simplex Virus 1 DNA, Herpesvirus Assembly, p. 135-150. *In* C. E. Catalano (ed.), Viral Genome Packaging Machines : Genetics, Structure, and Mechanism. Kluwer Academic/Plenum Publishers, New York, N.Y.

13. **Baker, M. L., W. Jiang, F. J. Rixon, and W. Chiu.** 2005. Common ancestry of herpesviruses and tailed DNA bacteriophages. J Virol **79:**14967-70.
14. **Bazinet, C., and J. King.** 1985. The DNA translocating vertex of dsDNA bacteriophage. Annu Rev Microbiol **39:**109-29.
15. **Beard, P. M., and J. D. Baines.** 2004. The DNA cleavage and packaging protein encoded by the UL33 gene of herpes simplex virus 1 associates with capsids. Virology **324:**475-82.
16. **Beard, P. M., C. Duffy, and J. D. Baines.** 2004. Quantification of the DNA cleavage and packaging proteins U(L)15 and U(L)28 in A and B capsids of herpes simplex virus type 1. J Virol **78:**1367-74.
17. **Beard, P. M., N. S. Taus, and J. D. Baines.** 2002. DNA cleavage and packaging proteins encoded by genes U(L)28, U(L)15, and U(L)33 of herpes simplex virus type 1 form a complex in infected cells. J Virol **76:**4785-91.
18. **Beilstein, F., M. R. Higgs, and N. D. Stow.** 2009. Mutational analysis of the herpes simplex virus type 1 DNA packaging protein UL33. J Virol **83:**8938-45.
19. **Bjerke, S. L., and R. J. Roller.** 2006. Roles for herpes simplex virus type 1 UL34 and US3 proteins in disrupting the nuclear lamina during herpes simplex virus type 1 egress. Virology **347:**261-76.
20. **Boehmer, P. E., and I. R. Lehman.** 1997. Herpes simplex virus DNA replication. Annu Rev Biochem **66:**347-84.
21. **Bogner, E.** 2002. Human cytomegalovirus terminase as a target for antiviral chemotherapy. Rev Med Virol **12:**115-27.
22. **Bogner, E., K. Radsak, and M. F. Stinski.** 1998. The gene product of human cytomegalovirus open reading frame UL56 binds the pac motif and has specific nuclease activity. J Virol **72:**2259-64.
23. **Booy, F. P., W. W. Newcomb, B. L. Trus, J. C. Brown, T. S. Baker, and A. C. Steven.** 1991. Liquid-crystalline, phage-like packing of encapsidated DNA in herpes simplex virus. Cell **64:**1007-15.
24. **Booy, F. P., B. L. Trus, W. W. Newcomb, J. C. Brown, J. F. Conway, and A. C. Steven.** 1994. Finding a needle in a haystack: detection of a small protein (the 12-kDa VP26) in a large complex (the 200-MDa capsid of herpes simplex virus). Proc Natl Acad Sci U S A **91:**5652-6.
25. **Borst, E. M., J. Kleine-Albers, I. Gabaev, M. Babic, K. Wagner, A. Binz, I. Degenhardt, M. Kalesse, S. Jonjic, R. Bauerfeind, and M. Messerle.** 2013. The human cytomegalovirus UL51 protein is essential for viral genome cleavage-packaging and interacts with the terminase subunits pUL56 and pUL89. J Virol **87:**1720-32.
26. **Brown, J. C., and W. W. Newcomb.** 2011. Herpesvirus capsid assembly: insights from structural analysis. Curr Opin Virol **1:**142-9.
27. **Campbell, M. E., J. W. Palfreyman, and C. M. Preston.** 1984. Identification of herpes simplex virus DNA sequences which encode a trans-acting polypeptide responsible for stimulation of immediate early transcription. J Mol Biol **180:**1-19.
28. **Cardone, G., J. B. Heymann, N. Cheng, B. L. Trus, and A. C. Steven.** 2012. Procapsid assembly, maturation, nuclear exit: dynamic steps in the production of infectious herpesvirions. Adv Exp Med Biol **726:**423-39.

29. **Cardone, G., W. W. Newcomb, N. Cheng, P. T. Wingfield, B. L. Trus, J. C. Brown, and A. C. Steven.** 2012. The UL36 tegument protein of herpes simplex virus 1 has a composite binding site at the capsid vertices. J Virol **86:**4058-64.
30. **Cardone, G., D. C. Winkler, B. L. Trus, N. Cheng, J. E. Heuser, W. W. Newcomb, J. C. Brown, and A. C. Steven.** 2007. Visualization of the herpes simplex virus portal in situ by cryo-electron tomography. Virology **361:**426-34.
31. **Caspar, D. L., and A. Klug.** 1962. Physical principles in the construction of regular viruses. Cold Spring Harb Symp Quant Biol **27:**1-24.
32. **Catalano, C. E.** 2005. Viral Genome Packaging Machines : Genetics, Structure, and Mechanism. Kluwer Academic/Plenum Publishers, New York, N.Y.
33. **Cavalcoli, J. D., A. Baghian, F. L. Homa, and K. G. Kousoulas.** 1993. Resolution of genotypic and phenotypic properties of herpes simplex virus type 1 temperature-sensitive mutant (KOS) tsZ47: evidence for allelic complementation in the UL28 gene. Virology **197:**23-34.
34. **Challberg, M. D.** 1986. A method for identifying the viral genes required for herpesvirus DNA replication. Proc Natl Acad Sci U S A **83:**9094-8.
35. **Chang, J. T., M. F. Schmid, F. J. Rixon, and W. Chiu.** 2007. Electron cryotomography reveals the portal in the herpesvirus capsid. J Virol **81:**2065-8.
36. **Chang, Y. E., A. P. Poon, and B. Roizman.** 1996. Properties of the protein encoded by the UL32 open reading frame of herpes simplex virus 1. J Virol **70:**3938-46.
37. **Chang, Y. E., C. Van Sant, P. W. Krug, A. E. Sears, and B. Roizman.** 1997. The null mutant of the U(L)31 gene of herpes simplex virus 1: construction and phenotype in infected cells. J Virol **71:**8307-15.
38. **Chou, J., and B. Roizman.** 1985. Isomerization of herpes simplex virus 1 genome: identification of the cis-acting and recombination sites within the domain of the a sequence. Cell **41:**803-11.
39. **Church, G. A., and D. W. Wilson.** 1997. Study of herpes simplex virus maturation during a synchronous wave of assembly. J Virol **71:**3603-12.
40. **Clements, J. B., R. J. Watson, and N. M. Wilkie.** 1977. Temporal regulation of herpes simplex virus type 1 transcription: location of transcripts on the viral genome. Cell **12:**275-85.
41. **Cockrell, S. K., J. B. Huffman, K. Toropova, J. F. Conway, and F. L. Homa.** 2011. Residues of the UL25 protein of herpes simplex virus that are required for its stable interaction with capsids. J Virol **85:**4875-87.
42. **Cockrell, S. K., M. E. Sanchez, A. Erazo, and F. L. Homa.** 2009. Role of the UL25 protein in herpes simplex virus DNA encapsidation. J Virol **83:**47-57.
43. **Coller, K. E., J. I. Lee, A. Ueda, and G. A. Smith.** 2007. The capsid and tegument of the alphaherpesviruses are linked by an interaction between the UL25 and VP1/2 proteins. J Virol **81:**11790-7.
44. **Conley, A. J., D. M. Knipe, P. C. Jones, and B. Roizman.** 1981. Molecular genetics of herpes simplex virus. VII. Characterization of a temperature-sensitive mutant produced by in vitro mutagenesis and defective in DNA synthesis and accumulation of gamma polypeptides. J Virol **37:**191-206.
45. **Conway, J. F., S. K. Cockrell, A. M. Copeland, W. W. Newcomb, J. C. Brown, and F. L. Homa.** 2010. Labeling and localization of the herpes simplex virus capsid protein

UL25 and its interaction with the two triplexes closest to the penton. J Mol Biol **397:**575-86.

46. **Conway, J. F., and F. L. Homa.** 2011. Nucleocapsid Structure, Assembly and DNA Packaging of Herpes Simplex Virus, p. 175-193. *In* S. K. Weller (ed.), Alphaherpesviruses: Molecular Virology. Caister Academic Press, Norfolk, UK.
47. **Costa, R. H., G. Cohen, R. Eisenberg, D. Long, and E. Wagner.** 1984. Direct demonstration that the abundant 6-kilobase herpes simplex virus type 1 mRNA mapping between 0.23 and 0.27 map units encodes the major capsid protein VP5. J Virol **49:**287-92.
48. **Costa, R. H., B. G. Devi, K. P. Anderson, B. H. Gaylord, and E. K. Wagner.** 1981. Characterization of a major late herpes simplex virus type 1 mRNA. J Virol **38:**483-96.
49. **Costa, R. H., K. G. Draper, T. J. Kelly, and E. K. Wagner.** 1985. An unusual spliced herpes simplex virus type 1 transcript with sequence homology to Epstein-Barr virus DNA. J Virol **54:**317-28.
50. **Costanzo, F., G. Campadelli-Fiume, L. Foa-Tomasi, and E. Cassai.** 1977. Evidence that herpes simplex virus DNA is transcribed by cellular RNA polymerase B. J Virol **21:**996-1001.
51. **Dasgupta, A., and D. W. Wilson.** 1999. ATP depletion blocks herpes simplex virus DNA packaging and capsid maturation. J Virol **73:**2006-15.
52. **Davison, A. J.** 1992. Channel catfish virus: a new type of herpesvirus. Virology **186:**9-14.
53. **Davison, A. J.** 2007. Comparative analysis of the genomes, p. 10-26. *In* A. Arvin, G. Campadelli-Fiume, E. Mocarski, P. Moore, B. Roizman, R. Whitley, and K. Yamanishi (ed.), Human Herpesviruses: Biology, Therapy, and Immunoprophylaxis. Cambridge University Press, Cambridge.
54. **Davison, A. J., D. J. Dargan, and N. D. Stow.** 2002. Fundamental and accessory systems in herpesviruses. Antiviral Res **56:**1-11.
55. **Davison, A. J., and N. M. Wilkie.** 1981. Nucleotide sequences of the joint between the L and S segments of herpes simplex virus types 1 and 2. J Gen Virol **55:**315-31.
56. **Davison, M. D., F. J. Rixon, and A. J. Davison.** 1992. Identification of genes encoding two capsid proteins (VP24 and VP26) of herpes simplex virus type 1. J Gen Virol **73 (Pt 10):**2709-13.
57. **Dawson, A. L., R. P. Dellavalle, and D. M. Elston.** 2012. Infectious skin diseases: a review and needs assessment. Dermatol Clin **30:**141-51, ix-x.
58. **de Bruyn Kops, A., and D. M. Knipe.** 1988. Formation of DNA replication structures in herpes virus-infected cells requires a viral DNA binding protein. Cell **55:**857-68.
59. **Deiss, L. P., J. Chou, and N. Frenkel.** 1986. Functional domains within the a sequence involved in the cleavage-packaging of herpes simplex virus DNA. J Virol **59:**605-18.
60. **Deiss, L. P., and N. Frenkel.** 1986. Herpes simplex virus amplicon: cleavage of concatemeric DNA is linked to packaging and involves amplification of the terminally reiterated a sequence. J Virol **57:**933-41.
61. **Delius, H., and J. B. Clements.** 1976. A partial denaturation map of herpes simplex virus type 1 DNA: evidence for inversions of the unique DNA regions. J Gen Virol **33:**125-33.
62. **Desai, P., and S. Person.** 1996. Molecular interactions between the HSV-1 capsid proteins as measured by the yeast two-hybrid system. Virology **220:**516-21.

63. **Desai, P., and S. Person.** 1999. Second site mutations in the N-terminus of the major capsid protein (VP5) overcome a block at the maturation cleavage site of the capsid scaffold proteins of herpes simplex virus type 1. Virology **261:**357-66.
64. **DiIanni, C. L., C. Mapelli, D. A. Drier, J. Tsao, S. Natarajan, D. Riexinger, S. M. Festin, M. Bolgar, G. Yamanaka, S. P. Weinheimer, and et al.** 1993. In vitro activity of the herpes simplex virus type 1 protease with peptide substrates. J Biol Chem **268:**25449-54.
65. **Dodding, M. P., and M. Way.** 2011. Coupling viruses to dynein and kinesin-1. EMBO J **30:**3527-39.
66. **Dolan, A., F. E. Jamieson, C. Cunningham, B. C. Barnett, and D. J. McGeoch.** 1998. The genome sequence of herpes simplex virus type 2. J Virol **72:**2010-21.
67. **Draper, B., and V. B. Rao.** 2007. An ATP hydrolysis sensor in the DNA packaging motor from bacteriophage T4 suggests an inchworm-type translocation mechanism. J Mol Biol **369:**79-94.
68. **Eisenberg, R. J., E. E. Heldwein, G. H. Cohen, and C. Krummenacher.** 2011. Recent Progress in Understanding Herpes Simplex Virus Entry: Relationship of Structure to Function, p. 131-152. *In* S. K. Weller (ed.), Alphaherpesviruses: Molecular Virology. Caister Academic Press, Norfolk, UK.
69. **Epstein, M. A.** 1962. Observations on the fine structure of mature herpes simplex virus and on the composition of its nucleoid. J Exp Med **115:**1-12.
70. **Farnsworth, A., T. W. Wisner, M. Webb, R. Roller, G. Cohen, R. Eisenberg, and D. C. Johnson.** 2007. Herpes simplex virus glycoproteins gB and gH function in fusion between the virion envelope and the outer nuclear membrane. Proc Natl Acad Sci U S A **104:**10187-92.
71. **Fatahzadeh, M., and R. A. Schwartz.** 2007. Human herpes simplex virus infections: epidemiology, pathogenesis, symptomatology, diagnosis, and management. J Am Acad Dermatol **57:**737-63; quiz 764-6.
72. **Feiss, M., and V. B. Rao.** 2012. The bacteriophage DNA packaging machine. Adv Exp Med Biol **726:**489-509.
73. **Fossum, E., C. C. Friedel, S. V. Rajagopala, B. Titz, A. Baiker, T. Schmidt, T. Kraus, T. Stellberger, C. Rutenberg, S. Suthram, S. Bandyopadhyay, D. Rose, A. von Brunn, M. Uhlmann, C. Zeretzke, Y. A. Dong, H. Boulet, M. Koegl, S. M. Bailer, U. Koszinowski, T. Ideker, P. Uetz, R. Zimmer, and J. Haas.** 2009. Evolutionarily conserved herpesviral protein interaction networks. PLoS Pathog **5:**e1000570.
74. **Frenkel, N., and B. Roizman.** 1972. Ribonucleic acid synthesis in cells infected with herpes simplex virus: controls of transcription and of RNA abundance. Proc Natl Acad Sci U S A **69:**2654-8.
75. **Fuchs, W., H. Granzow, B. G. Klupp, M. Kopp, and T. C. Mettenleiter.** 2002. The UL48 tegument protein of pseudorabies virus is critical for intracytoplasmic assembly of infectious virions. J Virol **76:**6729-42.
76. **Fuchs, W., B. G. Klupp, H. Granzow, T. Leege, and T. C. Mettenleiter.** 2009. Characterization of pseudorabies virus (PrV) cleavage-encapsidation proteins and functional complementation of PrV pUL32 by the homologous protein of herpes simplex virus type 1. J Virol **83:**3930-43.

77. **Furlong, D., H. Swift, and B. Roizman.** 1972. Arrangement of herpesvirus deoxyribonucleic acid in the core. J Virol **10:**1071-4.
78. **Gao, M., and D. M. Knipe.** 1991. Potential role for herpes simplex virus ICP8 DNA replication protein in stimulation of late gene expression. J Virol **65:**2666-75.
79. **Garber, D. A., S. M. Beverley, and D. M. Coen.** 1993. Demonstration of circularization of herpes simplex virus DNA following infection using pulsed field gel electrophoresis. Virology **197:**459-62.
80. **Gibson, W., and B. Roizman.** 1972. Proteins specified by herpes simplex virus. 8. Characterization and composition of multiple capsid forms of subtypes 1 and 2. J Virol **10:**1044-52.
81. **Gierasch, W. W., D. L. Zimmerman, S. L. Ward, T. K. Vanheyningen, J. D. Romine, and D. A. Leib.** 2006. Construction and characterization of bacterial artificial chromosomes containing HSV-1 strains 17 and KOS. J Virol Methods **135:**197-206.
82. **Godowski, P. J., and D. M. Knipe.** 1986. Transcriptional control of herpesvirus gene expression: gene functions required for positive and negative regulation. Proc Natl Acad Sci U S A **83:**256-60.
83. **Goldner, T., G. Hewlett, N. Ettischer, H. Ruebsamen-Schaeff, H. Zimmermann, and P. Lischka.** 2011. The novel anticytomegalovirus compound AIC246 (Letermovir) inhibits human cytomegalovirus replication through a specific antiviral mechanism that involves the viral terminase. J Virol **85:**10884-93.
84. **Goshima, F., D. Watanabe, H. Takakuwa, K. Wada, T. Daikoku, M. Yamada, and Y. Nishiyama.** 2000. Herpes simplex virus UL17 protein is associated with B capsids and colocalizes with ICP35 and VP5 in infected cells. Arch Virol **145:**417-26.
85. **Grunewald, K., P. Desai, D. C. Winkler, J. B. Heymann, D. M. Belnap, W. Baumeister, and A. C. Steven.** 2003. Three-dimensional structure of herpes simplex virus from cryo-electron tomography. Science **302:**1396-8.
86. **Hangen, E., K. Blomgren, P. Benit, G. Kroemer, and N. Modjtahedi.** 2010. Life with or without AIF. Trends Biochem Sci **35:**278-87.
87. **Hayward, G. S., R. J. Jacob, S. C. Wadsworth, and B. Roizman.** 1975. Anatomy of herpes simplex virus DNA: evidence for four populations of molecules that differ in the relative orientations of their long and short components. Proc Natl Acad Sci U S A **72:**4243-7.
88. **Heldwein, E. E., and C. Krummenacher.** 2008. Entry of herpesviruses into mammalian cells. Cell Mol Life Sci **65:**1653-68.
89. **Herrera, F. J., and S. J. Triezenberg.** 2004. VP16-dependent association of chromatin-modifying coactivators and underrepresentation of histones at immediate-early gene promoters during herpes simplex virus infection. J Virol **78:**9689-96.
90. **Heymann, J. B., N. Cheng, W. W. Newcomb, B. L. Trus, J. C. Brown, and A. C. Steven.** 2003. Dynamics of herpes simplex virus capsid maturation visualized by time-lapse cryo-electron microscopy. Nat Struct Biol **10:**334-41.
91. **Higgs, M. R., V. G. Preston, and N. D. Stow.** 2008. The UL15 protein of herpes simplex virus type 1 is necessary for the localization of the UL28 and UL33 proteins to viral DNA replication centres. J Gen Virol **89:**1709-15.
92. **Hodge, P. D., and N. D. Stow.** 2001. Effects of mutations within the herpes simplex virus type 1 DNA encapsidation signal on packaging efficiency. J Virol **75:**8977-86.

93. **Hodgson, A. J., J. M. Hyser, V. V. Keasler, Y. Cang, and B. L. Slagle.** 2012. Hepatitis B virus regulatory HBx protein binding to DDB1 is required but is not sufficient for maximal HBV replication. Virology **426:**73-82.
94. **Holland, L. E., K. P. Anderson, C. Shipman, Jr., and E. K. Wagner.** 1980. Viral DNA synthesis is required for the efficient expression of specific herpes simplex virus type 1 mRNA species. Virology **101:**10-24.
95. **Homa, F. L., and J. C. Brown.** 1997. Capsid assembly and DNA packaging in herpes simplex virus. Rev Med Virol **7:**107-122.
96. **Homa, F. L., T. M. Otal, J. C. Glorioso, and M. Levine.** 1986. Transcriptional control signals of a herpes simplex virus type 1 late (gamma 2) gene lie within bases -34 to +124 relative to the 5' terminus of the mRNA. Mol Cell Biol **6:**3652-66.
97. **Honess, R. W., and B. Roizman.** 1974. Regulation of herpesvirus macromolecular synthesis. I. Cascade regulation of the synthesis of three groups of viral proteins. J Virol **14:**8-19.
98. **Honess, R. W., and B. Roizman.** 1975. Regulation of herpesvirus macromolecular synthesis: sequential transition of polypeptide synthesis requires functional viral polypeptides. Proc Natl Acad Sci U S A **72:**1276-80.
99. **Honess, R. W., and D. H. Watson.** 1974. Herpes simplex virus-specific polypeptides studied by polyacrylamide gel electrophoresis of immune precipitates. J Gen Virol **22:**171-85.
100. **Hong, Z., M. Beaudet-Miller, J. Durkin, R. Zhang, and A. D. Kwong.** 1996. Identification of a minimal hydrophobic domain in the herpes simplex virus type 1 scaffolding protein which is required for interaction with the major capsid protein. J Virol **70:**533-40.
101. **Huang, E., E. M. Perkins, and P. Desai.** 2007. Structural features of the scaffold interaction domain at the N terminus of the major capsid protein (VP5) of herpes simplex virus type 1. J Virol **81:**9396-407.
102. **Huffman, J. B., W. W. Newcomb, J. C. Brown, and F. L. Homa.** 2008. Amino acids 143 to 150 of the herpes simplex virus type 1 scaffold protein are required for the formation of portal-containing capsids. J Virol **82:**6778-81.
103. **Iovine, B., M. L. Iannella, and M. A. Bevilacqua.** 2011. Damage-specific DNA binding protein 1 (DDB1): a protein with a wide range of functions. Int J Biochem Cell Biol **43:**1664-7.
104. **Jacobson, J. G., K. Yang, J. D. Baines, and F. L. Homa.** 2006. Linker insertion mutations in the herpes simplex virus type 1 UL28 gene: effects on UL28 interaction with UL15 and UL33 and identification of a second-site mutation in the UL15 gene that suppresses a lethal UL28 mutation. J Virol **80:**12312-23.
105. **Jessie, K., O. H. Hashim, and Z. H. A. Rahim.** 2008. Protein precipitation method for salivary proteins and rehydration buffer for two-dimensional electrophoresis. Biotechnology **7:**686-693.
106. **Johnson, D. C., and J. D. Baines.** 2011. Herpesviruses remodel host membranes for virus egress. Nat Rev Microbiol **9:**382-94.
107. **Jones, P. C., and B. Roizman.** 1979. Regulation of herpesvirus macromolecular synthesis. VIII. The transcription program consists of three phases during which both extent of transcription and accumulation of RNA in the cytoplasm are regulated. J Virol **31:**299-314.

108. **Kang, X., X. Chen, Y. He, D. Guo, L. Guo, J. Zhong, and H. B. Shu.** 2013. DDB1 is a cellular substrate of NS3/4A protease and required for hepatitis C virus replication. Virology **435:**385-94.
109. **Keller, A., A. I. Nesvizhskii, E. Kolker, and R. Aebersold.** 2002. Empirical statistical model to estimate the accuracy of peptide identifications made by MS/MS and database search. Anal Chem **74:**5383-92.
110. **Kieff, E. D., S. L. Bachenheimer, and B. Roizman.** 1971. Size, composition, and structure of the deoxyribonucleic acid of herpes simplex virus subtypes 1 and 2. J Virol **8:**125-32.
111. **Knipe, D. M., and A. Cliffe.** 2008. Chromatin control of herpes simplex virus lytic and latent infection. Nat Rev Microbiol **6:**211-21.
112. **Koslowski, K. M., P. R. Shaver, J. T. Casey, 2nd, T. Wilson, G. Yamanaka, A. K. Sheaffer, D. J. Tenney, and N. E. Pederson.** 1999. Physical and functional interactions between the herpes simplex virus UL15 and UL28 DNA cleavage and packaging proteins. J Virol **73:**1704-7.
113. **Koslowski, K. M., P. R. Shaver, X. Y. Wang, D. J. Tenney, and N. E. Pederson.** 1997. The pseudorabies virus UL28 protein enters the nucleus after coexpression with the herpes simplex virus UL15 protein. J Virol **71:**9118-23.
114. **Krosky, P. M., M. R. Underwood, S. R. Turk, K. W. Feng, R. K. Jain, R. G. Ptak, A. C. Westerman, K. K. Biron, L. B. Townsend, and J. C. Drach.** 1998. Resistance of human cytomegalovirus to benzimidazole ribonucleosides maps to two open reading frames: UL89 and UL56. J Virol **72:**4721-8.
115. **Krupovic, M., P. Forterre, and D. H. Bamford.** 2010. Comparative analysis of the mosaic genomes of tailed archaeal viruses and proviruses suggests common themes for virion architecture and assembly with tailed viruses of bacteria. J Mol Biol **397:**144-60.
116. **Lamberti, C., and S. K. Weller.** 1998. The herpes simplex virus type 1 cleavage/packaging protein, UL32, is involved in efficient localization of capsids to replication compartments. J Virol **72:**2463-73.
117. **Lamberti, C., and S. K. Weller.** 1996. The herpes simplex virus type 1 UL6 protein is essential for cleavage and packaging but not for genomic inversion. Virology **226:**403-7.
118. **Leach, N. R., and R. J. Roller.** 2010. Significance of host cell kinases in herpes simplex virus type 1 egress and lamin-associated protein disassembly from the nuclear lamina. Virology **406:**127-37.
119. **Liang, X., M. T. Pickering, N. H. Cho, H. Chang, M. R. Volkert, T. F. Kowalik, and J. U. Jung.** 2006. Deregulation of DNA damage signal transduction by herpesvirus latency-associated M2. J Virol **80:**5862-74.
120. **Liashkovich, I., W. Hafezi, J. M. Kuhn, H. Oberleithner, and V. Shahin.** 2011. Nuclear delivery mechanism of herpes simplex virus type 1 genome. J Mol Recognit **24:**414-21.
121. **Lilley, C. E., C. T. Carson, A. R. Muotri, F. H. Gage, and M. D. Weitzman.** 2005. DNA repair proteins affect the lifecycle of herpes simplex virus 1. Proc Natl Acad Sci U S A **102:**5844-9.
122. **Liu, F., and B. Roizman.** 1993. Characterization of the protease and other products of amino-terminus-proximal cleavage of the herpes simplex virus 1 UL26 protein. J Virol **67:**1300-9.

123. **Liu, F. Y., and B. Roizman.** 1991. The herpes simplex virus 1 gene encoding a protease also contains within its coding domain the gene encoding the more abundant substrate. J Virol **65:**5149-56.
124. **Liu, F. Y., and B. Roizman.** 1991. The promoter, transcriptional unit, and coding sequence of herpes simplex virus 1 family 35 proteins are contained within and in frame with the UL26 open reading frame. J Virol **65:**206-12.
125. **Locker, H., and N. Frenkel.** 1979. BamI, KpnI, and SalI restriction enzyme maps of the DNAs of herpes simplex virus strains Justin and F: occurrence of heterogeneities in defined regions of the viral DNA. J Virol **32:**429-41.
126. **Loret, S., G. Guay, and R. Lippe.** 2008. Comprehensive characterization of extracellular herpes simplex virus type 1 virions. J Virol **82:**8605-18.
127. **Marschall, M., S. Feichtinger, and J. Milbradt.** 2011. Regulatory roles of protein kinases in cytomegalovirus replication. Adv Virus Res **80:**69-101.
128. **Martinez, R., R. T. Sarisky, P. C. Weber, and S. K. Weller.** 1996. Herpes simplex virus type 1 alkaline nuclease is required for efficient processing of viral DNA replication intermediates. J Virol **70:**2075-85.
129. **Maul, G. G.** 1998. Nuclear domain 10, the site of DNA virus transcription and replication. Bioessays **20:**660-7.
130. **Mavromara-Nazos, P., M. Ackermann, and B. Roizman.** 1986. Construction and properties of a viable herpes simplex virus 1 recombinant lacking coding sequences of the alpha 47 gene. J Virol **60:**807-12.
131. **McGeoch, D. J., M. A. Dalrymple, A. J. Davison, A. Dolan, M. C. Frame, D. McNab, L. J. Perry, J. E. Scott, and P. Taylor.** 1988. The complete DNA sequence of the long unique region in the genome of herpes simplex virus type 1. J Gen Virol **69 (Pt 7):**1531-74.
132. **McNab, A. R., P. Desai, S. Person, L. L. Roof, D. R. Thomsen, W. W. Newcomb, J. C. Brown, and F. L. Homa.** 1998. The product of the herpes simplex virus type 1 UL25 gene is required for encapsidation but not for cleavage of replicated viral DNA. J Virol **72:**1060-70.
133. **McNamee, E. E., T. J. Taylor, and D. M. Knipe.** 2000. A dominant-negative herpesvirus protein inhibits intranuclear targeting of viral proteins: effects on DNA replication and late gene expression. J Virol **74:**10122-31.
134. **Mettenleiter, T. C., F. Muller, H. Granzow, and B. G. Klupp.** 2012. The way out: what we know and do not know about herpesvirus nuclear egress. Cell Microbiol **15:**170-8.
135. **Mingo, R. M., J. Han, W. W. Newcomb, and J. C. Brown.** 2012. Replication of herpes simplex virus: egress of progeny virus at specialized cell membrane sites. J Virol **86:**7084-97.
136. **Mocarski, E. S., L. P. Deiss, and N. Frenkel.** 1985. Nucleotide sequence and structural features of a novel US-a junction present in a defective herpes simplex virus genome. J Virol **55:**140-6.
137. **Mocarski, E. S., L. E. Post, and B. Roizman.** 1980. Molecular engineering of the herpes simplex virus genome: insertion of a second L-S junction into the genome causes additional genome inversions. Cell **22:**243-55.

138. **Mocarski, E. S., and B. Roizman.** 1981. Site-specific inversion sequence of the herpes simplex virus genome: domain and structural features. Proc Natl Acad Sci U S A **78:**7047-51.
139. **Mocarski, E. S., and B. Roizman.** 1982. Structure and role of the herpes simplex virus DNA termini in inversion, circularization and generation of virion DNA. Cell **31:**89-97.
140. **Mou, F., T. Forest, and J. D. Baines.** 2007. US3 of herpes simplex virus type 1 encodes a promiscuous protein kinase that phosphorylates and alters localization of lamin A/C in infected cells. J Virol **81:**6459-70.
141. **Muranyi, W., J. Haas, M. Wagner, G. Krohne, and U. H. Koszinowski.** 2002. Cytomegalovirus recruitment of cellular kinases to dissolve the nuclear lamina. Science **297:**854-7.
142. **Nadal, M., P. J. Mas, A. G. Blanco, C. Arnan, M. Sola, D. J. Hart, and M. Coll.** 2010. Structure and inhibition of herpesvirus DNA packaging terminase nuclease domain. Proc Natl Acad Sci U S A **107:**16078-83.
143. **Nahmias, A. J., F. K. Lee, and S. Beckman-Nahmias.** 1990. Sero-epidemiological and -sociological patterns of herpes simplex virus infection in the world. Scand J Infect Dis Suppl **69:**19-36.
144. **Nasseri, M., and E. S. Mocarski.** 1988. The cleavage recognition signal is contained within sequences surrounding an a-a junction in herpes simplex virus DNA. Virology **167:**25-30.
145. **Nellissery, J. K., R. Szczepaniak, C. Lamberti, and S. K. Weller.** 2007. A putative leucine zipper within the herpes simplex virus type 1 UL6 protein is required for portal ring formation. J Virol **81:**8868-77.
146. **Nesvizhskii, A. I., A. Keller, E. Kolker, and R. Aebersold.** 2003. A statistical model for identifying proteins by tandem mass spectrometry. Anal Chem **75:**4646-58.
147. **Newcomb, W. W., and J. C. Brown.** 1991. Structure of the herpes simplex virus capsid: effects of extraction with guanidine hydrochloride and partial reconstitution of extracted capsids. J Virol **65:**613-20.
148. **Newcomb, W. W., S. K. Cockrell, F. L. Homa, and J. C. Brown.** 2009. Polarized DNA ejection from the herpesvirus capsid. J Mol Biol **392:**885-94.
149. **Newcomb, W. W., F. L. Homa, and J. C. Brown.** 2006. Herpes simplex virus capsid structure: DNA packaging protein UL25 is located on the external surface of the capsid near the vertices. J Virol **80:**6286-94.
150. **Newcomb, W. W., F. L. Homa, and J. C. Brown.** 2005. Involvement of the portal at an early step in herpes simplex virus capsid assembly. J Virol **79:**10540-6.
151. **Newcomb, W. W., F. L. Homa, D. R. Thomsen, F. P. Booy, B. L. Trus, A. C. Steven, J. V. Spencer, and J. C. Brown.** 1996. Assembly of the herpes simplex virus capsid: characterization of intermediates observed during cell-free capsid formation. J Mol Biol **263:**432-46.
152. **Newcomb, W. W., F. L. Homa, D. R. Thomsen, B. L. Trus, N. Cheng, A. Steven, F. Booy, and J. C. Brown.** 1999. Assembly of the herpes simplex virus procapsid from purified components and identification of small complexes containing the major capsid and scaffolding proteins. J Virol **73:**4239-50.
153. **Newcomb, W. W., F. L. Homa, D. R. Thomsen, Z. Ye, and J. C. Brown.** 1994. Cell-free assembly of the herpes simplex virus capsid. J Virol **68:**6059-63.

154. **Newcomb, W. W., L. M. Jones, A. Dee, F. Chaudhry, and J. C. Brown.** 2012. Role of a reducing environment in disassembly of the herpesvirus tegument. Virology **431:**71-9.
155. **Newcomb, W. W., R. M. Juhas, D. R. Thomsen, F. L. Homa, A. D. Burch, S. K. Weller, and J. C. Brown.** 2001. The UL6 gene product forms the portal for entry of DNA into the herpes simplex virus capsid. J Virol **75:**10923-32.
156. **Newcomb, W. W., D. R. Thomsen, F. L. Homa, and J. C. Brown.** 2003. Assembly of the herpes simplex virus capsid: identification of soluble scaffold-portal complexes and their role in formation of portal-containing capsids. J Virol **77:**9862-71.
157. **Newcomb, W. W., B. L. Trus, F. P. Booy, A. C. Steven, J. S. Wall, and J. C. Brown.** 1993. Structure of the herpes simplex virus capsid. Molecular composition of the pentons and the triplexes. J Mol Biol **232:**499-511.
158. **Newcomb, W. W., B. L. Trus, N. Cheng, A. C. Steven, A. K. Sheaffer, D. J. Tenney, S. K. Weller, and J. C. Brown.** 2000. Isolation of herpes simplex virus procapsids from cells infected with a protease-deficient mutant virus. J Virol **74:**1663-73.
159. **Nicholson, P., C. Addison, A. M. Cross, J. Kennard, V. G. Preston, and F. J. Rixon.** 1994. Localization of the herpes simplex virus type 1 major capsid protein VP5 to the cell nucleus requires the abundant scaffolding protein VP22a. J Gen Virol **75 (Pt 5):**1091-9.
160. **Norberg, E., S. Orrenius, and B. Zhivotovsky.** 2010. Mitochondrial regulation of cell death: processing of apoptosis-inducing factor (AIF). Biochem Biophys Res Commun **396:**95-100.
161. **O'Hara, M., F. J. Rixon, N. D. Stow, J. Murray, M. Murphy, and V. G. Preston.** 2010. Mutational analysis of the herpes simplex virus type 1 UL25 DNA packaging protein reveals regions that are important after the viral DNA has been packaged. J Virol **84:**4252-63.
162. **O'Hare, P., and G. S. Hayward.** 1985. Evidence for a direct role for both the 175,000- and 110,000-molecular-weight immediate-early proteins of herpes simplex virus in the transactivation of delayed-early promoters. J Virol **53:**751-60.
163. **Ogasawara, M., T. Suzutani, I. Yoshida, and M. Azuma.** 2001. Role of the UL25 gene product in packaging DNA into the herpes simplex virus capsid: location of UL25 product in the capsid and demonstration that it binds DNA. J Virol **75:**1427-36.
164. **Park, R., and J. D. Baines.** 2006. Herpes simplex virus type 1 infection induces activation and recruitment of protein kinase C to the nuclear membrane and increased phosphorylation of lamin B. J Virol **80:**494-504.
165. **Patel, A. H., and J. B. MacLean.** 1995. The product of the UL6 gene of herpes simplex virus type 1 is associated with virus capsids. Virology **206:**465-78.
166. **Patel, A. H., F. J. Rixon, C. Cunningham, and A. J. Davison.** 1996. Isolation and characterization of herpes simplex virus type 1 mutants defective in the UL6 gene. Virology **217:**111-23.
167. **Patel, V. J., K. Thalassinos, S. E. Slade, J. B. Connolly, A. Crombie, J. C. Murrell, and J. H. Scrivens.** 2009. A comparison of labeling and label-free mass spectrometry-based proteomics approaches. J Proteome Res **8:**3752-9.
168. **Pellet, P. E., and B. Roizman.** 2007. The Family *Herpesviridae*: A Brief Introduction, p. 2479-2499. *In* D. M. Knipe and H. P. M. (ed.), Fields Virology, Fifth ed, vol. II. Wolters Kluwer Health/Lippincott Williams & Wilkins, Philadelphia.

169. **Pelletier, A., F. Do, J. J. Brisebois, L. Lagace, and M. G. Cordingley.** 1997. Self-association of herpes simplex virus type 1 ICP35 is via coiled-coil interactions and promotes stable interaction with the major capsid protein. J Virol **71:**5197-208.
170. **Perdue, M. L., J. C. Cohen, C. C. Randall, and D. J. O'Callaghan.** 1976. Biochemical studies of the maturation of herpesvirus nucleocapsid species. Virology **74:**194-208.
171. **Person, S., S. Laquerre, P. Desai, and J. Hempel.** 1993. Herpes simplex virus type 1 capsid protein, VP21, originates within the UL26 open reading frame. J Gen Virol **74 (Pt 10):**2269-73.
172. **Poffenberger, K. L., and B. Roizman.** 1985. A noninverting genome of a viable herpes simplex virus 1: presence of head-to-tail linkages in packaged genomes and requirements for circularization after infection. J Virol **53:**587-95.
173. **Poon, A. P., and B. Roizman.** 1993. Characterization of a temperature-sensitive mutant of the UL15 open reading frame of herpes simplex virus 1. J Virol **67:**4497-503.
174. **Post, L. E., S. Mackem, and B. Roizman.** 1981. Regulation of alpha genes of herpes simplex virus: expression of chimeric genes produced by fusion of thymidine kinase with alpha gene promoters. Cell **24:**555-65.
175. **Powell, K. L., D. J. Purifoy, and R. J. Courtney.** 1975. The synthesis of herpes simplex virus proteins in the absence of virus DNA synthesis. Biochem Biophys Res Commun **66:**262-71.
176. **Preston, V. G., J. A. Coates, and F. J. Rixon.** 1983. Identification and characterization of a herpes simplex virus gene product required for encapsidation of virus DNA. J Virol **45:**1056-64.
177. **Preston, V. G., J. Murray, C. M. Preston, I. M. McDougall, and N. D. Stow.** 2008. The UL25 gene product of herpes simplex virus type 1 is involved in uncoating of the viral genome. J Virol **82:**6654-66.
178. **Przech, A. J., D. Yu, and S. K. Weller.** 2003. Point mutations in exon I of the herpes simplex virus putative terminase subunit, UL15, indicate that the most conserved residues are essential for cleavage and packaging. J Virol **77:**9613-21.
179. **Reynolds, A. E., Y. Fan, and J. D. Baines.** 2000. Characterization of the U(L)33 gene product of herpes simplex virus 1. Virology **266:**310-8.
180. **Reynolds, A. E., L. Liang, and J. D. Baines.** 2004. Conformational changes in the nuclear lamina induced by herpes simplex virus type 1 require genes U(L)31 and U(L)34. J Virol **78:**5564-75.
181. **Reynolds, A. E., B. J. Ryckman, J. D. Baines, Y. Zhou, L. Liang, and R. J. Roller.** 2001. U(L)31 and U(L)34 proteins of herpes simplex virus type 1 form a complex that accumulates at the nuclear rim and is required for envelopment of nucleocapsids. J Virol **75:**8803-17.
182. **Reynolds, A. E., E. G. Wills, R. J. Roller, B. J. Ryckman, and J. D. Baines.** 2002. Ultrastructural localization of the herpes simplex virus type 1 UL31, UL34, and US3 proteins suggests specific roles in primary envelopment and egress of nucleocapsids. J Virol **76:**8939-52.
183. **Rigaut, G., A. Shevchenko, B. Rutz, M. Wilm, M. Mann, and B. Seraphin.** 1999. A generic protein purification method for protein complex characterization and proteome exploration. Nat Biotechnol **17:**1030-2.

184. **Rixon, F. J., C. Addison, A. McGregor, S. J. Macnab, P. Nicholson, V. G. Preston, and J. D. Tatman.** 1996. Multiple interactions control the intracellular localization of the herpes simplex virus type 1 capsid proteins. J Gen Virol **77 (Pt 9):**2251-60.
185. **Rixon, F. J., A. M. Cross, C. Addison, and V. G. Preston.** 1988. The products of herpes simplex virus type 1 gene UL26 which are involved in DNA packaging are strongly associated with empty but not with full capsids. J Gen Virol **69 (Pt 11):**2879-91.
186. **Rixon, F. J., and D. McNab.** 1999. Packaging-competent capsids of a herpes simplex virus temperature-sensitive mutant have properties similar to those of in vitro-assembled procapsids. J Virol **73:**5714-21.
187. **Roberts, K. L., and J. D. Baines.** 2010. Myosin Va enhances secretion of herpes simplex virus 1 virions and cell surface expression of viral glycoproteins. J Virol **84:**9889-96.
188. **Roizman, B.** 1979. The organization of the herpes simplex virus genomes. Annu Rev Genet **13:**25-57.
189. **Roizman, B.** 1979. The structure and isomerization of herpes simplex virus genomes. Cell **16:**481-94.
190. **Roizman, B., and D. Furlong.** 1974. The replication of herpesviruses, p. 229-403. *In* H. Fraenkel-Conrat and R. R. Wagner (ed.), Comprehensive Virology. Plenum Press, New York.
191. **Roizman, B., D. M. Knipe, and R. J. Whitley.** 2007. Herpes Simplex Viruses, p. 2501-2602. *In* D. M. Knipe and H. P. M. (ed.), Fields Virology, Fifth ed, vol. II. Wolters Kluwer Health/Lippincott Williams & Wilkins, Philadelphia.
192. **Roller, R. J., Y. Zhou, R. Schnetzer, J. Ferguson, and D. DeSalvo.** 2000. Herpes simplex virus type 1 U(L)34 gene product is required for viral envelopment. J Virol **74:**117-29.
193. **Romani, B., and E. A. Cohen.** 2012. Lentivirus Vpr and Vpx accessory proteins usurp the cullin4-DDB1 (DCAF1) E3 ubiquitin ligase. Curr Opin Virol **2:**755-63.
194. **Salmon, B., and J. D. Baines.** 1998. Herpes simplex virus DNA cleavage and packaging: association of multiple forms of U(L)15-encoded proteins with B capsids requires at least the U(L)6, U(L)17, and U(L)28 genes. J Virol **72:**3045-50.
195. **Salmon, B., C. Cunningham, A. J. Davison, W. J. Harris, and J. D. Baines.** 1998. The herpes simplex virus type 1 U(L)17 gene encodes virion tegument proteins that are required for cleavage and packaging of viral DNA. J Virol **72:**3779-88.
196. **Salmon, B., D. Nalwanga, Y. Fan, and J. D. Baines.** 1999. Proteolytic cleavage of the amino terminus of the U(L)15 gene product of herpes simplex virus type 1 is coupled with maturation of viral DNA into unit-length genomes. J Virol **73:**8338-48.
197. **Savva, C. G., A. Holzenburg, and E. Bogner.** 2004. Insights into the structure of human cytomegalovirus large terminase subunit pUL56. FEBS Lett **563:**135-40.
198. **Schaffer, P. A., G. M. Aron, N. Biswal, and M. Benyesh-Melnick.** 1973. Temperature-sensitive mutants of herpes simplex virus type 1: isolation, complementation and partial characterization. Virology **52:**57-71.
199. **Scheffczik, H., C. G. Savva, A. Holzenburg, L. Kolesnikova, and E. Bogner.** 2002. The terminase subunits pUL56 and pUL89 of human cytomegalovirus are DNA-metabolizing proteins with toroidal structure. Nucleic Acids Res **30:**1695-703.

200. **Scholz, B., S. Rechter, J. C. Drach, L. B. Townsend, and E. Bogner.** 2003. Identification of the ATP-binding site in the terminase subunit pUL56 of human cytomegalovirus. Nucleic Acids Res **31:**1426-33.
201. **Schrag, J. D., B. V. Prasad, F. J. Rixon, and W. Chiu.** 1989. Three-dimensional structure of the HSV1 nucleocapsid. Cell **56:**651-60.
202. **Sciortino, M. T., M. Suzuki, B. Taddeo, and B. Roizman.** 2001. RNAs extracted from herpes simplex virus 1 virions: apparent selectivity of viral but not cellular RNAs packaged in virions. J Virol **75:**8105-16.
203. **Severini, A., A. R. Morgan, D. R. Tovell, and D. L. Tyrrell.** 1994. Study of the structure of replicative intermediates of HSV-1 DNA by pulsed-field gel electrophoresis. Virology **200:**428-35.
204. **Sheaffer, A. K., W. W. Newcomb, M. Gao, D. Yu, S. K. Weller, J. C. Brown, and D. J. Tenney.** 2001. Herpes simplex virus DNA cleavage and packaging proteins associate with the procapsid prior to its maturation. J Virol **75:**687-98.
205. **Sherman, G., and S. L. Bachenheimer.** 1988. Characterization of intranuclear capsids made by ts morphogenic mutants of HSV-1. Virology **163:**471-80.
206. **Sherman, G., and S. L. Bachenheimer.** 1987. DNA processing in temperature-sensitive morphogenic mutants of HSV-1. Virology **158:**427-30.
207. **Simpson-Holley, M., R. C. Colgrove, G. Nalepa, J. W. Harper, and D. M. Knipe.** 2005. Identification and functional evaluation of cellular and viral factors involved in the alteration of nuclear architecture during herpes simplex virus 1 infection. J Virol **79:**12840-51.
208. **Singer, G. P., W. W. Newcomb, D. R. Thomsen, F. L. Homa, and J. C. Brown.** 2005. Identification of a region in the herpes simplex virus scaffolding protein required for interaction with the portal. J Virol **79:**132-9.
209. **Smiley, J. R., J. Duncan, and M. Howes.** 1990. Sequence requirements for DNA rearrangements induced by the terminal repeat of herpes simplex virus type 1 KOS DNA. J Virol **64:**5036-50.
210. **Smiley, J. R., B. S. Fong, and W. C. Leung.** 1981. Construction of a double-jointed herpes simplex viral DNA molecule: inverted repeats are required for segment inversion, and direct repeats promote deletions. Virology **113:**345-62.
211. **Spaete, R. R., and N. Frenkel.** 1982. The herpes simplex virus amplicon: a new eucaryotic defective-virus cloning-amplifying vector. Cell **30:**295-304.
212. **Spaete, R. R., and N. Frenkel.** 1985. The herpes simplex virus amplicon: analyses of cis-acting replication functions. Proc Natl Acad Sci U S A **82:**694-8.
213. **Spear, P. G.** 2004. Herpes simplex virus: receptors and ligands for cell entry. Cell Microbiol **6:**401-10.
214. **Spear, P. G., and B. Roizman.** 1967. Buoyant density of herpes simplex virus in solutions of caesium chloride. Nature **214:**713-4.
215. **Spear, P. G., and B. Roizman.** 1972. Proteins specified by herpes simplex virus. V. Purification and structural proteins of the herpesvirion. J Virol **9:**143-59.
216. **Steven, A. C., J. B. Heymann, N. Cheng, B. L. Trus, and J. F. Conway.** 2005. Virus maturation: dynamics and mechanism of a stabilizing structural transition that leads to infectivity. Curr Opin Struct Biol **15:**227-36.
217. **Stow, N. D.** 2001. Packaging of genomic and amplicon DNA by the herpes simplex virus type 1 UL25-null mutant KUL25NS. J Virol **75:**10755-65.

218. **Stow, N. D., and E. C. McMonagle.** 1983. Characterization of the TRS/IRS origin of DNA replication of herpes simplex virus type 1. Virology **130:**427-38.
219. **Stow, N. D., E. C. McMonagle, and A. J. Davison.** 1983. Fragments from both termini of the herpes simplex virus type 1 genome contain signals required for the encapsidation of viral DNA. Nucleic Acids Res **11:**8205-20.
220. **Strang, B. L., and N. D. Stow.** 2005. Circularization of the herpes simplex virus type 1 genome upon lytic infection. J Virol **79:**12487-94.
221. **Su, Y. H., M. J. Moxley, A. K. Ng, J. Lin, R. Jordan, N. W. Fraser, and T. M. Block.** 2002. Stability and circularization of herpes simplex virus type 1 genomes in quiescently infected PC12 cultures. J Gen Virol **83:**2943-50.
222. **Tatman, J. D., V. G. Preston, P. Nicholson, R. M. Elliott, and F. J. Rixon.** 1994. Assembly of herpes simplex virus type 1 capsids using a panel of recombinant baculoviruses. J Gen Virol **75 (Pt 5):**1101-13.
223. **Taus, N. S., and J. D. Baines.** 1998. Herpes simplex virus 1 DNA cleavage/packaging: the UL28 gene encodes a minor component of B capsids. Virology **252:**443-9.
224. **Taylor, M. P., O. O. Koyuncu, and L. W. Enquist.** 2011. Subversion of the actin cytoskeleton during viral infection. Nat Rev Microbiol **9:**427-39.
225. **Tengelsen, L. A., N. E. Pederson, P. R. Shaver, M. W. Wathen, and F. L. Homa.** 1993. Herpes simplex virus type 1 DNA cleavage and encapsidation require the product of the UL28 gene: isolation and characterization of two UL28 deletion mutants. J Virol **67:**3470-80.
226. **Thoma, C., E. Borst, M. Messerle, M. Rieger, J. S. Hwang, and E. Bogner.** 2006. Identification of the interaction domain of the small terminase subunit pUL89 with the large subunit pUL56 of human cytomegalovirus. Biochemistry **45:**8855-63.
227. **Thomsen, D. R., W. W. Newcomb, J. C. Brown, and F. L. Homa.** 1995. Assembly of the herpes simplex virus capsid: requirement for the carboxyl-terminal twenty-five amino acids of the proteins encoded by the UL26 and UL26.5 genes. J Virol **69:**3690-703.
228. **Thomsen, D. R., L. L. Roof, and F. L. Homa.** 1994. Assembly of herpes simplex virus (HSV) intermediate capsids in insect cells infected with recombinant baculoviruses expressing HSV capsid proteins. J Virol **68:**2442-57.
229. **Thurlow, J. K., M. Murphy, N. D. Stow, and V. G. Preston.** 2006. Herpes simplex virus type 1 DNA-packaging protein UL17 is required for efficient binding of UL25 to capsids. J Virol **80:**2118-26.
230. **Thurlow, J. K., F. J. Rixon, M. Murphy, P. Targett-Adams, M. Hughes, and V. G. Preston.** 2005. The herpes simplex virus type 1 DNA packaging protein UL17 is a virion protein that is present in both the capsid and the tegument compartments. J Virol **79:**150-8.
231. **Tischer, B. K., J. von Einem, B. Kaufer, and N. Osterrieder.** 2006. Two-step red-mediated recombination for versatile high-efficiency markerless DNA manipulation in Escherichia coli. Biotechniques **40:**191-7.
232. **Toropova, K., J. B. Huffman, F. L. Homa, and J. F. Conway.** 2011. The herpes simplex virus 1 UL17 protein is the second constituent of the capsid vertex-specific component required for DNA packaging and retention. J Virol **85:**7513-22.
233. **Trilling, M., V. T. Le, M. Fiedler, A. Zimmermann, E. Bleifuss, and H. Hengel.** 2011. Identification of DNA-damage DNA-binding protein 1 as a conditional essential

factor for cytomegalovirus replication in interferon-gamma-stimulated cells. PLoS Pathog **7:**e1002069.

234. **Trus, B. L., F. P. Booy, W. W. Newcomb, J. C. Brown, F. L. Homa, D. R. Thomsen, and A. C. Steven.** 1996. The herpes simplex virus procapsid: structure, conformational changes upon maturation, and roles of the triplex proteins VP19c and VP23 in assembly. J Mol Biol **263:**447-62.
235. **Trus, B. L., N. Cheng, W. W. Newcomb, F. L. Homa, J. C. Brown, and A. C. Steven.** 2004. Structure and polymorphism of the UL6 portal protein of herpes simplex virus type 1. J Virol **78:**12668-71.
236. **Trus, B. L., W. W. Newcomb, N. Cheng, G. Cardone, L. Marekov, F. L. Homa, J. C. Brown, and A. C. Steven.** 2007. Allosteric signaling and a nuclear exit strategy: binding of UL25/UL17 heterodimers to DNA-Filled HSV-1 capsids. Mol Cell **26:**479-89.
237. **Umene, K., S. Oohashi, M. Yoshida, and Y. Fukumaki.** 2008. Diversity of the a sequence of herpes simplex virus type 1 developed during evolution. J Gen Virol **89:**841-52.
238. **Underwood, M. R., R. J. Harvey, S. C. Stanat, M. L. Hemphill, T. Miller, J. C. Drach, L. B. Townsend, and K. K. Biron.** 1998. Inhibition of human cytomegalovirus DNA maturation by a benzimidazole ribonucleoside is mediated through the UL89 gene product. J Virol **72:**717-25.
239. **van Genderen, I. L., R. Brandimarti, M. R. Torrisi, G. Campadelli, and G. van Meer.** 1994. The phospholipid composition of extracellular herpes simplex virions differs from that of host cell nuclei. Virology **200:**831-6.
240. **van Leeuwen, H., M. Okuwaki, R. Hong, D. Chakravarti, K. Nagata, and P. O'Hare.** 2003. Herpes simplex virus type 1 tegument protein VP22 interacts with TAF-I proteins and inhibits nucleosome assembly but not regulation of histone acetylation by INHAT. J Gen Virol **84:**2501-10.
241. **Varmuza, S. L., and J. R. Smiley.** 1985. Signals for site-specific cleavage of HSV DNA: maturation involves two separate cleavage events at sites distal to the recognition sequences. Cell **41:**793-802.
242. **Vasilenko, N. L., M. Snider, S. L. Labiuk, V. A. Lobanov, L. A. Babiuk, and S. van Drunen Littel-van den Hurk.** 2012. Bovine herpesvirus-1 VP8 interacts with DNA damage binding protein-1 (DDB1) and is monoubiquitinated during infection. Virus Res **167:**56-66.
243. **Visalli, R. J., J. Knepper, B. Goshorn, K. Vanover, D. M. Burnside, K. Irven, R. McGauley, and M. Visalli.** 2009. Characterization of the Varicella-zoster virus ORF25 gene product: pORF25 interacts with multiple DNA encapsidation proteins. Virus Res **144:**58-64.
244. **Visalli, R. J., D. M. Nicolosi, K. L. Irven, B. Goshorn, T. Khan, and M. A. Visalli.** 2007. The Varicella-zoster virus DNA encapsidation genes: Identification and characterization of the putative terminase subunits. Virus Res **129:**200-11.
245. **Vizoso Pinto, M. G., V. R. Pothineni, R. Haase, M. Woidy, A. S. Lotz-Havla, S. W. Gersting, A. C. Muntau, J. Haas, M. Sommer, A. M. Arvin, and A. Baiker.** 2011. Varicella zoster virus ORF25 gene product: an essential hub protein linking encapsidation proteins and the nuclear egress complex. J Proteome Res **10:**5374-82.

246. **Vlazny, D. A., A. Kwong, and N. Frenkel.** 1982. Site-specific cleavage/packaging of herpes simplex virus DNA and the selective maturation of nucleocapsids containing full-length viral DNA. Proc Natl Acad Sci U S A **79:**1423-7.
247. **Wadsworth, S., R. J. Jacob, and B. Roizman.** 1975. Anatomy of herpes simplex virus DNA. II. Size, composition, and arrangement of inverted terminal repetitions. J Virol **15:**1487-97.
248. **Wagner, M. J., and W. C. Summers.** 1978. Structure of the joint region and the termini of the DNA of herpes simplex virus type 1. J Virol **27:**374-87.
249. **Walker, J. E., M. Saraste, M. J. Runswick, and N. J. Gay.** 1982. Distantly related sequences in the alpha- and beta-subunits of ATP synthase, myosin, kinases and other ATP-requiring enzymes and a common nucleotide binding fold. EMBO J **1:**945-51.
250. **Wang, J. B., Y. Zhu, M. A. McVoy, and D. S. Parris.** 2012. Changes in subcellular localization reveal interactions between human cytomegalovirus terminase subunits. Virol J **9:**315.
251. **Ward, S. A., and S. K. Weller.** 2011. HSV-1 DNA Replication, p. 89-112. *In* S. K. Weller (ed.), Alphaherpesviruses: Molecular Virology. Caister Academic Press, Norfolk, UK.
252. **Warner, S. C., P. Desai, and S. Person.** 2000. Second-site mutations encoding residues 34 and 78 of the major capsid protein (VP5) of herpes simplex virus type 1 are important for overcoming a blocked maturation cleavage site of the capsid scaffold proteins. Virology **278:**217-26.
253. **Watson, R. J., and J. B. Clements.** 1980. A herpes simplex virus type 1 function continuously required for early and late virus RNA synthesis. Nature **285:**329-30.
254. **Weber, P. C., M. D. Challberg, N. J. Nelson, M. Levine, and J. C. Glorioso.** 1988. Inversion events in the HSV-1 genome are directly mediated by the viral DNA replication machinery and lack sequence specificity. Cell **54:**369-81.
255. **Weinheimer, S. P., P. J. McCann, 3rd, D. R. O'Boyle, 2nd, J. T. Stevens, B. A. Boyd, D. A. Drier, G. A. Yamanaka, C. L. DiIanni, I. C. Deckman, and M. G. Cordingley.** 1993. Autoproteolysis of herpes simplex virus type 1 protease releases an active catalytic domain found in intermediate capsid particles. J Virol **67:**5813-22.
256. **Weller, S. K., E. P. Carmichael, D. P. Aschman, D. J. Goldstein, and P. A. Schaffer.** 1987. Genetic and phenotypic characterization of mutants in four essential genes that map to the left half of HSV-1 UL DNA. Virology **161:**198-210.
257. **Weller, S. K., and D. M. Coen.** 2012. Herpes simplex viruses: mechanisms of DNA replication. Cold Spring Harb Perspect Biol **4:**a013011.
258. **White, C. A., N. D. Stow, A. H. Patel, M. Hughes, and V. G. Preston.** 2003. Herpes simplex virus type 1 portal protein UL6 interacts with the putative terminase subunits UL15 and UL28. J Virol **77:**6351-8.
259. **Whitley, R. J., and B. Roizman.** 2001. Herpes simplex virus infections. Lancet **357:**1513-8.
260. **Wilcock, D., and D. P. Lane.** 1991. Localization of p53, retinoblastoma and host replication proteins at sites of viral replication in herpes-infected cells. Nature **349:**429-31.
261. **Wildy, P., W. C. Russell, and R. W. Horne.** 1960. The morphology of herpes virus. Virology **12:**204-22.

262. **Wilkinson, D. E., and S. K. Weller.** 2004. Recruitment of cellular recombination and repair proteins to sites of herpes simplex virus type 1 DNA replication is dependent on the composition of viral proteins within prereplicative sites and correlates with the induction of the DNA damage response. J Virol **78:**4783-96.
263. **Wills, E., L. Scholtes, and J. D. Baines.** 2006. Herpes simplex virus 1 DNA packaging proteins encoded by UL6, UL15, UL17, UL28, and UL33 are located on the external surface of the viral capsid. J Virol **80:**10894-9.
264. **Wood, L. J., M. K. Baxter, S. M. Plafker, and W. Gibson.** 1997. Human cytomegalovirus capsid assembly protein precursor (pUL80.5) interacts with itself and with the major capsid protein (pUL86) through two different domains. J Virol **71:**179-90.
265. **Wu, C. A., N. J. Nelson, D. J. McGeoch, and M. D. Challberg.** 1988. Identification of herpes simplex virus type 1 genes required for origin-dependent DNA synthesis. J Virol **62:**435-43.
266. **Yang, K., and J. D. Baines.** 2008. Domain within herpes simplex virus 1 scaffold proteins required for interaction with portal protein in infected cells and incorporation of the portal vertex into capsids. J Virol **82:**5021-30.
267. **Yang, K., and J. D. Baines.** 2006. The putative terminase subunit of herpes simplex virus 1 encoded by UL28 is necessary and sufficient to mediate interaction between pUL15 and pUL33. J Virol **80:**5733-9.
268. **Yang, K., F. Homa, and J. D. Baines.** 2007. Putative terminase subunits of herpes simplex virus 1 form a complex in the cytoplasm and interact with portal protein in the nucleus. J Virol **81:**6419-33.
269. **Yang, K., A. P. Poon, B. Roizman, and J. D. Baines.** 2008. Temperature-sensitive mutations in the putative herpes simplex virus type 1 terminase subunits pUL15 and pUL33 preclude viral DNA cleavage/packaging and interaction with pUL28 at the nonpermissive temperature. J Virol **82:**487-94.
270. **Yang, K., E. Wills, and J. D. Baines.** 2009. The putative leucine zipper of the UL6-encoded portal protein of herpes simplex virus 1 is necessary for interaction with pUL15 and pUL28 and their association with capsids. J Virol **83:**4557-64.
271. **Yang, K., E. G. Wills, and J. D. Baines.** 2011. A mutation in UL15 of herpes simplex virus 1 that reduces packaging of cleaved genomes. J Virol **85:**11972-80.
272. **Yu, D., A. K. Sheaffer, D. J. Tenney, and S. K. Weller.** 1997. Characterization of ICP6::lacZ insertion mutants of the UL15 gene of herpes simplex virus type 1 reveals the translation of two proteins. J Virol **71:**2656-65.
273. **Yu, D., and S. K. Weller.** 1998. Genetic analysis of the UL 15 gene locus for the putative terminase of herpes simplex virus type 1. Virology **243:**32-44.
274. **Yu, D., and S. K. Weller.** 1998. Herpes simplex virus type 1 cleavage and packaging proteins UL15 and UL28 are associated with B but not C capsids during packaging. J Virol **72:**7428-39.
275. **Zhang, X., S. Efstathiou, and A. Simmons.** 1994. Identification of novel herpes simplex virus replicative intermediates by field inversion gel electrophoresis: implications for viral DNA amplification strategies. Virology **202:**530-9.
276. **Zhang, Y. F., and E. K. Wagner.** 1987. The kinetics of expression of individual herpes simplex virus type 1 transcripts. Virus Genes **1:**49-60.
277. **Zhou, G., and B. Roizman.** 2000. Wild-type herpes simplex virus 1 blocks programmed cell death and release of cytochrome c but not the translocation of mitochondrial

apoptosis-inducing factor to the nuclei of human embryonic lung fibroblasts. J Virol **74:**9048-53.

278. **Zhou, Z. H., D. H. Chen, J. Jakana, F. J. Rixon, and W. Chiu.** 1999. Visualization of tegument-capsid interactions and DNA in intact herpes simplex virus type 1 virions. J Virol **73:**3210-8.

279. **Zhou, Z. H., B. V. Prasad, J. Jakana, F. J. Rixon, and W. Chiu.** 1994. Protein subunit structures in the herpes simplex virus A-capsid determined from 400 kV spot-scan electron cryomicroscopy. J Mol Biol **242:**456-69.